

Annual Report 2003

Institute of Bioinorganic and
Radiopharmaceutical Chemistry



Forschungszentrum
Rossendorf

Wissenschaftlich-Technische Berichte
FZR-394
2004

Annual Report 2003

**Institute of Bioinorganic and
Radiopharmaceutical Chemistry**

Editor: Dr. H. Spies

Editorial staff: Dr. S. Seifert



**Forschungszentrum
Rossendorf**

Cover Picture:

Distribution of [^{18}F]fluoride in the Wistar rat skeleton measured with a MicroPET camera (Concorde Microsystems Inc.) one hour after application.

FOREWORD

In 2003 the Institute of Bioinorganic and Radiopharmaceutical Chemistry, one of five institutes in the Forschungszentrum Rossendorf e.V., continued and further developed its basic and application-oriented research. Research was focused on radiotracers as molecular probes to make the human body biochemically transparent with regard to individual molecular reactions.

As illustrated by the majority of contributions in this report, the Institute is predominantly engaged in radiopharmaceutical chemistry of both radiometals and the PET nuclides. While the improvement of labelling methods for carbon-11 and fluorine-18 continued to remain an area of considerable endeavour, the completion of laboratories for production of PET-radiopharmaceuticals according to GMP regulations and investigations on computer-assisted movement corrections in PET are new and important issues.

The Institute's chemically and radiopharmacologically oriented activities were complemented by more clinically oriented activities in the Positron Emission Tomography (PET) Centre Rossendorf, which closely links the Institute with the Department of Nuclear Medicine of the Medical Faculty of the Technische Universität Dresden.

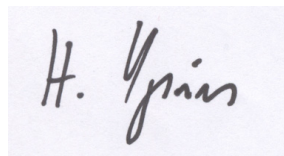
Our chemical, biological and medical activities in the PET Centre were further extended as well as our engagement in the coordination chemistry and radiopharmacology of technetium, rhenium and other metals. The studies on bioactive substances as they are present in food have been continued. This line of activity was set up one year ago. Bioactive substances may cause a health risk or may exert effects not yet fully understood. New biotechnological procedures in food processing also give rise to new questions that can be addressed by PET.

As for the radiometals, chemical and radiopharmaceutical studies meet more and more the radiotherapeutic aspect. This involves both the search for stable chelators for radiometals as well as attempts to better understand and adjust the *in vivo* behaviour of the molecule into which the chelate unit is integrated.

During the period under review cooperations with external partners, particularly from the pharmaceutical industry, could be substantially extended.

Because the former Director of the Institute, Prof. Johannsen, became the Scientific Director of the Research Centre, Dr. Spies has assumed the role of Acting Director since March 1, 2003.

The Institute would like to thank all partners from universities, industry and research institutes who supported its progress, as well as all members and guests of the Institute for their active contributions in 2003. The Institute wishes to acknowledge in particular the support and assistance received from the Executive Board of the Forschungszentrum Rossendorf, from the competent authorities and funding agencies.

A handwritten signature in black ink on a light blue background. The signature reads "H. Spies" in a cursive, slightly slanted script.

Dr. habil. Hartmut Spies

Contents

I. RESEARCH REPORTS.....	1
RADIOTRACERS IN TUMOUR AND METABOLISM RESEARCH	3
Behavioural Disturbances and Regional Cerebral Metabolism in Probable Alzheimer's Disease.....	5
V. Holthoff, K. Herholz, S. Lüdecke, S. Spirling, E. Kalbe, O. Lenz, G. Zündorf, B. Beuthien-Baumann	
Monitoring Postradiotherapeutic Changes of Lung Tissue with PET and SPECT.....	7
B. Beuthien-Baumann, M. Eckhardt, Th. Herrmann, R. Hliscs, L. Oehme, J. van den Hoff, R. Kumpf, P. Geyer, H. Blank, M. Baumann	
Impact of FDG PET Imaging on the Therapy Decision in Patients with Early Stage Hodgkin's Lymphoma.....	9
B. Beuthien-Baumann, R. Naumann, A. Reiß, J. Schulze, A. Hänel, J. Bredow, G. Kühnel, J. Kropp, M. Hänel, M. Laniado, J. Kotzerke, G. Ehniger	
Concorde MicroPET P4 – a PET Scanner for Animal Studies.....	10
E. Will, P. Bühler	
Improvement of the Tomographic Reconstruction at the MicroPET-Scanner	11
F. Pönisch, P. Bühler	
Correction of Body Motion Artifacts in PET - Continued	12
P. Bühler, J. Langner, U. Just, E. Will, J. van den Hoff	
Respiratory Gating for Improved Image Resolution and Tumour Detection in PET Thorax Investigations.....	13
U. Just, P. Bühler, E. Will, J. van den Hoff	
Radiolabelling of an Oligonucleotide Aptamer by Conjugation with N-Succinimidyl-4-[¹⁸ F]Fluorobenzoate.....	14
M. Grote, F. Wüst, B. Noll, A. Stephens, M. Friebe	
Inhibition Studies with FMHGB as a New Pattern for Monitoring Gene Expression.....	15
M. Grote, St. Noll, B. Noll	
¹⁸ F- Labelling of Cytosine at the 2-Position	16
B. Noll, St. Noll	
The Microwave-Assisted Synthesis of 5-Hydroxymethylcytosine	17
B. Noll, B. Grosse, St. Noll	
Z/E-Isomerism of N ⁴ -(p-Toluenesulphonyloxy)cytosine Derivatives	18
St. Noll, B. Noll, H. Stephan, W. Kraus, M. Findeisen, L. Hennig, K. Yoshizuka	
Syntheses of Novel Acyclic Pyrimidine Nucleosides as Precursors for ¹⁸ F- Labelling	19
B. Noll, St. Noll	
Syntheses of Novel Acyclic Pyrimidine Nucleosides as Potential Substrates of the HSV1-TK.....	20
St. Noll, B. Noll	
Neurotensin(8-13) Labelled with ^{99m} Tc Using the '4+1' Mixed-Ligand Chelate System – Part 1: Chemistry.....	21
J.-U. Kuentler, S. Seifert, H.-J. Pietzsch, H. Spies	
Neurotensin(8-13) Labelled with ^{99m} Tc Using the '4+1' Mixed-Ligand Chelate System – Part 2: Basic Stability Considerations	22
B. Pawelke, J.-U. Kuentler, S. Seifert, R. Bergmann, H.-J. Pietzsch, H. Spies	
^{99m} Tc-Cytectrene Complexes – Chemical Structure and Biobehaviour Part 1: Chemical Characterisation of Tc and Re Complexes.....	23
M. Saidi, S. Seifert, M. Kretzschmar, R. Bergmann, H.-J. Pietzsch	
^{99m} Tc-Cytectrene Complexes – Chemical Structure and Biobehaviour Part 2: Biological Characterisation	24
M. Saidi, M. Kretzschmar, R. Bergmann, S. Seifert, H.-J. Pietzsch	

Synthesis of 4-[¹⁸ F]Fluoromethyl-2-Chloro-O-Succinimidyl-Benzoate as Novel Bifunctional ¹⁸ F- Labelling Agent.....	25
F. Wüst, M. Müller, H. Kasper	
Radiosynthesis and Biodistribution of a ¹⁸ F-Labelled Corticosteroid for Mapping Brain Glucocorticoid Receptors (GR)	26
F. Wüst, T. Kniess, R. Bergmann	
Synthesis of ¹⁸ F-Labelled Nucleosides Using Stille Cross-Coupling Reactions with [4- ¹⁸ F]Fluoriodobenzene.....	27
F. Wüst, T. Kniess, H. Kasper	
Radiolabelled Flavonoids and Polyphenols	
I. Introduction and Radiolabelling Concept	28
S. Gester, F. Wüst, R. Bergmann, J. Pietzsch	
Radiolabelled Flavonoids and Polyphenols	
II. Synthesis Towards [¹⁸ F]Fluorine Labelled Resveratrol.....	29
S. Gester, F. Wüst, R. Bergmann, J. Pietzsch	
Synthesis of a ¹⁸ F-Labelled COX-2 Inhibitor	30
A. Höhne, F. Wüst	
¹⁸ F- Labelling of a Potent Nonpeptide CCR1 Antagonist: Synthesis of [¹⁸ F]ZK811460 in an Automated Module	31
P. Mäding, F. Füchtner, B. Johannsen, J. Steinbach, C. S. Hilger, R. Mohan	
¹¹ C- Labelling of a Taxane Derivative Using [1- ¹¹ C]Acetyl Chloride	32
P. Mäding, J. Zessin, U. Pleiß, F. Wüst	
Synthesis of Sodium [1- ¹¹ C]Acetate for Clinical Applications	33
P. Mäding, J. Zessin, F. Füchtner, F. Wüst	
Tissue Transglutaminase: a Minireview	35
J. Pietzsch, R. Bergmann	
Synthesis of Fluorinated <i>N</i> -Benzoylpolyamines as Substrates of Tissue Transglutaminase	36
K. Knop, C. Hultsch, K. Rode, T. Kniess, F. Wüst, R. Bergmann, J. Pietzsch	
Biological Evaluation of Fluorinated <i>N</i> -Benzoylpolyamines as Substrates of Tissue Transglutaminase Activity: Polyamination of <i>N,N'</i> -Dimethylcasein.....	37
J. Pietzsch, K. Knop, K. Rode, R. Bergmann	
Biological Evaluation of Fluorinated <i>N</i> -Benzoylpolyamines as Substrates of Tissue Transglutaminase Activity: Insights from Animal PET Studies	38
J. Pietzsch, R. Bergmann, K. Knop, K. Rode, F. Wüst, J. van den Hoff	
Measurement of 5-Hydroxy-2-Aminovaleric Acid as a Specific Marker of Iron-Mediated Oxidation of Proline and Arginine Residues of Low Density Lipo-protein Apolipoprotein B-100 in Human Atherosclerotic Lesions.....	39
J. Pietzsch, R. Bergmann	
Increased Cholesteryl Ester Transfer Protein (CETP) Activity in Impaired Glucose Tolerance: Relationship to High Density Lipoprotein Metabolism.....	40
J. Pietzsch, S. Nitzsche, K. Fuecker	
RADIOMETAL THERAPEUTICS	41
Novel Procedures for Preparing '4+1' ¹⁸⁸ Re Complexes	43
S. Seifert, E. Schiller, H.-J. Pietzsch	
Hydrophilic Rhenium-188 Complexes for Attaching the Metal to Biomolecules	
1. General Considerations.....	44
E. Schiller, H.-J. Pietzsch, H. Spies	
Hydrophilic Rhenium-188 Complexes for Attaching the Metal to Biomolecules	
2. Synthesis and Characterisation of a Novel Hydrophilic Ligand	45
E. Schiller, W. Kraus, H.-J. Pietzsch, H. Spies	
Hydrophilic Rhenium-188 Complexes for Attaching the Metal to Biomolecules	
3. Physicochemical and Biological Evaluation of Model Complexes	46
E. Schiller, S. Seifert, R. Bergmann, H.-J. Pietzsch, H. Spies	

Routes to Modification of Rhenium Cluster Core Ligand Environment with Organic Ligands.....	47
K. Brylev, H.-J. Pietzsch, H. Stephan, V. E. Fedorov, H. Spies	
Characterization of Cu(II)-Cyclam Complexes by Laser-Induced Fluorescence Spectroscopy	48
D. Appelhans, D. Tabuani, B. Voit, G. Geipel, G. Bernhard, H. Spies, H. Stephan	
Calorimetric and Potentiometric Study of PAMAM Dendrimers: Protonation and Interactions with Human Serum Albumin	49
R. Kirchner, J. Seidel, H. Stephan, B. Johannsen	
Hydrolytic Stability of Polyoxotungstates	50
H. Stephan, D. John, A. S. Raji, A.-K. Sawatzki, L. Jelínek, P. Houserová, Z. Matějka	
PET IN DRUG AND FOOD RESEARCH.....	51
Biodistribution and Catabolism of ¹⁸ F-Labelled Isopeptide N ^ε -(γ-Glutamyl)-L-Lysine	53
C. Hultsch, R. Bergmann, B. Pawelke, F. Wüst, J. Pietzsch, T. Knieß, B. Johannsen, T. Henle	
CYCLOTRON OPERATION	55
Operation of the Rossendorf PET Cyclotron "CYCLONE 18/9" in 2003.....	57
St. Preusche, F. Wüst	
Ion Beam Tests on the Solid Target System of the Rossendorf CYCLONE 18/9 Cyclotron	59
St. Preusche, H. Roß	
Factors Affecting the Specific Activity of [¹⁸ F]Fluoride from a Water Target.....	60
F. Füchtner, S. Preusche, J. Steinbach	
II. PUBLICATIONS, LECTURES, PATENTS AND AWARDS OF THE INSTITUTE AND THE PET-CENTRE ROSSENDORF	61
III. SCIENTIFIC COOPERATION.....	75
IV. SEMINARS.....	81
V. ACKNOWLEDGEMENTS.....	85
VI. PERSONNEL	89

I. RESEARCH REPORTS

**RADIOTRACERS IN TUMOUR AND METABOLISM
RESEARCH**

Behavioural Disturbances and Regional Cerebral Metabolism in Probable Alzheimer's Disease

V. Holthoff¹, K. Herholz², S. Lüddecke¹, S. Spirling¹, E. Kalbe², O. Lenz², G. Zündorf², B. Beuthien-Baumann³.

¹Klinik und Poliklinik für Psychiatrie und Psychotherapie, Universitätsklinikum der TU Dresden; ²Max-Planck Institut für Neurologische Forschung, Köln, ³Klinik und Poliklinik für Nuklearmedizin/PET-Zentrum Rossendorf, Universitätsklinikum der TU Dresden

The data were obtained by the European Network for Efficiency and Standardisation of Dementia Diagnosis (NEST-DD) with support from the European Commission Framework V.

Introduction

Alzheimer's disease (AD) is clinically characterized by cognitive impairment and behavioural disturbances, that significantly interfere with activities of daily living. The following study examines the association between regional changes in cerebral glucose metabolism and behavioural abnormalities in patients suffering from AD. The aim of the study was the identification of brain areas implicated in behavioural disturbances in AD. Behavioural assessment included the interview of the caregiver with the neuropsychiatric inventory (NPI) [1]. The NPI uses screening questions to ask whether a behavioural change is present or not. The domains assessed include depression, apathy, anxiety, agitation, abnormal motor behaviour, disinhibition, euphoria, delusion and hallucination. The behavioural domains are then rated using scales for frequency and severity.

Methods

•Patient and normal control group:
41 patients with probable AD according to NINCDS-ADRDA criteria.
mean age: 68.1 years, SD: 8.3
MMSE score range 18-28, mean: 22.2; SD: 3.9

range Clinical Dementia score CDR: 0.5-2, mean:1, SD: 0.6

109 controls; mean age: 61.5 years, SD: 11.7

•Behavioural assessment: NPI

•FDG-PET:ECAT Exact HR+ (Siemens/CTI), 300 MBq ¹⁸F-FDG, measured attenuation correction, Acquisition: 40-60 min post injection

•Data analysis: SPM99 (Statistical Parametric Imaging) [2] using a one-way ANOVA comparing patients with and without the behavioural disturbance under study and an age-matched control group. We retained as significant those clusters with a corrected $p < 0.05$.

Results and Discussion

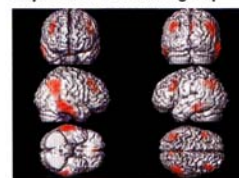
Depressive symptoms are associated with bilateral prefrontal hypometabolism. Apathy is associated with bilateral prefrontal and orbitofrontal hypometabolism. Aberrant motor behaviour is associated with bilateral dorsolateral prefrontal hypometabolism. Irritability is associated with bilateral orbitofrontal and left prefrontal hypometabolism. These findings support the hypothesis of a neuroanatomical brain circuit involving the prefrontal cortex that mediate behavioural abnormalities in AD [3].

AD group with depression

(n=16; 70.8±9.2, MMSE=22.6±3.3)

Comparison	Size	P (corr.)	Z	x, y, z	Brodman area/gyrus
Depression vs. control group	5279	0.0001	5.64	52, -54, 26	39 (r) sup.temp
			5.35	68, -24, -18	20 (r) inf.temp
			5.22	66, -32, -14	21 (l) mid.temp
	1457	0.0001	4.57	-40, -64, 44	7 (l) inf.pariet.
	1299	0.0001	4.27	-42, -72, 32	39 (l) angular
			4.48	0, -44, 36	31 (l) cingulate
Depression-free control group			4.35	2, -56, 28	31 (r) cingulate
	806	0.005	4.46	-42, 20, 42	20 (l) inf.temp
			4.08	-50, 24, 26	8 (l) mid.front.
	1051	0.061	4.23	-62, -36, -16	46 (l) mid.front.
	890	0.004	4.15	40, 28, 42	8 (r) mid.front.
			3.92	44, 38, 28	9 (r) sup.front.
Depression-free vs control group	5230	0.0001	6.19	66, -24, -26	20 (r) inf.temp
			5.64	50, -56, 22	39 (r) sup.temp
			5.41	2, -60, 26	31 (r) cingulate
			4.55	-46, -62, 36	39 (l) inf.pariet.
	4303	0.0001	4.55	-38, -66, 44	7 (l) inf.pariet.
			4.90	-62, -42, -20	20 (l) inf.temp
Depression vs depression-free group	1511	0.0001	4.90	-62, -42, -20	20 (l) inf.temp
			4.10	8, 50, -30	11 (r) orbital
	855	0.004	4.08	4, 58, -8	10 (r) sup.front.
			3.63	10, 30, -30	11 (r) orbital
Depression vs depression-free group	5188	0.020	2.91	-48, -4, 22	6 (l) sup.front.
			2.86	-54, -14, 18	43 (l) pariet.
			2.82	-52, 18, 18	45 (l) inf.front.

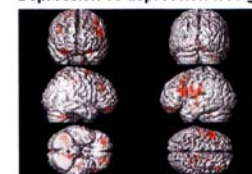
Depression vs control group



Depression-free vs control group



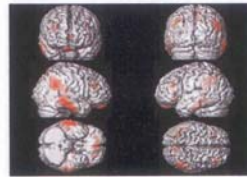
Depression vs depression-free group



AD group with aberrant motor behavior
(Abmotor.;n=7; 69.7±9.2, MMSE=18.7±5.7)

Comparison	Size	P (corr.)	Z	x, y, z	Brodman area/gyrus
Abmotor. vs. control group	5021	0.0001	4.59	50, -54, 28	39 (r) sup.temp.
			4.17	56, -26, -20	20 (r) inf.temp
			3.17	-36, -62, 46	7 (l) inf.pariet.
	2746	0.001	3.12	-48, -52, 32	40 (l) parietal
			3.09	-40, -36, 10	41 (l) sup.temp.
Abmotor.-free vs control group	5102	0.0001	4.41	48, -58, 28	39 (r) sup.temp.
			3.40	6, -72, 54	7 (r) precuneus, pariet.
			3.15	30, -66, 44	19 (r) precuneus, pariet.
	3154	0.0001	3.50	-36, -64, 44	7 (l) sup.pariet.
			3.48	-48, -44, 40	40 (l) inf.pariet.
			3.24	-40, -68, 28	39 (l) mid.temp.
Abmotor. vs abmotor.-free group	1486	0.03	3.78	34, 34, 28	9 (r) mid.front.
			2.92	46, 40, 2	44 (r) inf.front.
			2.65	22, 40, 22	9 (r) med.front.
	4944	0.0001	3.55	-44, 28, -8	47 (l) inf.front.
			3.05	-32, 54, 2	10 (l) mid.front.
			3.01	-12, 12, 34	32 (l) cingulate

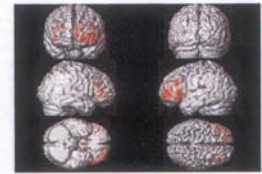
Abmotor. vs control group



Abmotor.-free vs control group



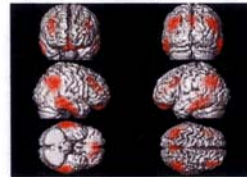
Abmotor vs Abmotor.-free group



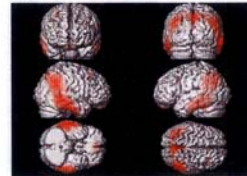
AD group with apathy
(n=18; 67.4±10.5 years, MMSE=21.6±3.9)

Comparison	Size	P (corr.)	Z	x, y, z	Brodman area/gyrus
Apathy vs. control group	6422	0.0001	6.22	46, -56, 32	39 (r), sup.temp.
			5.39	66, -26, -22	40 (r) postcentr.
			5.07	62, -16, -32	20 (r) inf.temp
	6731	0.0001	5.32	-42, -62, 38	39 (l) angular
			4.26	-58, -28, -14	21 (l) mid.temp.
			4.25	-60, -40, -12	21 (l) mid.temp.
3605	0.001	4.39	0, -40, 34	7 (l) precuneus, pariet.	
		4.23	-2, -58, 28	31 (l) cingulate	
2567	0.004	4.03	2, 52, -24	11 (r) rectal	
		3.37	-24, 36, -22	11 (l) rectal	
		2.36	24, 50, -20	11 (r) sup.front.	
1731	0.03	3.78	-42, 24, 30	9 (l) mid.front.	
		3.30	-44, 4, 32	9(l) inf.front.	
		2.70	-32, 48, 12	10 (l) mid.front.	
1773	0.03	3.53	40, 28, 40	9 (r) mid.front.	
		3.33	38, 50, 20	10 (r) sup.front.	
		3.27	44, 36, 28	9 (r) sup.front.	
Apathy-free vs control group	6942	0.0001	6.26	48, -56, 30	39 (r) sup.temp.
			5.98	62, -22, -30	20 (r) fusiform, temp.
			5.72	62, -44, -8	21 (r) mid.temp.
5530	0.0001	5.01	-40, -66, 34		
		4.81	6, -68, 50		
		4.67	0, -46, 36		
2099	0.0001	4.64	-56, -34, -10		
		4.23	-60, -28, -28		
		3.97	-54, -48, -24		
Apathy vs apathy-free group		n.s.			

Apathy vs control group



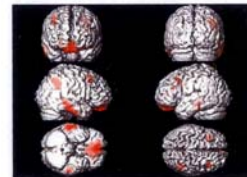
Apathy-free vs control group



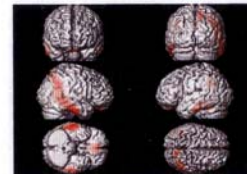
AD group with irritability
(n=10; 67.1±8.2, MMSE=23.3±2.0)

Comparison	Size	P (corr.)	Z	x, y, z	Brodman area/gyrus
Irritability vs. control group	1555	0.03	5.30	64, -22, -28	20 (r) fusiform
			4.77	54, -36, -8	20 (r) mid.temp
			4.50	-10, 28, -32	11 (l) orbital
	3593	0.0001	3.93	2, 52, -18	11 (r) med.front.
			3.81	8, 30, -32	11 (r) orbital
Irritability-free vs control group	4648	0.0001	5.05	64, -22, -28	20 (r) fusiform
			4.27	46, -54, 28	39 (r), sup.temp.
			3.94	56, -42, -8	20 (r) mid.temp.
Irritability vs irritability-free group	2357	0.005	3.14	28, 52, -4	10 (r) mid.front
			2.95	44, 34, -14	11 (r) mid.front.
			2.91	-22, 56, -12	11 (l) sup. front.

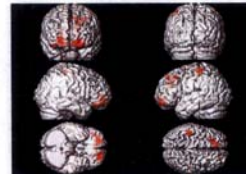
Irritability vs control group



Irritability-free vs control group



Irritability vs non-Irritability



References

[1] Cummings, J. L. *et al.*, J. Neurology 44 (1994) 2308-14.

[2] Friston, K., Statistical Parametric Imaging (1994).

[3] Cummings, J. L., Neurobiol. Aging 21 (2000) 845-861.

Monitoring Postradiotherapeutic Changes of Lung Tissue with PET and SPECT

B. Beuthien-Baumann¹, M. Eckhardt², Th. Herrmann², R. Hliscs¹, L. Oehme¹, J. van den Hoff, R. Kumpf³, P. Geyer², H. Blank², M. Baumann^{2,3}

¹Klinik und Poliklinik für Nuklearmedizin/PET-Zentrum Rossendorf, ²Klinik und Poliklinik für Strahlentherapie und Radioonkologie, ³Experimentelles Zentrum, Universitätsklinikum der TU Dresden

Introduction

Damage to surrounding lung is a substantial problem in radiation treatment (RT) of malignant disease in the thoracic region. Experimental data suggest, that certain regions of the lung show different vulnerability for the development of pneumonitis and fibrosis. Modern 3D-treatment planning systems in radiotherapy allow to spare normal lung tissue in especially vulnerable regions. As part of an ongoing study aimed to define the relative radiosensitivity of different regions of the lung, the present investigation explores the usefulness of different diagnostic procedures for qualitative and quantitative monitoring of the development of early and late radiation damage in the lung of minipigs.

Methods

The right lung of 6 minipigs (age 6 months) was irradiated with a single dose of 12 Gy. Before irradiation and at 2, 4, 8, 12 and 24 weeks after irradiation of the lung the animals were investigated with 1. HR-CT to follow morphologic changes of lung tissue 2. perfusion SPECT with ^{99m}Tc-macroaggregated albumin (MAA) 3. ventilation SPECT with Xenon-133 (¹³³Xe) 4. [¹⁸F]Fluoro-deoxyglucose-PET (FDG) 5. [¹⁵O]H₂O-PET (H₂O). Data sets of all imaging modalities were matched using the HERMES[®] software (Nuclear Diagnostics, Sweden). Regions of interest were defined in different parts of the lung using CT and transferred to the functional imaging modalities.

Results and Discussion

Table 1. Radiographic changes in CT. Infiltrations post irradiation become visible as early as 2 weeks (w) post irradiation in half of the animals. After 4 weeks infiltrations are apparent in all animals.

	0 w	2 w	4 w	8 w	12 w	24 w
# 1	0	0	(+)	0	0	0
# 2	0	0	+	(+)	0	(+)
# 3	0	(+)	(+)	0	0	0
# 4	0	(+)	++	++	++	+
# 5	0	+	+	(+)	0	0
# 6	0	0	++	++	++	++

(+) fine infiltrations

+ distinct infiltrations, partly spotted

++ spotted, partly confluent

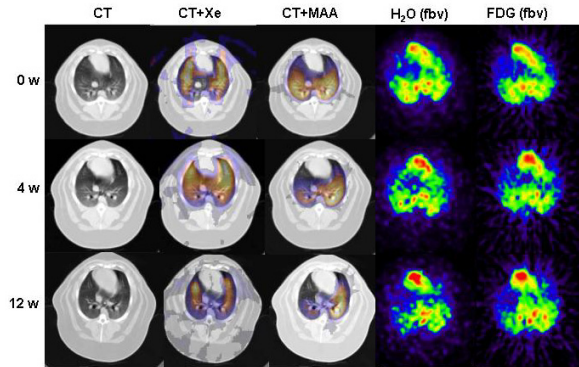


Fig. 1. CT, ventilation- and perfusion-SPECT, and FDG- and H₂O-PET at different time points in pig No. 3. Although in CT no or only very subtle changes are seen at 4 weeks post irradiation, clear diminished perfusion of the irradiated lung is visible (MAA) with unchanged ventilation status (¹³³Xe). With H₂O-PET and FDG-PET a decline of the fractional blood volume is visible at 12 weeks post RT.

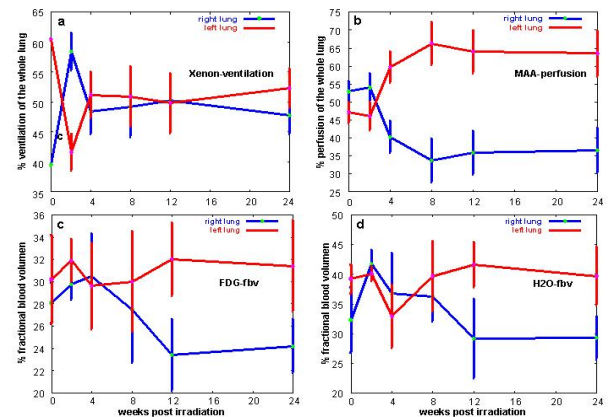


Fig. 2a-d. Quantitative changes in SPECT and PET.

a) In ventilation-SPECT no clear changes occur. The first two datapoints (pre- and 2w post RT) have to be interpreted with caution due to technical limitations.

b) Starting 4 weeks after RT perfusion of the irradiated lungs significantly decreases.

c) The FDG-signal is significantly lower in the irradiated lung at 12 w post RT.

d) The fractional blood volume of the irradiated lung is significantly lower in the irradiated lung at 12 w post RT. The curves of FDG-PET and H₂O-PET show a similar course.

- While the morphologic changes in CT are reversible in 4 of 6 animals, the functional parameter perfusion remains reduced over the time investigated.

- Ventilation was not significantly affected by irradiation. In animal investigations ¹³³Xe-SPECT is not the ideal tracer (no active inhalation, low breathing under anaesthesia and

accumulation of ^{133}Xe in fat tissue during SPECT acquisition).

- Perfusion changes are clearly visible with MAA-SPECT as early as 4 w post RT.
- Absolute quantification of perfusion of the lung with H_2O -PET was not feasible because of identical shapes of the input functions from the right ventricle (blood curve) and the lung tissue curve. In contrast, the calculation of the fractional blood volume (fbv) is possible even on pixel by pixel basis, yielding parametric maps for this parameter. Similar to the perfusion evaluated with MAA-SPECT, a reduction of fbv is seen in the irradiated lung, but at a later timepoint.

- Lung itself shows very low glucose metabolism. In some animals subtle accumulation was seen in the pleura post irradiation, indicating inflammation (not shown). Because of identical shapes of the input function from the right ventricle (blood curve) and the lung tissue curve, the low glucose metabolism of lung tissue and the small percentage of lung tissue with respect to air, calculation of the absolute glucose metabolism according to the Patlak-plot did not show reasonable results. The FDG-data were therefore quantified according to the fractional blood volume model. The results show comparable to the H_2O -data a decline of the fbv of the irradiated lung.

=> Perfusion SPECT was the most robust imaging modality for functional changes of the lung post irradiation in this animal model.

Impact of FDG PET Imaging on the Therapy Decision in Patients with Early Stage Hodgkin's Lymphoma

B. Beuthien-Baumann, R. Naumann, A. Reiß, J. Schulze, A. Hänel, J. Bredow, G. Kühnel, J. Kropp, M. Hänel, M. Laniado, J. Kotzerke, G. Ehninger

Introduction

Today, Hodgkin's lymphoma (HL) is one of the malignant diseases with the highest rate of cure in adults based on improved chemotherapy and radiotherapy. The most important objective of staging is the exact detection of all nodal and extranodal lymphoma manifestations present to be able to administer the optimal therapy according to the stage and to the risk situation [1]. The criteria for detecting involvement are mainly based on the assessment of the size of the lymph nodes, mainly revealed with computed tomography (CT), regarding lymph nodes with a diameter of more than 1 cm as pathologic. This prospective study assessed the impact of ^{18}F -fluorodeoxyglucose (^{18}F -FDG) positron emission tomography (PET) on staging and possible consequential changes of treatment regimen in patients with Hodgkin's lymphoma (HL).

Patients and Methods

88 consecutive patients with histological verified Hodgkin's lymphoma underwent a PET scan in addition to conventional staging procedures (physical examination, chest X-ray, ultrasound, contrast-enhanced CT of the neck, chest, abdomen and pelvis, erythrocyte sedimentation rate, posterior iliac crest biopsy). The clinical stage of the patients was assessed according to the Ann Arbor classification [2]. Treatment was based on the conventional staging only, the results of the ^{18}F -FDG-PET did not affect the treatment strategy. Evaluation focused on the suggested change in clinical stage according to the Ann Arbor classification and on the suggested change in treatment strategy rather than on a lesion-by-lesion analysis.

Results and Discussion

Using all the methods performed as the standard of reference, ^{18}F -FDG-PET staging was concordant with conventional staging in 70/88 patients (80 %). ^{18}F -FDG-PET suggested a change to a different clinical stage in 18 patients (20 %): eleven patients (13 %) would have been upstaged and 7 patients (8 %) would have been downstaged. The same treatment strategy would have been defined in 72/88 patients (82 %). Management would have been changed in 16 patients (18 %): intensification of treatment in 9 patients (10 %) and minimization of treatment in seven patients

(8 %). In the 44 patients with early disease (stage IA-IIIB), treatment would have been intensified in 9/44 patients (20 %).

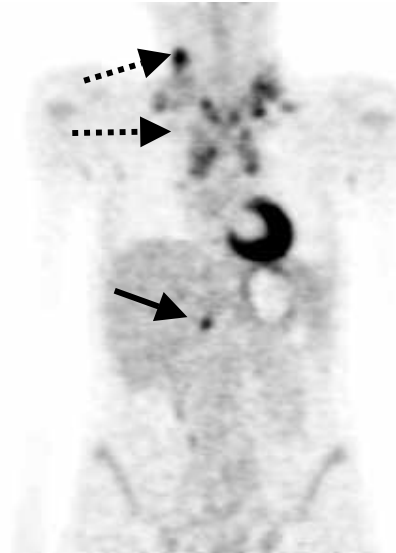


Fig. 1. Additional focal liver uptake (solid arrow) changed former stage II (cervical and mediastinal involvement, dashed arrows) to stage III.

In the literature the value of ^{18}F -FDG-PET for the staging of lymphoma is well documented [3, 4], but only limited numbers of studies concentrate solely on HL or focus on the impact on change of treatment [5, 6]. The results of our study underline the value of ^{18}F -FDG-PET for the staging of HL and indicate a substantial impact on the treatment strategy, particularly in patients in which conventional staging procedures indicate a limited stage of disease [7]. ^{18}F -FDG-PET is a relevant noninvasive method that supplements conventional staging procedures and should therefore be used routinely to stage Hodgkin's lymphoma.

References

- [1] Lister, T. A. *et al.*, *J. Clin. Oncol.* 7 (1989) 1630-1636.
- [2] Carbone *et al.*, *Cancer Res.* 31 (1971) 1860-1861.
- [3] Naumann, R. *et al.*, *Br. J. Haematol.* 115 (2001) 793-800.
- [4] Jerusalem, G. *et al.*, *Haematologica* 86 (2001) 266-273.
- [5] Bangerter, M. *et al.*, *Ann. Oncol.* 9 (1998) 1117-1122.
- [6] Hueltenschmidt, B. *et al.*, *Cancer* 91 (2001) 302-310.
- [7] Naumann, R. *et al.*, *Br. J. Cancer*, *in press*.

Concorde MicroPET P4 – a PET Scanner for Animal Studies

E. Will, P. Bühler¹

¹Klinik und Poliklinik für Nuklearmedizin/PET-Zentrum Rossendorf

Introduction

A Concorde microPET P4 PET scanner [1] was installed in November 2002 at the PET Centre Rossendorf. It is a four-ring scanner with a ring diameter of 26 cm, and is equipped with LSO detectors. The detectors consist of arrays of 8 x 8 crystals of 2.2 x 2.2 x 10 mm³ and are arranged in 42 detector blocks per ring. The axial field of view is 7.8 cm and the transaxial field of view (FOV) is 19 cm. The resolution in the centre is about 1.8 mm. The system is operated in full 3D mode and data are acquired in list mode. Here we report on the measured performance of the microPET.

Results and Discussion

Two dedicated line phantoms were developed to evaluate the resolution and other camera parameters, one with a length of 50 mm and Ø100 mm, one with a length of 100 mm and Ø50 mm. The phantoms consist of segments with holes of 1, 1.5, 2, 2.5 and 3 mm diameter respectively. Each segment can be filled independently. The phantoms were manufactured by BS Industrieelektronik & Medizintechnik - Herbert Schöppy (www.bsi-schoeppy.de).

The list mode data of the presented measurements were sorted in full 3D sinograms and reconstructed with Fourier rebinning (FORE) and the OSEM2D algorithm. For transmission measurements an 18 MBq ⁶⁸Ge point source was used. In Fig. 1 an image of the Line Phantom with 50 mm diameter is shown. Fig. 2 shows the activity profile along the horizontal line in Fig. 1. The distance between the 1.5 mm holes in this segment is 6 mm. The measured full width of the peaks at half maximum is ~1.9 mm near the centre and ~2.5 mm at the edge. The linearity of the scanner was measured with a mice "phantom" (60 cm³ syringe) filled with 500 MBq of a ¹¹C-solution. The time dependence is shown in Fig. 3. The scanner is linear up to 60 MBq = 1.2 MBq/cm³ for this phantom. The measured linearity over all planes is ~6 %.

Data volumes in animal PET studies

Acquisition in list mode results in large data volumes. Typical values are presented in Table 1 for a two-hour investigation with 35 MBq FDG. To store this amount of data a 6 TB raid system was installed.

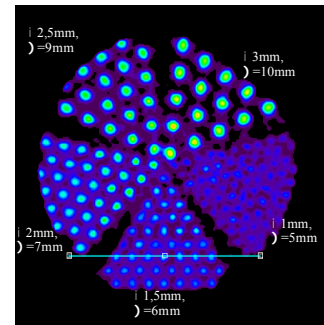


Fig. 1. Image of the Ø 50mm Line Phantom.

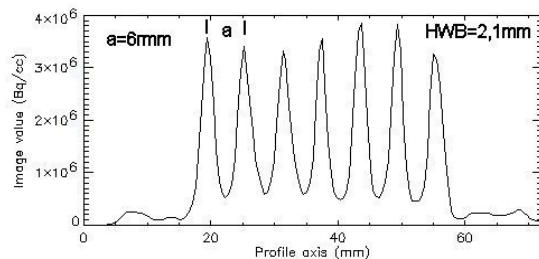


Fig. 2. Profile of a line in the 1.5 mm hole segment 3 cm off the centre.

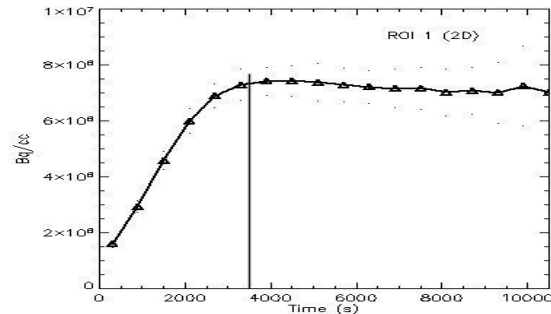


Fig. 3. Decay measurement for 500 MBq ¹¹C.

Table 1. Data volumes in animal PET studies

	Typical	Typical (30 Frames)
List mode file	<20 GByte	~10 GByte
FDG Rate		
Dynamic sinogram	90.7 MByte/Frame	2.7 GByte
Transmission list mode file	<15 GByte	~5 GByte
Attenuation file	90 MByte	90 MByte
Image file:		
128x128	4.1 MByte/Frame	124 MByte
256x256	16.5 MByte/Frame	495 MByte
Volume/measurement:		~18 GByte

Reference

[1] Tai, Y. C. *et al.*, Phys. Med. Biol. 46 (2001) 1845-1862.

Improvement of the Tomographic Reconstruction at the MicroPET-Scanner

F. Pönisch, P. Bühler

The method for improving the tomographic reconstruction at the MicroPET scanner is described. The presented algorithm will result in a better quality of the reconstructed PET images.

Introduction

Since 2003 a microPET scanner of Concorde Microsystems Inc. (CMS) is used at the PET Centre of the FZR for rats and mice imaging. The dedicated positron emission tomograph (PET) operates in 3D mode, i.e. without using tungsten septa and a spatial resolution of less than 2 mm is achieved [1]. However, the resolution is deteriorated with increasing distance from the scanner axis. This results in a reduced practical usability of the tomograph. Furthermore, the existing reconstruction code supplied from CMS provides only 2D reconstruction algorithms: filtered back projection and 2D Ordered Subsets Expectation Maximization (OSEM). The restriction to 2D determines the fixed voxel size in axial direction which further limits the intrinsic resolution along this axis. The aim of the current work is to develop a 3D reconstruction code for this scanner.

Materials and Methods

The microPET scintillation crystals (block detector design) are half the size in comparison with a conventional PET scanner (e.g. CTI HR+). This on one hand improves the spatial resolution for small animal imaging but on the other hand enhances a wrong detector classification caused by Compton Scatter within the scintillator crystal. Unconsidered this results in a blurring of the detector response function and a reduced spatial resolution.

A feasible solution for this problem is to model all physical processes within the tomographic iterative reconstruction. The basis of the reconstruction algorithm is the transition matrix \mathbf{A} . Its element a_{ij} denotes the probability for detecting a positron emission in voxel site j , $j = 1, \dots, J$ at coincidence channel i , $i = 1, \dots, I$. In order to reduce the size of \mathbf{A} , the matrix can be divided into two factors:

$$\mathbf{A} = \mathbf{A}_{geom} \times \mathbf{A}_{cryst}.$$

The geometrical component transition matrix \mathbf{A}_{geom} is stored in a file with a sparse matrix format (ca. 2 GB). The crystal blurring component \mathbf{A}_{cryst} will be calculated in dependence of the projection distance by means of GEANT4-simulations [2] and stored as blurring kernel according to [3]. The applied OSEM algorithm [4] is a modification of the Maximum Likelihood Expectation Maximization (MLEM) algorithm of Shepp and Vardi [5]. It starts with an initial

image estimation. With OSEM, the projection data are grouped in ordered subsets. The standard MLEM algorithm, i.e. forward- and backward-projection, is then applied to each of the subsets in turn. The resulting reconstructed image becomes the starting value for use with the next subset.

Results

The matrix \mathbf{A}_{geom} was calculated in dependence of the voxel size and the dimension of the image. The calculations considered the solid angle for each combination of detector pair and voxel and the intersection length of the coincidence line with the voxel. Fig. 1 shows the sinogram of the forward projection of a point source using the matrix \mathbf{A}_{geom} .

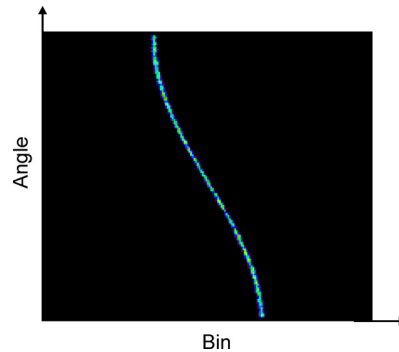


Fig. 1. Sinogram of the forward projection of a point source using the matrix \mathbf{A}_{geom} after the first iteration step.

First results of the GEANT4 simulation are obtained for the block detector geometry. This will allow the estimation of the factor \mathbf{A}_{cryst} in the near future.

References

- [1] Will, E. *et al.*, *this report*, p. 10.
- [2] GEANT-Collaboration, <http://geant4.web.cern.ch/geant4/>
- [3] Qi *et al.*, *Phys. Med. Biol.* 43 (1998) 1001-1013.
- [4] Hudson, M. *et al.*, *IEEE Trans. Med. Imag.* 13 (1994) 601-609.
- [5] Shepp, L. A. *et al.*, *IEEE Trans. Med. Imag.* 1 (1982) 113-122.

Correction of Body Motion Artifacts in PET - Continued

P. Bühler¹, J. Langner, U. Just, E. Will, J. van den Hoff¹
¹PET-Zentrum Rossendorf and Klinik und Poliklinik für Nuklearmedizin

Introduction

Correction for patient motion during PET investigations is a persistent issue. Common methods to correct head motion in PET are based on reorientation of multiple frame images to a common reference position. These methods allow the correction of movements between frames (time windows) but can not account for motion occurring within frame boundaries. For this purpose a list mode-based method is needed [1]. The PET data are acquired in list mode (each single event is saved) and simultaneously the head motion is tracked with a suitable device. According to the motion data each detected event is corrected to a reference point in time. Potentially, this results in a fully corrected list mode stream and, after binning and reconstruction, in motion free images. Last year we reported on the development of the basic event based correction algorithm [2]. Here we report on the completion of the implementation and demonstrate the capabilities of the method.

For the measurement of movements of the head during PET acquisition, we use the infrared camera system ARTrack1, which is able to track a target of retroreflecting spheres. For PET measurements the target is mounted on the head of the patient using a glasses frame. With a maximum sampling rate of 60 Hz, the system delivers measures of the six degrees of freedom of the target. The data stream also contains time tags, which allows to synchronize the tracking data with the PET list mode stream. In order to apply the tracking information to the PET data the tracking information has to be converted from the tracking systems coordinate system to the coordinate system of the PET camera. The transformation is found by a dedicated crosscalibration measurement.

Results and Discussion

The accuracy of the entire setup including the tracking system, the crosscalibration procedure, and movement correction algorithm was validated with several test measurements. Here results of a test with a point like Ge-68 source are shown. During PET acquisition the source was displaced and the displacement was measured with the tracking system. The data were then movement corrected, reconstructed, and the resulting image was compared with the image of the source in the reference position. At displacements in transaxial direction of up to 5 cm (see Fig. 1) the difference between corrected and nominal central

position of the point source as well as the broadening of the image (FWHM) is less than 0.2 mm. In axial direction the accuracy of the correction is limited by the finite extent of the PET crystals of 4.85 mm in axial direction.

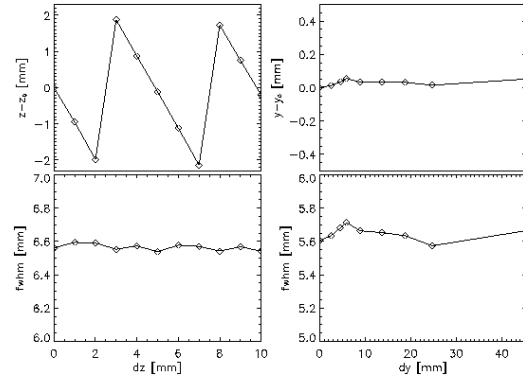


Fig. 1. Test measurements with a point-like Ge-68 source, which was displaced during data acquisition in axial (left column of panels) and transaxial direction. The upper row shows the difference between corrected and original position as function of maximum displacement during acquisition. The lower row of panels shows the resolution (FWHM) of the point source in the corrected image.

The method was also tested under realistic conditions. A volunteer patient was asked to intentionally turn the head during a six-minute acquisition (250 MBq FDG). Analysis of the registered tracking data shows, that the movement was dominated by a rotation about the scanner z axis of approximately 20 degrees. Images of the uncorrected and corrected data sets are shown in Fig. 2. The uncorrected movement results in a strong blurring of the image. This is significantly improved after application of the movement correction.

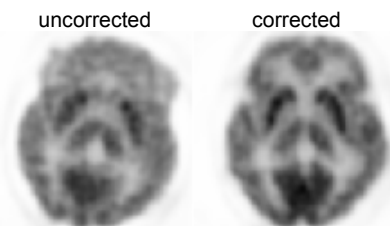


Fig. 2. Images of a test measurement with volunteer patient who was asked to turn the head during PET acquisition. The blurring caused by this motion is clearly reduced after application of the movement correction.

The next step will be to introduce the method in routine operation.

References

- [1] Bloomfield, P. *et al.*, Phys. Med. Biol. 48 (2003) 959.
- [2] Bühler, P. *et al.*, Annual Report 2002, FZR-363, p. 29.

Respiratory Gating for Improved Image Resolution and Tumour Detection in PET Thorax Investigations

U. Just, P. Bühler¹, E. Will, J. van den Hoff¹

¹PET Zentrum Rossendorf and Klinik und Poliklinik für Nuklearmedizin

Respiratory gated patient studies of the thorax were acquired and evaluated by comparing the image data of non gated studies with data sets of selected respiration phases. Significant tumour motions up to 12-14 mm between inhaled and exhaled respiration state were found in 7 of 10 patient image datasets. The reduced motion in gated images provides a better image contrast improving the detection of small tumours.

Introduction

Based on the development of listmode software [1] for the ECAT HR+ scanner (Siemens/CTI) respiratory gated patient studies were acquired. Respiratory gating provides image datasets for defined respiratory phases reducing largely motion effects in thorax acquisitions. The gated image datasets were evaluated for possible improvements on thoracic tumour detection.

Methods

Thorax acquisitions of 10 patients were performed using listmode. The patients respiratory motion was measured with a respiratory belt. A PC equipped with an A/D converter card digitized and recorded the respiration sensors signal. The respiratory motion data was further processed with the listmode software. Taking advantage of variable acquisition parameters available in listmode, gated and static image datasets were created and compared for each measurement. The position and volume of each tumour lesion was determined. In cases where no tumour was available, the position of the heart apex was evaluated. The accumulated activity in tumour volumes was quantified to show possible improvements on the detection of small tumour lesions.

Results

Respiratory gating allows to locate thoracic tumours more precisely. Motions of tumour or heart apex larger than 5 mm caused by respiratory motion were found in 7 of the 10 patient image datasets. Large axial shifts up to 12-14

mm between the inhaled and exhaled respiration phase were detected in close approximation to the diaphragm (Fig. 1).

Gated image datasets showed up to 40 % higher maximum values of the activity distribution in tumour volumes. Additionally the tumour volume derived from a threshold value for the activity concentration was reduced by 15 % - 35 % (for typical tumour volumes of 2 - 4 cm³). Higher maximum activity concentrations and smaller lesion volumes result in increased image contrast as shown in Fig. 2. Especially smaller lesions are differentiated better relative to the surrounding background thus providing an improvement for tumour detection.

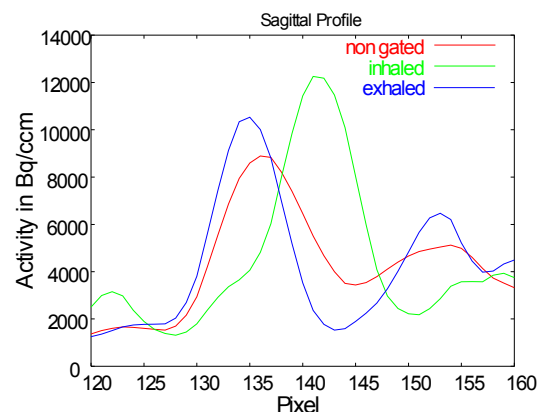


Fig. 2. Axial profile through the centre of a tumour taken from a sagittal slice view. The location and the slope of the tumours activity concentration is shown for a non gated study, the inhaled and exhaled respiratory study.

Reference

[1] Just, U. *et al.*, *Annual Report 2001*, FZR-340, p. 72.

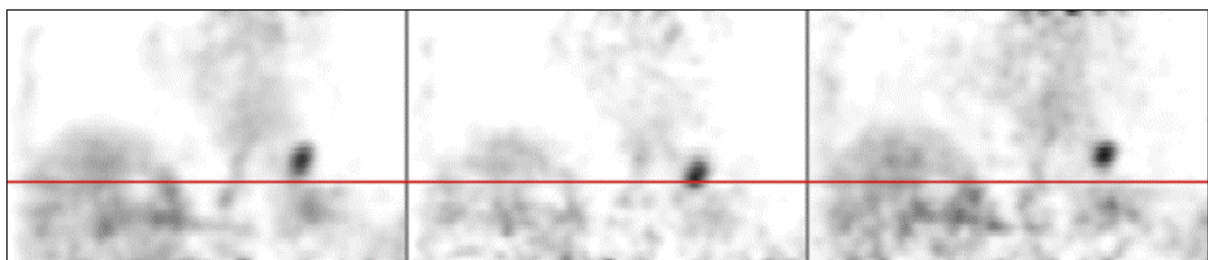


Fig. 1. Coronal views of a thorax acquisition with FDG: Images of a lung tumour close to the diaphragm (from left to right) of a non gated study, the inhaled and the exhaled respiratory phase, respectively.

Inhibition Studies with FMHBG as a New Pattern for Monitoring Gene Expression

M. Grote, St. Noll, B. Noll

*N*¹-Methyl-9-[(3-fluoro-1-hydroxy-2-propoxy)methyl]guanine **1** (FMHBG), a substance which was originally synthesized together with a couple of compounds as potential substrate for Herpes Simplex Virus Thymidine Kinase (HSV-1 TK) [1] showed no characteristics of a substrate but of an inhibitor for HSV-1 TK in cell tests. Additional studies with the isolated enzyme were performed to affirm this preliminary results.

The herpes simplex virus type-1 thymidine kinase gene (HSV-1 tk) is a commonly studied suicide gene for cancer gene therapy. The expressed enzyme HSV-1 TK phosphorylates a broad spectrum of compounds in contrast to its mammalian counterpart. Combined with molecules labelled with positron-emitting isotopes monitoring of the expression of the suicide gene product and its location is possible [2]. One premise for successful monitoring is that the used tracer is a substrate of HSV-1 TK and the phosphorylating rate is proportional to the amount of expressed enzyme. Now, our intention is that an inhibitor of HSV-1 TK can also be used, and an eligible candidate for this purpose is FMHBG **1**, the methylated analogue of FHBG **2**.

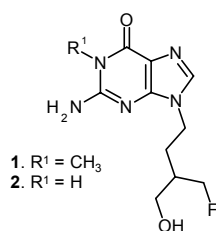


Fig. 1. Structures of FMHBG **1** and FHBG **2**.

A screening test of **1** with HSV-1 TK in presence of ATP and Mg²⁺ showed no monophosphorylated product. However, in transduced MC 38 cells (murine mamma carcinoma) an uptake of [¹⁸F]FMHBG was noted whereas in the presence of thymidine the accumulation was decreased (Fig. 2). This led to the assumption that **1** may be an inhibitor of HSV-1 TK.

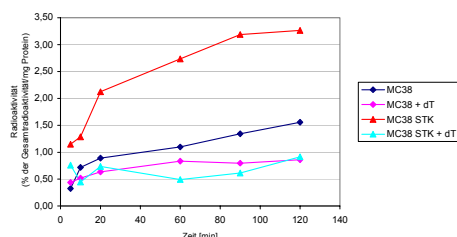


Fig. 2. Cell uptake studies of FMHBG **2**.

Competition experiments with thymidine (dT) and FMHBG **1** analyzed by ion-pair chromatography indicated a decrease of thymidine

monophosphate (TMP) formulation when the concentration of **1** is arised.

To characterize the efficacy of the inhibitor, the K_i values were evaluated. In general, the lower the K_i value, the tighter the binding and hence the more effective is the inhibitor. Initial velocities (V_i) were measured using the DEAE paper method and various concentrations of tritium labelled thymidine in presence of compound **1** and the binding affinity calculated as K_i value using a double-reciprocal plot (Fig. 3) [3].

Reactions were carried out in a final volume of 30 µl containing 50 mM Tris buffer (pH 7.2), 0.25 mM FMHBG, 5 mM ATP, 5 mM MgCl₂ and 1.5 mg/ml BSA and 0.2 ng enzyme; the concentration of [³H]dT varied from 0.2 µM – 2.0 µM in consideration to *Michaelis-Menten* conditions for initial velocity measurements [4].

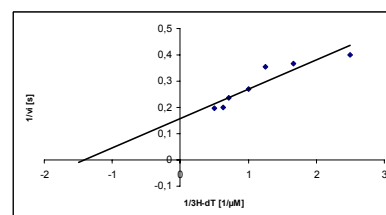


Fig. 3. Calculation of binding affinity using a double-reciprocal plot.

The binding affinity (K_i) of FMHBG was determined with 0.1 mM and this result implied that the inhibitory strength is comparable with structural related purine derivatives. Further investigations whether this compound in radiolabelled form is capable for monitoring gene expression are in progress.

The authors thank Prof. L. Scapozza, ETH Zurich, for providing the HSV-1 TK and helpful discussions.

References

- [1] Noll, St. *et al.*, *Annual Report 2000*, FZR-312, pp. 68-73.
- [2] Wiebe, L. *et al.*, *Curr. Pharm. Res.* (2001) 1893-1906.
- [3] Eisenthal, R., Danson, M. J., *Enzyme Assays – A practical Approach* (1992), IRL Press, Oxford.
- [4] Pospisil, P. *et al.*, *Helv. Chim. Acta* 85 (2002) 3237-3250.

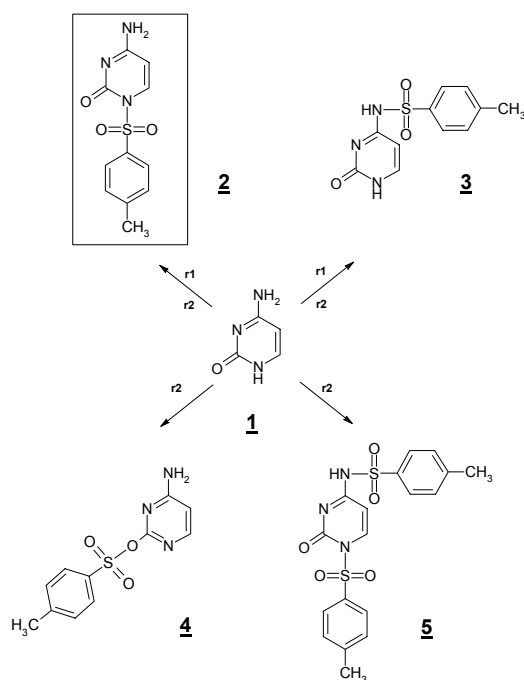
¹⁸F-Labeling of Cytosine at the 2-Position

B. Noll, St. Noll

4-Amino-2-(p-toluenesulphonyloxy)-pyrimidine was radiolabelled with a $K[^{18}F]F/kryptofix\ 2.2.2^{TM}$ complex in acetonitrile to obtain the 4-amino-2-[¹⁸F]fluoropyrimidine. The identity of the labelling product was proved by mass spectrometry.

For monitoring gene therapy with substrates of cytosine deaminase several methods to label cytosine with fluorine-18 have been described [1]. The labelling was carried out either from elemental [¹⁸F]F₂ in glacial acetic acid or [¹⁸F]-acetylhypofluorite at the 5-position of cytosine [2, 3]. This labelling procedure starting from elemental [¹⁸F]F₂ is accompanied by arising several by-products and lowering the radiochemical yield.

We found out an other method to label cytosine with a $K[^{18}F]F/kryptofix\ 2.2.2^{TM}$ complex in acetonitrile. Studying the tosylation of cytosine with p-toluenesulphonyl chloride both in pyridine (r1) and acetonitrile/triethyl amine (r2) several tosylation products were obtained and are described following:

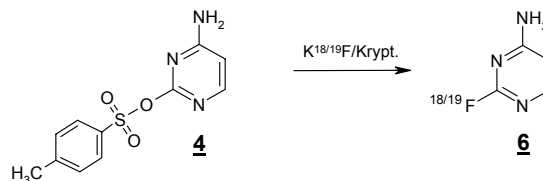


In dependence on the reaction conditions four products were obtained. According to the paths r1 and r2 1-(p-toluenesulphonyl)-cytosine **2** is the main product (80 %) and N⁴-(p-toluenesulphonyl)-cytosine **3** (5-10 %) the by-product. Additional by-products are only formed according to r2 as 4-amino-2-(p-toluenesulphonyloxy)-pyrimidine **4** (10 %) and 1-(p-toluenesulphonyl)-N⁴-(p-toluenesulphonyl)-cytosine **5** (5 %). The products were purified by column chromatography on silica gel and dichloromethane/methanol as eluent. All syn-

thesized substances were characterized by elemental analysis and ¹H NMR spectroscopy. Compound **4** was used as precursor to label cytosine at the 2-position.

¹⁸F-Labeling

A [¹⁸F]KF/K2.2.2 complex was received after azeotropic distillation with acetonitrile, kryptofix 2.2.2 and potassium carbonate. This complex was allowed to react with the precursor **4** (5 mg) dissolved in acetonitrile for 25 min at 160 °C. Then, the whole reaction mixture was given over a silica Sep-Pak cartridge and eluted with dichloromethane/methanol (85/15 v/v). The cartridge held back K₂CO₃, kryptand and non-converted [¹⁸F]KF whereas the desired ¹⁸F-labelled tracer (**6**) was eluted.



Comparison of non-eluted to eluted radioactivity led to the labelling yield amounted to about 55 % (50 min reaction time). HPLC analysis (Phenomenex C-18, PBS/MeCN 80:20) of the reaction mixture after Si Sep-Pak elution yielded a radiochemical purity > 98 %. The "carrier-added" preparation carried out by adding 10 µl 0.1 M KF solution to the distillation vessel was also purified as described for the "nca"-preparation. The isolated fraction containing the expected ¹⁸F-tracer **6** was analyzed by mass spectrometry. The ESI⁺ spectrum showed one peak at m/z 114 (M+H) corresponding to the mol peak of component **6** with M = 113. The occurrence of this mol peak proves the existence of the ¹⁸F-labelled cytosine derivative at the 2-position. It is expected that this tracer will be accepted as substrate of the cytosine deaminase and is a potential tracer for monitoring gene therapy.

References

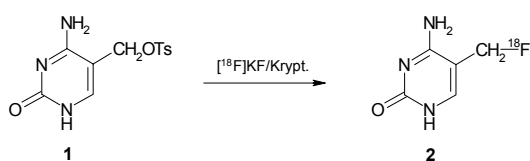
- [1] Haberkorn, U. *et al.*, J. Nucl. Med. 37 (1996) 87-94.
- [2] Shiue, C.-Y. *et al.*, J. Labelled Compd. Radiopharm. XXI (1984) 865-873.
- [3] Visser, G. W. M. *et al.*, Nucl. Med. Commun. 6 (1985) 455-459.

The Microwave-Assisted Synthesis of 5-Hydroxymethylcytosine

B. Noll, B. Grosse, St. Noll

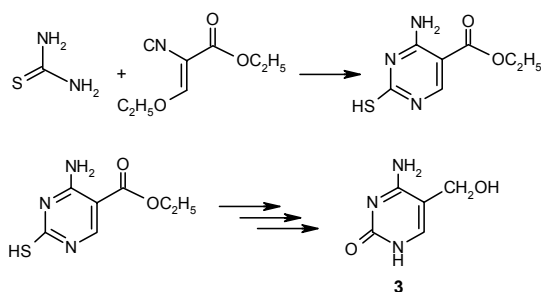
A time-reduced one-step synthesis of 5-hydroxymethylcytosine using a microwave equipment and the following purification is described.

Suicide gene therapy tries to make use of the bacterial cytosine deaminase / 5-fluorocytosine system. Therefore Escherichia coli (CD) gene in transfected cancer cells expresses the cytosine deaminase. Our intention consists in developing new ^{18}F -labelled tracers which are substrates of the CD for monitoring gene therapy and will be trapped in the cells. One approach is the labelling of 5-p-toluenesulphonyloxymethylcytosine **1** with a $[^{18}\text{F}]\text{KF}$ /kryptofix complex yielding 5- $[^{18}\text{F}]$ fluoromethylcytosine **2**.



The following enzymatic hydrolysis results in 5- $[^{18}\text{F}]$ fluoromethyluracil and should be involved as thymine analogous in DNA synthesis.

1 can be prepared by tosylation of 5-hydroxymethylcytosine **3** available by a conventional four-step synthesis [1].



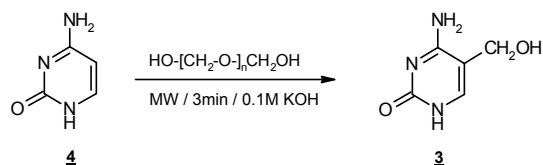
In order to reduce the time exposure of the synthesis we used a less time-consuming approach assisted by a microwave oven. Microwave enhanced reactions becomes more and more commonly used in the synthesis of complicated organic compounds and are often more time-serving than the conventional multi-level syntheses. They are uncomplicated and their realization is very simple.

We adapted a method for the synthesis of 5-hydroxymethylcytosine **3** starting from cytosine **4** and paraformaldehyde in an one-step reaction described by Adel et al. [2] to our microwave equipment MLS ($\mu\text{Chemist}$).

The synthesis was optimized by variation of the amounts of cytosine **4** and paraformaldehyde,

the amount of potassium hydroxide and the irradiation time and energy.

Our optimized synthesis was carried out by heating an aqueous solution of 555 mg (5 mmole) cytosine **4**, 200 mg paraformaldehyde and 5.0 ml of a 0.1 M potassium hydroxide solution in a microwave oven. The solution was irradiated in a special bottle for 3 min at 1000 Watt.



After irradiation the solution was neutralized and then analyzed by HPLC on a C-18 column (Phenomenex aqua 250 x 4 mm, flow rate 1.0 ml/min) and 0,07 M PBS (pH 7.0) as eluent. The yield of 5-hydroxymethylcytosine **3** amounts to 40 %. Besides **3** unreacted cytosine (about 50 %), uracil and 5-hydroxymethyluracil were detected as by-products in different ratios.

Cytosine **4** and its 5-hydroxymethyl derivative **3** were separated by treatment of the crude solution with a cation exchange resin in the H^+ -form (DOWEX W50X8). Both compounds remained on the resin and were eluted with 2.5 % ammonia and subsequently separated by column chromatography on Sephadex G10 and water as eluent.

The final product 5-hydroxymethylcytosine **3** was identified by ^1H NMR and elemental analysis.

^1H NMR (DMSO- d_6 400 MHz): $\delta = 4.13\text{-}4.14$ (d, 2H, CH_2), 4.90-4.93 (t, 1H, OH), 6.44-7.14 (2H, NH_2), 7.24 (s, 1H, H_6), 10.36 (s, 1H, NH).

Our described optimized synthesis in the microwave field yields an efficient and easy method for the synthesis of 5-hydroxymethylcytosine **3**.

References

- [1] Ulbricht, T. L. V. *et al.*, Contribution from the Dep. of Chem. Univ. of Notre Dame 21 (1956) 567-570.
- [2] Adel, A.-H. *et al.*, Synlett 12 (2002) 2043-2044.

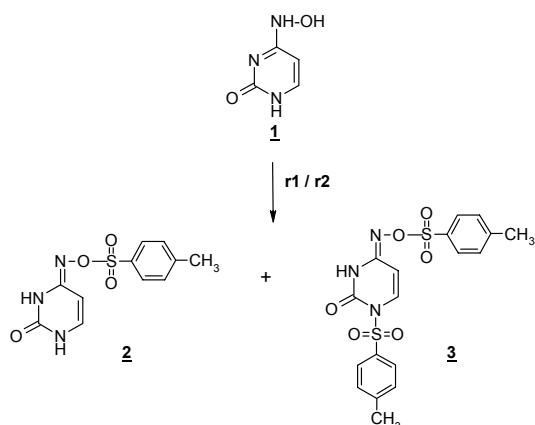
Z/E-Isomerism of N⁴-(p-Toluenesulphonyloxy)cytosine Derivatives

St. Noll, B. Noll, H. Stephan, W. Kraus¹, M. Findeisen², L. Hennig², K. Yoshizuka³
¹BAM Berlin, ²Universität Leipzig, ³University of Kitakyushu, Japan

Tosylation of N⁴-hydroxycytosine results in dependence on the reaction conditions both in the formation of the N⁴-(p-toluenesulphonyloxy)cytosine and the two-fold tosylated 1-(p-toluenesulphonyl)-N⁴-(p-toluenesulphonyloxy)cytosine. The N⁴-(p-toluenesulphonyloxy)cytosine crystallizes as a dimeric Z-isomer. Both NMR studies and DFT calculations point to the formation of Z/E-isomers.

Monitoring cytosine deaminase expression should be possible by using ¹⁸F-labelled cytosine derivatives [1]. As part of an ongoing development of a ¹⁸F-labelled cytosine derivative systematic investigations were carried out to introduce leaving groups preferably the tosyl group. N⁴-hydroxycytosine was tosylated and the reaction products were analyzed.

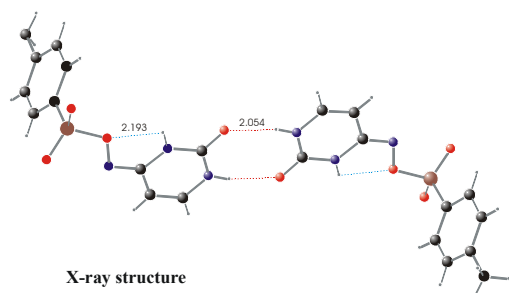
The introduction of the p-toluenesulphonyl group into N⁴-hydroxycytosine **1** was carried out with p-toluenesulphonyl chloride in a five-fold molar excess both in pyridine (route 1, **r1**) and acetonitrile/triethyl amine (route 2, **r2**).



Both approaches resulted in N⁴-(p-toluenesulphonyloxy)cytosine **2** and 1-(p-toluenesulphonyl)-N⁴-(p-toluenesulphonyloxy)cytosine **3** but in different quantities.

By using approach **r2** N⁴-hydroxy-1-(p-toluenesulphonyl)cytosine was additionally formed.

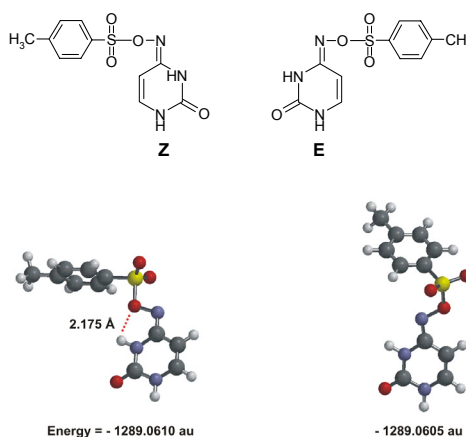
N⁴-(p-toluenesulphonyloxy)cytosine **2** was chromatographically purified on silica gel with dichloromethane / methanol 50:1 as eluent. **2** crystallized from ethanol as colourless plates. The X-ray structure shows a dimer of **2** forming intermolecular hydrogen bonds between N¹



X-ray structure

and C²=O (2.054 Å) of each molecule. Additionally an intramolecular hydrogen bond is formed between N³ and the N⁴-oxy group (2.193 Å) resulting in the Z configuration of this derivative.

NMR measurements in d⁶-DMSO point to the formation of two isomeric structures having a molecular ratio of about 2:3. A dynamic hydrogen exchange between both structures was proven by 2D-NOESY measurements. In contradiction to other crosspeaks, those of the olefinic protons at 7.1/7.0 ppm and 5.8/5.4 ppm show the same phase like the diagonal peaks. These could be interpreted as cross peaks due to chemical exchange by the formation of Z/E-isomers. This finding is also corroborated by DFT calculations (*Gaussian 98*, BLYP, 6-31G). Both isomers calculated have almost the same energy making the simultaneous formation plausible.



DFT calculations

Comparing the NMR-spectra of the different tosylation products of N⁴-hydroxycytosine with the corresponding cytosine derivatives results also in the conclusion: Only the tosylation products of N⁴-hydroxycytosine show the typical pattern caused by the Z/E-isomers.

Reference

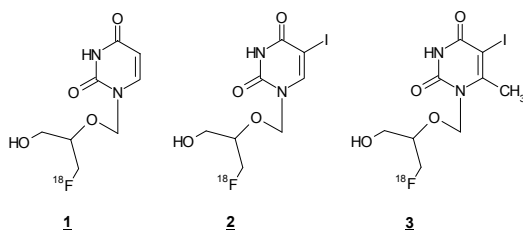
[1] Grote, M. *et al.*, *Annual Report 2002*, FZR-363, p. 21.

Syntheses of Novel Acyclic Pyrimidine Nucleosides as Precursors for ^{18}F -Labelling

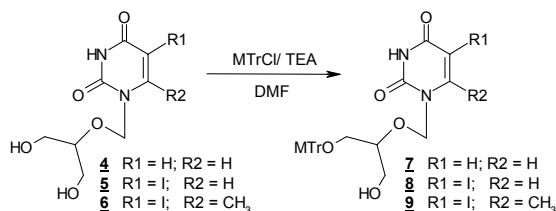
B. Noll, St. Noll

The synthesis of three new uracil-based acyclic nucleoside precursors for monitoring gene expression of herpes simplex virus type 1 thymidine kinase gene (HSV1-tk) is described.

Three new precursors for ^{18}F -labelling have been synthesized to get new potential substrates **1**, **2** and **3** for monitoring gene expression of herpes simplex virus type 1 thymidine kinase gene (HSV1-tk).



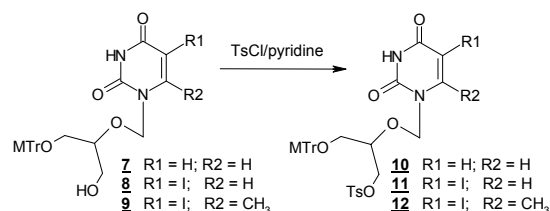
Our strategy to label the nucleosides at the acyclic chain with ^{18}F requires the protection of the opposite hydroxyl group. Therefore 1-[(1,3-dihydroxy-2-propoxy)methyl]uracil (Acyclur **4**), 5-iodo-1-[(1,3-dihydroxy-2-propoxy)methyl]uracil (Iodacyclur **5**) and 5-iodo-6-methyl-1-[(1,3-dihydroxy-2-propoxy)methyl]uracil (Iodmetacyclur **6**) were treated with p-anisylchloro-diphenylmethane in dimethyl formamide. Triethylamine and traces of dimethylamino pyridine were added and the mixture was allowed to react for 2 hours at room temperature. Thus 1-[[1-(p-anisyl-diphenyl-methoxy)-3-hydroxy-2-propoxy]methyl]uracil **7**, 5-iodo-1-[[1-(p-anisyl-diphenyl-methoxy)-3-hydroxy-2-propoxy]methyl]uracil **8** and 5-iodo-6-methyl-1-[[1-(p-anisyl-diphenyl-methoxy)-3-hydroxy-2-propoxy]methyl]uracil **9** were formed in a yield of about 65 %.



The ditritylated compounds being occurred as by-products in the syntheses were separated by column chromatography on silica gel and dichloromethane/methanol 25:1 as eluent. The precursors 1-[[1-(p-anisyl-diphenyl-methoxy)-3-(p-toluenesulphonyloxy)-2-propoxy]methyl]uracil **10**, 5-iodo-1-[[1-(p-anisyl-diphenyl-methoxy)-3-(p-toluenesulphonyloxy)-2-propoxy]methyl]uracil **11** and 5-iodo-6-methyl-1-[[1-(p-anisyl-diphenyl-methoxy)-3-(p-toluenesulphonyloxy)-2-propoxy]methyl]uracil **12** were obtained with 53 % from **7**, **8** and **9** by introduction of an eligible leaving group for the subsequent fluorination.

Tosyl chloride in anhydrous pyridine reacted with the methoxytrityl protected acyclic nucleosides for 2 hours at room temperature.

Tosyl chloride in anhydrous pyridine reacted with the methoxytrityl protected acyclic nucleosides for 2 hours at room temperature.



The tosylation reaction is accompanied by the partial splitting off the trityl protecting group forming the by-products 1-[(1-hydroxy-3-(p-toluenesulphonyloxy)-2-propoxy)-methyl]uracil **13**, 5-iodo-1-[(1-hydroxy-3-(p-toluenesulphonyloxy)-2-propoxy)methyl]uracil **14** and 5-iodo-6-methyl-1-[(1-hydroxy-3-(p-toluenesulphonyloxy)-2-propoxy)methyl]uracil **15**.

We did not succeed in the re-protection of the tosylated by-products because of an unrequested chlorination reaction.

The precursors were separated from the by-products and purified by column chromatography on silica gel and dichloromethane/methanol 20:1 as eluent.

Orientating tests were carried out to label the precursors with a ^{18}F KF/kryptofix complex. **1**, **2** and **3** were obtained in a radiochemical yield of about 12 %. Fluorination of the unprotected precursors **13**, **14** and **15** resulted also in **1**, **2** and **3**, but with diminished yield (about 7 %) [1].

All synthesized substances were identified by elemental analysis and ^1H NMR spectroscopy. Fluorine-19 reference compounds were also determined by ^{19}F NMR.

Reference

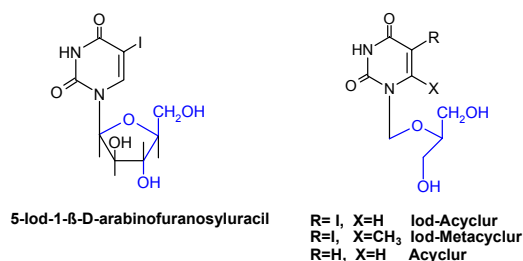
[1] Grote, M., *PhD Thesis* (2002), TU Dresden.

Syntheses of Novel Acyclic Pyrimidine Nucleosides as Potential Substrates of the HSV1-TK

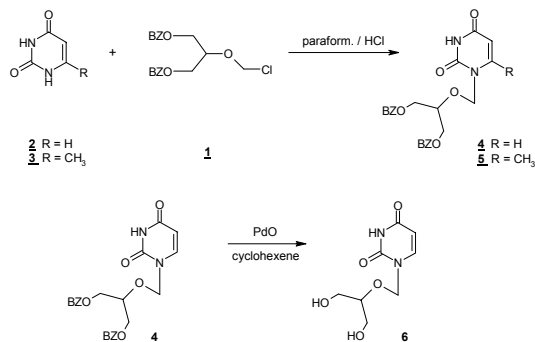
St. Noll, B. Noll

Syntheses of three novel acyclic nucleosides as potential substrates of HSV1-TK are described which are derived from the cyclic 5-iodo-1-β-D-arabinofuranosyluracil.

Substrates that have been studied to date as reporter probes for HSV1-TK can be classified into two main classes of compounds: pyrimidine nucleoside derivatives and acyclo-guanosine derivatives. The former category of reporter probes includes 5-iodo-1-β-D-arabinofuranosyluracil and its 2'-fluorine derivative FIAU as most established ¹²⁵I-labelled PET-tracer for monitoring gene expression [1]. Our aim was to prepare corresponding acyclic derivatives as potential substrates of HSV1-TK in conformance with the acyclic guanosine derivatives FHPG or FHBG.

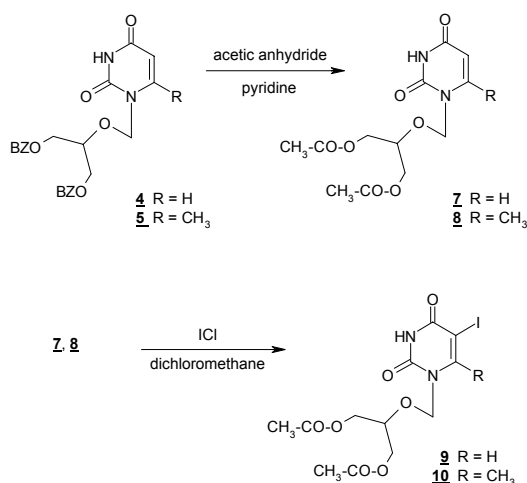


We used 1,3-dichloro-2-propanol, sodium hydride and benzyl alcohol to produce 1,3-dibenzoyloxy-2-propanol, which was added to 1,2-dichloroethane followed by paraformaldehyde and hydrogen chloride gas to obtain 1,3-dibenzoyloxy-2-chloro-methoxypropane **1**. Then the bases uracil **2** and 6-methyluracil **3** were coupled to **1** in dichloromethane with tetrabutylammonium iodide to produce 1-[(1,3-dibenzoyloxy-2-propoxy)methyl]uracil **4** and 6-methyl-1-[(1,3-dibenzoyloxy-2-propoxy)methyl]uracil **5**. Treatment of **4** with palladium oxide and cyclohexene split off the benzyl protection groups yielding 1-[(1,3-dihydroxy-2-propoxy)methyl]uracil (Acyclur **6**).

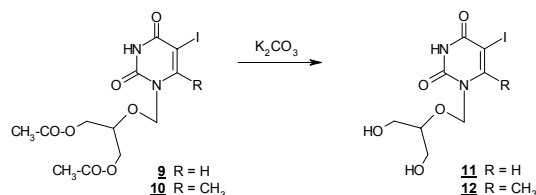


To synthesize the iodine compounds the protection groups at **4** and **5** were replaced with

acetyl groups by treatment with acetic anhydride in pyridine yielding 1-[(1,3-diacetoxy-2-propoxy)methyl]uracil **7** and 6-methyl-1-[(1,3-diacetoxy-2-propoxy)methyl]uracil **8**, followed by reaction with iodine monochloride in dichloromethane to get 5-iodo-1-[(1,3-diacetoxy-2-propoxy)methyl]uracil **9** and 5-iodo-6-methyl-1-[(1,3-diacetoxy-2-propoxy)methyl]uracil **10**.



Subsequently the protection groups at **9** and **10** were split off by potassium carbonate yielding 5-iodo-1-[(1,3-dihydroxy-2-propoxy)methyl]uracil (Iodacyclur **11**) and 5-iodo-6-methyl-1-[(1,3-dihydroxy-2-propoxy)methyl]uracil (Iodmetacyclur **12**).



In the following steps the acyclic pyrimidine nucleosides will be labelled with fluorine-18 and tested concerning their uptake into HSV1-TK expressing cell cultures. The preparation of the corresponding precursors is described in [2].

References

- [1] Brust, P. *et al.*, Eur. J. Nucl. Med. 28 (2001) 721-729.
- [2] Noll, B. *et al.*, *this report*, p. 19.

Neurotensin(8-13) Labelled with ^{99m}Tc Using the '4+1' Mixed-Ligand Chelate System – Part 1: Chemistry

J.-U. Kuenstler, S. Seifert, H.-J. Pietzsch, H. Spies

The isocyanide group and a rhenium complex of the '4+1' mixed-ligand type were linked to the neurotensin derivative NT(8-13) as well as to Arg-Arg and Arg using active esters. ^{99m}Tc complexes of isocyanide-functionalized NT(8-13), Arg-Arg and Arg were obtained in yields of about 80 %.

Introduction

Radiolabelled neurotensin (NT) analogues are of interest for targeting neuro-endocrine tumours. ^{99m}Tc -labelling of stabilised NT analogues via the tricarbonyl concept were already studied extensively [1].

Here we describe the synthesis and characterization of ^{99m}Tc and $^{185/187}\text{Re}$ labelled NT(8-13), Arg-Arg and Arg using the '4+1' mixed-ligand chelate system, where technetium(III) and rhenium(III) are coordinated by the tripodal 2,2',2''-nitritoltris(ethanethiol) and a monodentate isocyanide [2].

Results and Discussion

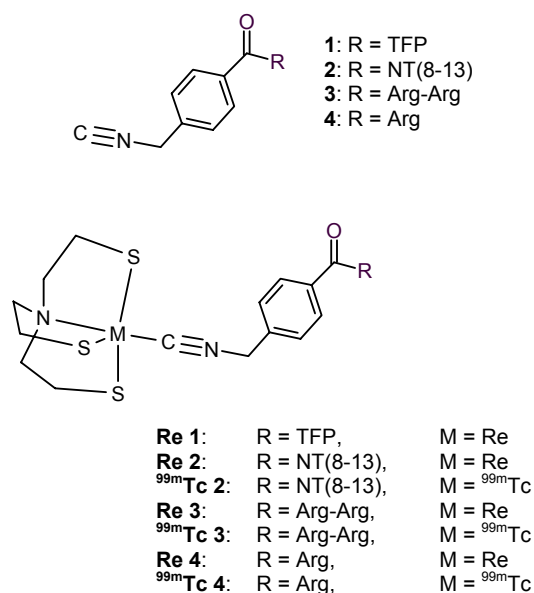


Fig. 1. Compounds prepared in this study.

NT(8-13) was reacted with the tetrafluorophenyl esters **1** and **Re 1** in DMF/Et₃N to give **2** and **Re 2**. Arg-Arg and Arg were reacted with **1** and **Re 1** in DMF/H₂O/Et₃N to get **3**, **4**, **Re 3** and **Re 4** (Fig. 1). The coupling had to be performed in organic or organic/aqueous media because of the lipophilicity of the active esters. The crude products were purified by RP-HPLC using MeCN/H₂O/0.1%TFA as eluent and then lyophilised (yield: 40 – 50 %). Immediately after semipreparative HPLC of **2**, **3** and **4** the fractions were neutralised. In acidic media the

free isocyanide group is unstable and forms the N-formyl derivative. The derivative was also detected in samples **2**, **3**, **4** by ESI-MS but its content was found to be small.

The obtained compounds were characterised by RP-HPLC and ESI-MS: HPLC (Jupiter (250 x 4.6 mm), 1 ml/min, 20 % to 80 % A in 20 min; A = MeCN/0.1% THF, B = H₂O/0.1 % TFA; R_t [min]: 10.1 (**2**), 14.9 (**Re 2**), 4.9 (**3**), 12.5 (**Re 3**), 5.6 (**4**), 13.8 (**Re 4**); MS: m/z calc. (found): 961 (961) for [**2**]⁺; 1341, 1343 (1341, 1343) for [**Re 2**]⁺; 474 (474) for [**3**]⁺; 854, 856 (854, 856) for [**Re 3**]⁺; 318 (318) for [**4** + H]⁺; 698, 700 (698, 700) for [**Re 4** + H]⁺; two peaks according to ^{185}Re or ^{187}Re , respectively.

^{99m}Tc -labelling was performed in a two-step procedure according to [3]. ^{99m}Tc -EDTA (100 to 500 MBq) was formed with a yield of about 95 %. For the following ligand exchange 0.5 mg 2,2',2''-nitritoltris(ethanethiol) and 50 µg **2**, **3** or **4** were added. The exchange reaction was completed within 30 min at 50 °C or 2 h at RT (yield: about 80 %). ^{99m}Tc **2**, ^{99m}Tc **3** and ^{99m}Tc **4** were obtained after semipreparative RP-HPLC. Radiochemical purity exceeded 95% as determined by HPLC (after co-injection of the analogous ^{99m}Tc and **Re 2** compounds, practically identical R_t values were observed) and TLC (RP-18 Merck, MeCN/H₂O/TFA (4/1/0.01, v/v/v), R_f ≈ 0.8; Silufol/acetone, R_f ≈ 0 – 0.1).

Basic stability studies of ^{99m}Tc **2** are described in [4]. ^{99m}Tc **3** and ^{99m}Tc **4** were synthesized to get reference compounds for catabolism studies.

Experiments show that the '4+1' mixed-ligand system is suitable for binding technetium and rhenium to peptides.

References

- [1] Schibli, R. *et al.*, Eur. J. Nucl. Med. 29 (2002) 1529-1542.
- [2] Pietzsch, H.-J. *et al.*, Bioconjugate Chem. 12 (2001) 538-544.
- [3] Seifert, S. *et al.*, Annual Report 2001, FZR-340, p. 49.
- [4] Pawelke, B. *et al.*, this report, p. 22.

Neurotensin(8-13) Labelled with ^{99m}Tc Using the '4+1' Mixed-Ligand Chelate System – Part 2: Basic Stability Considerations

B. Pawelke, J.-U. Kuenstler, S. Seifert, R. Bergmann, H.-J. Pietzsch, H. Spies

^{99m}Tc -NT(8-13) labelled via the '4+1' mixed-ligand concept [$^{99m}\text{Tc}(\text{NS}_3)\text{CN-NT}(8-13)$] was quickly catabolised after injection in rats. [$^{99m}\text{Tc}(\text{NS}_3)\text{CN-Arg}$] was the main catabolite. However, the chelate unit and the bond between the complex and the peptide exhibited high catabolic stability. The affinity of the labelled NT(8-13) towards the neurotensin receptor was decreased by the factor of about 15 compared with native NT(8-13).

Introduction

In this report, we present stability and receptor affinity studies of ^{99m}Tc 2.

The compounds ^{99m}Tc 2 [$^{99m}\text{Tc}(\text{NS}_3)\text{CN-NT}(8-13)$], ^{99m}Tc 3 [$^{99m}\text{Tc}(\text{NS}_3)\text{CN-Arg-Arg}$], ^{99m}Tc 4 [$^{99m}\text{Tc}(\text{NS}_3)\text{CN-Arg}$] and **Re 4** [$\text{Re}(\text{NS}_3)\text{CN-NT}(8-13)$] were prepared according to [1]. ^{99m}Tc 3, ^{99m}Tc 4 served as references for catabolism studies of ^{99m}Tc 2. The neurotensin receptor affinity was determined using **Re 4**.

Results and Discussion

^{99m}Tc 2 was very quickly catabolised after injection in rats as well as after in vitro incubation in blood or plasma. Only two catabolites were observed. The main catabolite could be identified as ^{99m}Tc 4 (Figs. 1, 2; Table 1). The catabolites were formed by proteolysis of the monodentate ligand.

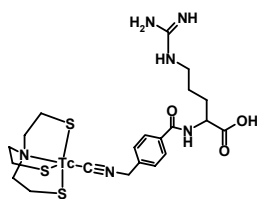


Fig. 1. Main catabolite ^{99m}Tc 4.

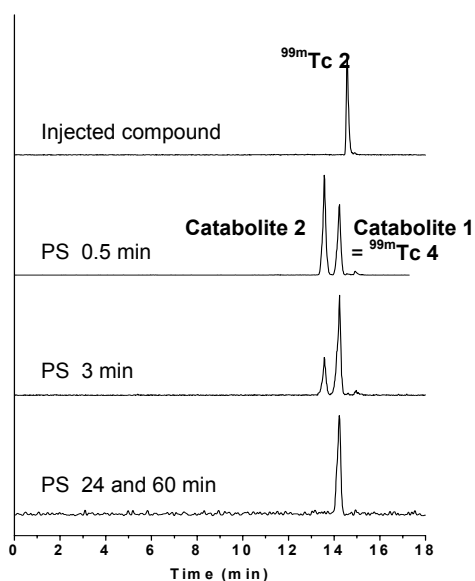


Fig. 2. Radiochromatograms (HPLC, RP-18, MeCN/H₂O/TFA) of catabolism studies of ^{99m}Tc 2; plasma samples (PS) at various times after i.v. injection in rats.

Table 1. *In vitro* stability of ^{99m}Tc 2 in rat blood and plasma analysed by HPLC (RP-18, MeCN/H₂O/TFA).

Catabolite	Blood, 120 min	Plasma, 120 min
Catabolite 1	85 %	90 %
Catabolite 2	13 %	8 %

The '4+1' chelate unit and the amide bond between the complex and the peptide or amino acid exhibited high catabolic stability. Subsequent studies had to be performed using stabilised peptides. The results are consistent with early stability studies showing that no trans-chelating reactions of the used complex type occurs [2].

Since ^{99m}Tc 4 exhibited a high catabolic stability, its biodistribution in rats was determined. The radioactivity was selectively taken up by the liver and then excreted into the intestine (Table 2).

Table 2. Biodistribution of ^{99m}Tc 4 in rats (% ID/g tissue, mean \pm S.D., n = 4) 5 and 120 min after i.v. injection.

Organ	5 min	120 min
Brain	< 0.1	< 0.1
Pancreas	< 0.1	< 0.1
Spleen	< 0.1	< 0.1
Kidney	3.0 \pm 0.4	1.2 \pm 0.3
Hart	< 0,1	< 0,1
Lungs	0.42 \pm 0.06	0.14 \pm 0.04
Thymus	< 0.1	< 0.1
Thyroid	< 0.1	< 0.1
Liver	72.0 \pm 5.1	16.8 \pm 5.0
Femur	0.11 \pm 0.03	< 0.1
Testicle	0.10 \pm 0.03	< 0.1
Intestine	19.3 \pm 4.5	80.1 \pm 6.1
Stomach	4.3 \pm 2.4	1.2 \pm 0.9

The affinity of **Re 4** towards the neurotensin receptor of HT29 cells (colorectal carcinoma cell line) was determined. The obtained IC₅₀ value of 23 \pm 8 nM indicates an approximately 15 times lowered affinity of **Re 4** compared to native NT(8-13).

Since the amide bond between the chelate moiety and the peptide is catabolically stable, the '4+1' mixed-ligand complexes are suitable for ^{99m}Tc -labelling of peptides.

References

- [1] Kuenstler, J.-U. *et al.*, *this report*, p. 21.
- [2] Pietzsch, H.-J. *et al.*, *Bioconjugate Chem.* 12 (2001) 538-544.

^{99m}Tc-Cyctectrene Complexes – Chemical Structure and Biobehaviour

Part 1: Chemical Characterisation of Tc and Re Complexes

M. Saidi¹, S. Seifert, M. Kretzschmar, R. Bergmann, H.-J. Pietzsch
¹Centre National des Sciences et Technologies Nucleaires, Tunis Carthage, Tunisia

Technetium and rhenium tricarbonyl complexes with a derivatised cyclopentadienyl ligand were prepared starting from pertechnetate and a ferrocene ligand as well as the tricarbonyl precursor complexes [^{99m}Tc(CO)₃(H₂O)₃]⁺ and [Re(CO)₃Br₃]²⁻. Their chemical identity was confirmed by chromatographic methods and electron spray mass spectrometry.

Introduction

A high receptor-affine ^{99m}Tc complex (cyctectrene II) prepared from the ferrocene complex N-(isopropyl)-piperidino-4[bis(pentahaptocyclopentadienyl)iron]-carboxylate was described in the *Annual Report 2002* of our institute [1]. The labelling method involved reaction of the ferrocene ligand with pertechnetate in the presence of Mn(CO)₅Br in dimethyl formamide at 150 °C for 1 h in an oil bath [2]. The proposed structure of the ^{99m}Tc cyctectrene complexes is given in Fig. 1.

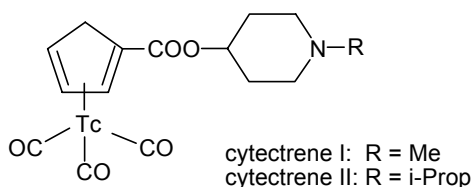


Fig. 1. Proposed structure of cyctectrene complexes

The goal of this work was to elucidate the structure of such kinds of complexes. For that reason, carrier added (c.a.) technetium preparations following the above mentioned preparation route and non carrier added (n.c.a.) preparations as well as cold rhenium preparations using the IsoLink carbonyl kit and the precursor complex (NEt₄)₂[Re(CO)₃Br₃] were performed with the methyl derivative of the ferrocene ligand. The chromatographic behaviour of preparation products was compared and electron spray mass spectrometry (ESI-MS) analyses were carried out to determine the composition of final products.

Results and Discussion

The preparation of the cyctectrene I complex following the method of Wenzel [2] leads to yields between 70 and 80 % determined by TLC [Silufol/ether/triethylamine (95/5), R_f ~ 0.5]. In HPLC, the complex is eluted at about 9 min (PRP-1 column (250 x 4.1 mm), acetonitrile/0.1 %TFA (A)//water/0.1 % TFA (B); gradient elution in 5 min from 20 % A to 50 % A, flow rate: 1.0 ml/min). It is possible to prepare the c.a. ^{99/99m}Tc complex in similar yields adding 10⁻⁷ mol ⁹⁹TcO₄⁻ to the reaction mixture. That allows to perform ESI-MS analyses of

such a preparation. The spectrum shows the expected molecular mass of 390 (Fig. 2).

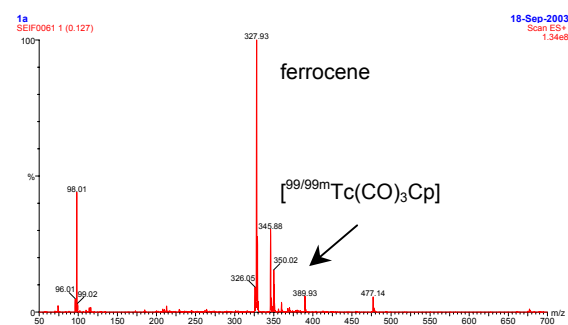


Fig. 2. ESI-MS of the c.a. preparation

If the tricarbonyl complex is really formed under this reaction conditions, the same result should be observed, when the complex is prepared from the precursor complex [^{99m}Tc(CO)₃(H₂O)₃]⁺ using a tricarbonyl kit. In fact, a comparable preparation is obtained following the reaction of the precursor complex in acidic solution with 1.0 mg of the ferrocene ligand dissolved in DMF for 1 h at 150 °C. In accordance with this result, the reaction of the rhenium tricarbonyl complex with the ferrocene ligand also leads to the tricarbonyl cyclopentadienyl complex as demonstrated by the mass spectrum in Fig. 3 (m/z = 476/478).

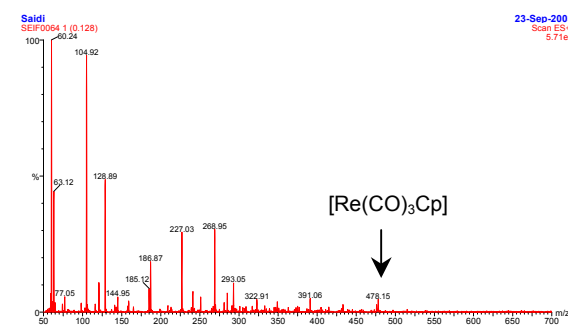


Fig. 3. ESI-MS of the ^{185/187}Re preparation

References

- [1] Kretzschmar, M. *et al.*, *Annual Report 2002*, FZR-363, p. 53.
- [2] Saidi, M. *et al.*, *J. Labelled Compd. Radiopharm.* 44 (2001) 603-618.

^{99m}Tc-Cytectrene Complexes – Chemical Structure and Biobehaviour

Part 2: Biological Characterisation

M. Saidi¹, M. Kretzschmar, R. Bergmann, S. Seifert, H.-J. Pietzsch
¹Centre National des Sciences et Technologies Nucleaires, Tunis Carthage, Tunisia

The biodistribution of cytectrene I and II in Wistar rats was studied. Both compounds show high uptake in the brain and fast blood clearance. The pattern of regional distribution in the brain demonstrated in autoradiographic studies indicates binding to the 5-HT_{1A} and α₁ adrenergic receptors.

Introduction

The wide interest in the 5-HT_{1A} receptor at present is due to its implicated role in several major neuropsychiatric disorders such as depression, eating disorders or anxiety. For the diagnosis of these pathophysiological processes it is important to develop radioligands for the binding on the 5-HT_{1A} receptor in order to allow brain imaging. After confirmation of the composition of the cytectrene complexes described in [1] their biodistribution in Wistar rats was studied. Additionally, the brain uptake of cytectrene I was investigated autoradiographically and compared with that of cytectrene II which was studied in the past [2].

Results and Discussion

The ^{99m}Tc cytectrene complexes penetrate the blood-brain barrier and accumulate strongly in the brain with fast blood clearance.

Table 1. Biodistribution of cytectrene I in selected rat organs (mean ± SD; n = 4).

Time p.i. [min]	5	60
	%ID/g organ	
Blood	0.30±0.04	0.17±0.72
front. Cortex	6.15±1.20	1.46±0.34
Cerebellum	4.38±1.08	1.61±0.37
Striatum	5.28±1.08	1.33±0.37
Hippocampus	5.41±1.49	1.63±0.53
Brown fat	3.25±0.17	0.80±0.21
Skin & hair	1.05±0.20	0.72±0.49
Brain	5.22±1.17	1.51±1.26
Pancreas	4.89±1.01	3.75±1.34
Spleen	1.35±0.28	1.34±0.26
Adrenals	5.27±0.94	1.27±4.48
Kidneys	8.26±1.38	9.53±4.78
Fat	1.87±1.21	0.71±0.17
Muscle	1.02±0.14	0.48±0.10
Heart	1.71±0.28	0.44±1.12
Lungs	7.73±1.29	2.29±0.80
Thymus	2.29±0.32	1.20±0.26
Harderian glands	3.58±0.87	3.90±2.92
Liver	4.26±1.19	9.27±4.61
Femur	1.13±0.03	0.66±0.26
Testes	1.03±0.12	1.08±0.59

Cytectrene I is eliminated through the liver and kidneys (Fig. 1).

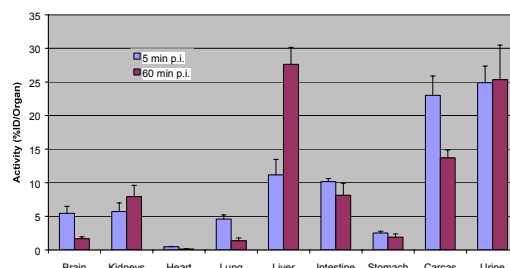


Fig. 1. Biodistribution and elimination of cytectrene I in the rat (mean ± SD; n = 4).

The autoradiograms of rat brain (Fig. 2) show an enrichment of activity in brain areas which are rich in 5-HT_{1A} receptors, such as hippocampus and entorhinal cortex as well as in regions for α₁ adrenergic receptors, such as thalamus, cortex and cerebellum. The ^{99m}Tc cytectrene I complex exhibits a higher nonspecific binding than cytectrene II. Receptor binding assays in rat brain homogenates and blocking studies are necessary to determine further data concerning affinity, specificity, selectivity and non-specific binding of the compounds.

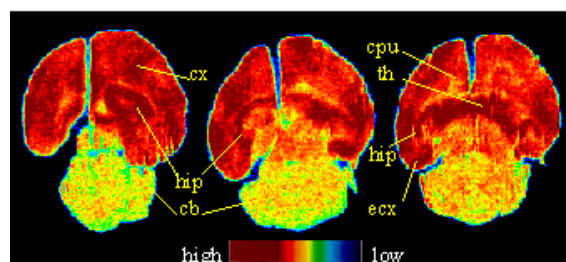


Fig. 2. Ex vivo autoradiograms of rat brain in horizontal section levels and radioactivity standard 20 min after i.v. application of the ^{99m}Tc cytectrene I complex. Hip= hippocampus, cx = frontal cortex, th = thalamus, ecx = entorhinal cortex, cpu = caudate-putamen, cb = cerebellum.

References

- [1] Saidi, M. *et al.*, *this report*, p. 23.
- [2] Kretzschmar, M. *et al.*, *Annual Report 2002*, FZR-363, p. 53.

Synthesis of 4- ^{18}F Fluoromethyl-2-Chloro-*O*-Succinimidyl-Benzoate as Novel Bifunctional ^{18}F -Labelling Agent

F. Wüst, M. Müller, H. Kasper

In this report we describe the radiosynthesis of 4- ^{18}F fluoromethyl-2-chloro-*O*-succinimidyl-benzoate as a novel bifunctional ^{18}F -labelling agent via nucleophilic displacement of the corresponding nosylate precursor with ^{18}F fluoride.

Introduction

The incorporation of ^{18}F with high specific radioactivity into biologically active peptides, proteins, oligonucleotides or antibodies represents a special challenge. Recently we have reported the one-step synthesis of a ^{18}F -labelled benzylfluoride containing a isothiocyanate group as novel prosthetic group [1]. Now we describe the single-step synthesis of ^{18}F -labelled 3-chloro-benzyl-fluoride **8** containing an *N*-hydroxysuccinimide (NHS) active ester functional group for conjugation with primary amines usually found in peptides, proteins and antibodies.

Results and Discussion

In a previous work we have shown that the nosylate group is an excellent leaving group for the one-step incorporation of ^{18}F fluoride into the benzylic positions under mild conditions [1]. Thus, labelling precursor **7** was synthesized in six steps starting from 2-amino-dimethylterephthalate **1**. The synthesis is depicted in Fig. 1.

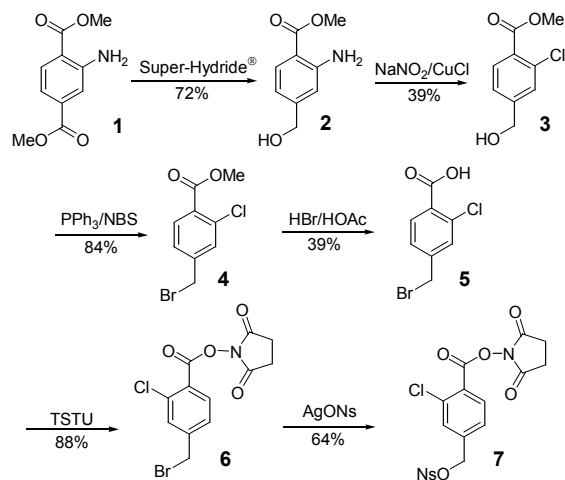


Fig. 1. Synthesis of the labelling precursor **7**

Starting from commercially available 2-amino-dimethylterephthalate **1** a regioselective reduction with Super-Hydride® provided amino alcohol **2** in 72 % yield. Subsequent application of a Sandmeyer-reaction gave the desired chloro-substituted alcohol **3** in 39 % yield. Further treatment of compound **3** with PPh_3/NBS afforded benzylbromide **4** in 84 % yield.

Cleavage of the ester group in **4** was performed under acidic conditions to give carboxylic acid **5** in 39 % yield. The carboxyl group in **5** was converted into succinimidyl active ester **6** by means of *O*-(*N*-succinimidyl)-*N,N,N',N'*-tetramethyluronium tetrafluoroborate (TSTU) in 88 % yield. Benzyl bromide **6** was finally treated with AgONs to give nosylate precursor **7** in 64 % yield. The radiosynthesis of **8** was performed in a remotely-controlled synthesis module according to [1] with nosylate precursor **7** (Fig. 2).

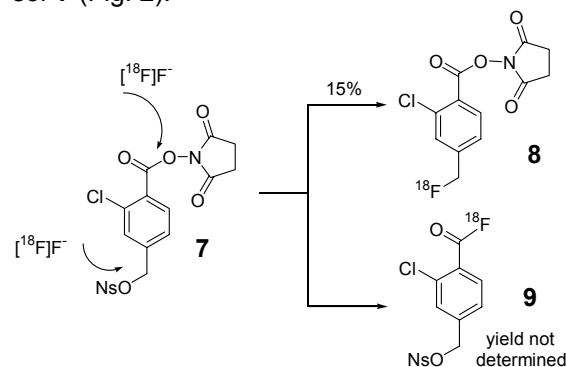


Fig. 2: ^{18}F -labelling of nosylate precursor **7**

When acetonitrile was used as the solvent, only low radiochemical yields of 5 - 10 % could be obtained at room temperature and 45 °C. Changing the solvent from acetonitrile to acetone gave slightly better but still low radiochemical yields of up to 15 % at 45 °C. The radiochemical yields could not be improved by further variation of the reaction temperature to 0 °C and 80 °C. The found low radiochemical yield and the fact that acetone is a better solvent compared to acetonitrile are consistent with reports on the synthesis of other NHS-substituted ^{18}F benzylfluorides [2, 3]. In these reports Eckelman *et al.* discussed the formation of a corresponding acid fluoride like **9** as competitive reaction of ^{18}F fluoride with the NHS active ester group.

References

- [1] Müller, M. *et al.*, *Annual Report 2002*, FZR-363, p. 46.
- [2] Lang, L. *et al.*, *Appl. Radiat. Isot.* 45 (1994) 1155-1163.
- [3] Lang, L. *et al.*, *Appl. Radiat. Isot.* 48 (1997) 169-173.

Radiosynthesis and Biodistribution of a ^{18}F -Labelled Corticosteroid for Mapping Brain Glucocorticoid Receptors (GR)

F. Wüst, T. Kniess, R. Bergmann

The radiosynthesis and biological evaluation of pyrazolo steroid 2'-(4-fluorophenyl)-21-[^{18}F]fluoro-20-oxo-11 β ,17 α -dihydroxy-pregn-4-eno[3,2-c]pyrazole is described. The radiolabelling was accomplished in 4-5 % decay-corrected radiochemical yield within 80 min at an effective specific radioactivity of 40-75 Ci/mmol. Biodistribution studies in male Wistar rats showed an initial brain uptake of 0.43 ± 0.12 % ID/g after 5 min and selective uptake in the pituitary which could be blocked by corticosterone pre-treatment.

Introduction

Corticosteroids are implicated in neuropsychiatric disorders such as severe depression and anxiety. The development of corticosteroids appropriately labelled with ^{18}F would allow the non-invasive in vivo imaging and mapping of brain GRs by means of PET. Recently we have prepared a series of novel fluorophenyl pyrazolo corticosteroids which showed relative binding affinities (RBA) to the GR of up to 56 % in comparison to dexamethasone (100 %) [1]. In this report we present the radiosynthesis of 2'-(4-fluorophenyl)-21-[^{18}F]fluoro-20-oxo-11 β ,17 α -di-hydroxy-pregn-4-eno[3,2-c]pyrazole **2** and its preliminary radiopharmacological evaluation by means of biodistribution studies in rats.

Results and Discussion

The radiolabelling was accomplished by [^{18}F]fluoride ion displacement on the corresponding α -keto iodide **1** to give 21-[^{18}F]fluoro compound **2** in 4-5 % decay-corrected radiochemical yield after HPLC purification at an effective specific radioactivity of 40-70 Ci/mmol (Fig. 1). The synthesis including HPLC separation was accomplished within 80 min after EOB, and the radiochemical purity exceeded 98 %. The found low effective specific radioactivity stems from the co-eluting oxetanone **3** which was formed inevitably during the radiolabelling process.

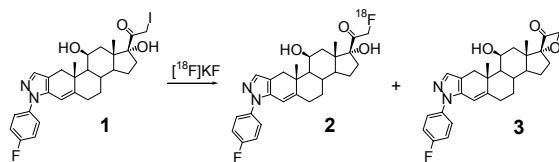


Fig. 1. Radiosynthesis of GR-ligand **2**

Biodistribution in male Wistar rats showed an initial brain uptake of 0.43 ± 0.12 % ID/g after 5 min which slightly decreased to 0.37 ± 0.06 % ID/g after 60 min. Brain to blood ratios at 5 min and 60 min p. i. were 4.3 and 2.8, respectively. The low accumulation of radioactivity in the bone (0.55 ± 0.08 % ID/g after 5 min and

0.41 ± 0.09 % ID/g after 60 min, respectively) is indicative of a low *in vivo* radiodefluorination of corticosteroid **2** in comparison to similar compounds reported in the literature [2, 3]. The pituitary and thymus as major targets of corticosteroid hormones showed uptakes of 1.64 ± 0.41 % ID/g and 0.55 ± 0.11 % ID/g after 5 min, and 1.95 ± 0.15 % ID/g and 0.68 ± 0.10 % ID/g after 60 min, respectively. The pituitary uptake of the radiotracer seems to be receptor-mediated since the uptake could be blocked by the co-injection of 2 mg of corticosterone per animal, being 0.87 ± 0.05 ID/g after 5 min and 1.39 ± 0.29 ID/g after 60 min (Table 1).

Table 1. Biodistribution (% ID/g) of **2** in male Wistar rats (^aPre-treatment with 2 mg of corticosterone)

Time p.i.	5 min	60 min	5 min (blocked) ^a	60 min (blocked) ^a
Organ				
Blood	0.10 ± 0.04	0.13 ± 0.02	0.11 ± 0.01	0.15 ± 0.02
Pituitary	1.64 ± 0.41	1.95 ± 0.15	0.87 ± 0.05	1.39 ± 0.29
Brain	0.43 ± 0.12	0.37 ± 0.06	0.44 ± 0.07	0.42 ± 0.08
Pancreas	1.38 ± 0.14	1.49 ± 0.12	1.39 ± 0.07	1.42 ± 0.15
Spleen	0.63 ± 0.11	0.66 ± 0.07	0.67 ± 0.04	0.74 ± 0.10
Adrenals	1.81 ± 0.48	2.93 ± 0.31	2.01 ± 0.29	3.27 ± 0.21
Kidneys	1.03 ± 0.29	1.24 ± 0.09	1.08 ± 0.19	1.46 ± 0.30
Muscle	0.53 ± 0.19	0.49 ± 0.08	0.51 ± 0.06	0.55 ± 0.21
Heart	0.99 ± 0.29	0.90 ± 0.12	1.03 ± 0.13	1.11 ± 0.17
Lungs	0.99 ± 0.32	1.08 ± 0.18	1.00 ± 0.11	1.11 ± 0.07
Thymus	0.55 ± 0.11	0.68 ± 0.10	0.62 ± 0.02	0.67 ± 0.20
Liver	2.02 ± 0.63	3.19 ± 0.29	2.13 ± 0.42	3.59 ± 0.37
Brown fat	1.10 ± 0.19	1.44 ± 0.38	1.31 ± 0.17	1.53 ± 0.30
Testes	0.26 ± 0.03	0.11 ± 0.06	0.30 ± 0.04	0.13 ± 0.02
Femur	0.53 ± 0.08	0.41 ± 0.09	0.56 ± 0.05	0.38 ± 0.04

In conclusion we have synthesized ^{18}F -labelled corticosteroid **2** showing moderate brain uptake comparable with the best ligands reported in the literature. In association with the good *in vivo* stability in terms of *in vivo* radiodefluorination we are encouraged to continue the work by using other ^{18}F -labelled corticosteroids to further improve brain uptake.

References

- [1] Wüst, F. *et al.*, Steroids 68 (2003) 177-191.
- [2] Pomper, M. G. *et al.*, Nucl. Med. Biol. 19 (1992) 461-480.
- [3] Feliu, A. L. *et al.*, J. Nucl. Med. 28 (1986) 998-1005.

Synthesis of ^{18}F -Labelled Nucleosides Using Stille Cross-Coupling Reactions with $[4\text{-}^{18}\text{F}]$ Fluoroiodobenzene

F. Wüst, T. Kniess, H. Kasper

The radiosyntheses of 5-([4'- ^{18}F]fluorophenyl)-uridine ^{18}F -**11** and 5-([4'- ^{18}F]fluorophenyl)-2'-deoxy-uridine ^{18}F -**12** are described. The $[4\text{-}^{18}\text{F}]$ fluorophenyl-substituted nucleosides were prepared via a Stille cross-coupling reaction with $[4\text{-}^{18}\text{F}]$ fluoroiodobenzene followed by basic hydrolysis. The Stille cross-coupling was optimised by screening various palladium catalysts, additives and solvents. Optimised reaction conditions ($\text{Pd}_2(\text{dba})_3/\text{CuI}/\text{AsPh}_3$ in DMF/dioxane 1:1, 20 min at 65 °C) provided the Stille cross-coupling products in radiochemical yields of up to 70 % related to $[4\text{-}^{18}\text{F}]$ fluoroiodobenzene.

Introduction

Recently we have described the synthesis of 5-([4'- ^{18}F]fluorophenyl)-2'-chloro-2'-deoxy-3',5'-diacetyl-uridine via a Stille cross-coupling reaction using $[4\text{-}^{18}\text{F}]$ fluoroiodobenzene [1]. Now we present the radiosynthesis of two new nucleosides bearing a $[4\text{-}^{18}\text{F}]$ fluorophenyl substituent at position 5 of the pyrimidine ring via a Stille cross-coupling with $[4\text{-}^{18}\text{F}]$ fluoro-iodobenzene. The reaction conditions were optimised by screening various palladium catalysts, additives and solvents.

Results and Discussion

The syntheses of labelling precursors **7** and **8** and reference compounds **11** and **12** are depicted in Fig. 1.

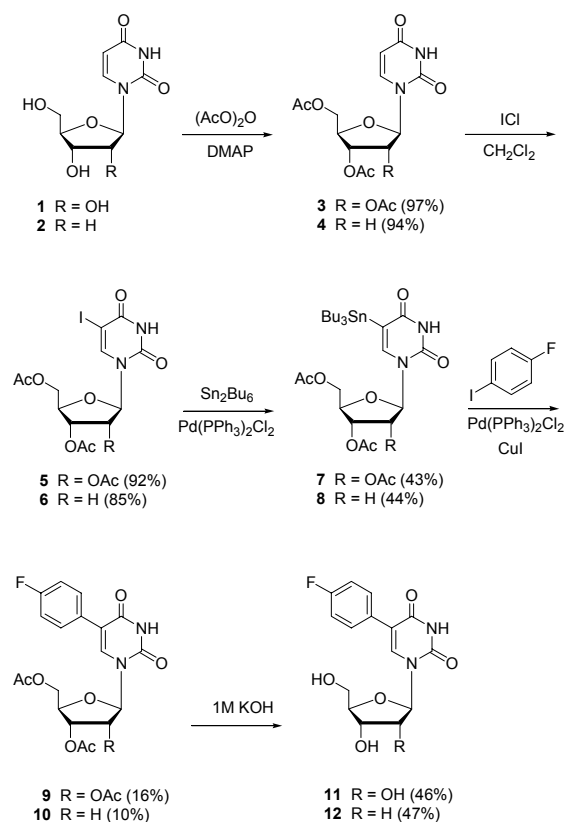


Fig. 1. Synthesis of labelling precursors and reference compounds

The radiosynthesis was performed using an one-pot procedure including the Stille cross-coupling reaction followed by basic hydrolysis of the acetyl protecting groups in $[^{18}\text{F}]$ -**9** and $[^{18}\text{F}]$ -**10** (Fig. 2.).

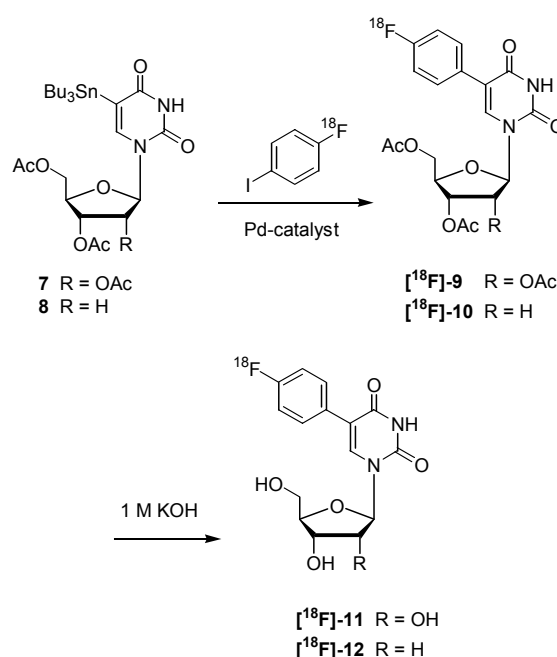


Fig. 2. Stille reaction with $[4\text{-}^{18}\text{F}]$ fluoro-iodobenzene and subsequent basic hydrolysis

By screening various palladium catalysts, additives and solvents the following reaction conditions were found to give the highest radiochemical yields of up to 70 % (related to $[4\text{-}^{18}\text{F}]$ fluoroiodobenzene, monitored by analytical radio-HPLC) for the Stille cross-coupling reaction: Heating a mixture of $[4\text{-}^{18}\text{F}]$ fluoro-iodobenzene/ $\text{Pd}_2(\text{dba})_3$ /tin precursor/ CuI/AsPh_3 in 1 ml of DMF/dioxane (1:1) for 20 min at 65 °C. In a typical large-scale experiment, 550 MBq of $[4\text{-}^{18}\text{F}]$ fluoroiodobenzene could be converted into 120 MBq (33 %, decay-corrected) of 5-([4'- ^{18}F]fluorophenyl)-2'-deoxy-uridine ^{18}F -**12** within 40 min, including HPLC purification.

Reference

[1] Kniess, T. *et al.*, *Annual Report 2002*, FZR-363, p. 45.

Radiolabelled Flavonoids and Polyphenols

I. Introduction and Radiolabelling Concept

S. Gester, F. Wüst, R. Bergmann, J. Pietzsch

The development of suitable concepts for the radiolabelling of flavonoids and polyphenols with ^{11}C and ^{18}F is described. Appropriately ^{11}C - and ^{18}F -labelled compounds will allow studies on some still unknown biological and biochemical pathways of specific flavonoid and polyphenolic substances by means of positron emission tomography (PET).

Introduction

Flavonoids are the most common occurring plant polyphenols and represent a group of phytochemicals exhibiting a wide range of biological activities arising mainly from their antioxidant properties and ability to modulate several enzymes or cell receptors [1]. Their wide occurrence, complex diversity and manifold functions have made flavonoids a very attractive target for chemical, biological and medical studies. In this context, flavonoids have been recognized to exert antibacterial and antiviral activity, anti-inflammatory, anti-angiogenic, analgesic, anti-allergic effects, hepatoprotective, cytostatic, apoptotic, estrogenic, and anti-estrogenic properties.

Flavonoids are chemically defined as substances composed of a common phenylchromanone structure with one or more hydroxyl substituents, including derivatives. Divided into several subclasses, the flavonoids include the anthocyanidins, responsible for the red and blue colors of fruits and flowers; the catechins, concentrated in tea; the flavanones and flavanone glycosides, found in citrus and honey, and the flavones, flavonols, and flavonol glycosides, found in tea, fruits, vegetables, and honey, as well as isoflavonoids found in soya food products (see Fig. 1).

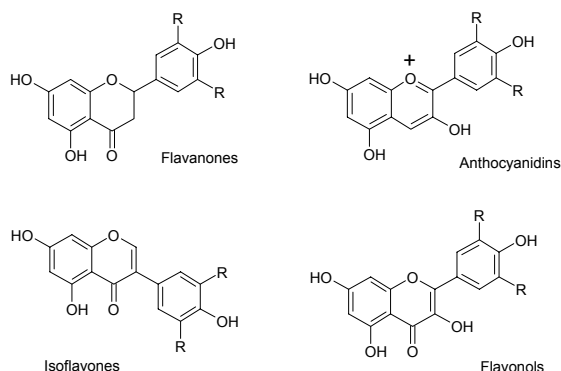


Fig. 1. Chemical structures of several classes of flavonoids

Other flavonoid-like compounds, derived from caffeic acid or *trans*-2-hydroxycinnamic acid, comprise dihydrochalcones, chlorogenic acid,

and different stilbenes, especially resveratrol (3,5,4'-trihydroxy-*trans*-stilbene).

This substance is found in red wine and was shown to reduce LDL-oxidation and act against arteriosclerotic processes.

Nevertheless, the biological pathways of many flavonoids in humans are still poorly understood. Understanding the potential link between the ingestion of individual flavonoids as dietary agents and the effect of health promotion or health risk requires the metabolic characterization of flavonoids *in vivo*. A solution could be the radiolabelling of flavonoids or flavonoid-like compounds with short-lived positron emitters (e.g. ^{11}C or ^{18}F) [2] and the subsequent radiopharmacological and physicochemical evaluation (informations on biodistribution, metabolism, lipophilicity data, binding properties to liposomes, lipoproteins etc.) by means of positron emission tomography (PET). The synthesis of ^{11}C -labelled flavonoids can be accomplished by using either standard methylation reactions with [^{11}C]methyl iodide or several ^{11}C -C bond forming reactions. The potential advantage of this approach consists of the isotopic labelling of flavonoids resulting in radiotracers which do not interfere with the physiological steady state, and which allow the external detection and monitoring of their *in vivo* biochemical fate.

Another important radioisotope in PET imaging is ^{18}F which can be used as an isosteric replacement for hydrogen or imitating a hydroxy group. The major advantage of ^{18}F -labelled radiotracers compared to ^{11}C -labelled compounds is the longer half-life of 110 min which allows the performance of more complex radiosyntheses and prolonged imaging protocols.

References

- [1] Middleton, E. *et al.*, Pharmacol. Rev. 52 (2000) 673-751.
- [2] Pietzsch, J. *et al.*, Bioforum 6 (2003) 384-385.

Radiolabelled Flavonoids and Polyphenols

II. Synthesis Towards [¹⁸F]Fluorine Labelled Resveratrol

S. Gester, F. Wüst, R. Bergmann, J. Pietzsch

4-[¹⁸F]fluorobenzaldehyde was coupled with diethyl-(3,5-dimethoxybenzyl)phosphonate under Wittig-Horner-Emmons conditions to form a [¹⁸F]fluorine labelled resveratrol derivative in 76 % yield related to 4-[¹⁸F]fluorobenzaldehyde.

Introduction

Resveratrol is a phytoalexin found in grapes and certain other plants. It exhibits a variety of useful biological properties (antileukemic, antibacterial, antifungal, antiplatelet aggregation, antioxidative, anti-inflammatory, and coronary vasodilator activities) and has been suggested as a possible cancer chemo-preventive agent on the basis of inhibitory effects on tumour initiation, promotion and progression. In this context, the synthesis of ¹⁸F-labelled resveratrol [¹⁸F]-**1** was initiated to evaluate radiopharmacological and physico-chemical properties (biodistribution, metabolism, binding properties etc.) by means of positron emission tomography (PET).

Results and Discussion

Diethyl-(3,5-dimethoxybenzyl)phosphonate **3**, the precursor for the radiosynthesis was obtained by the Michaelis-Arbuzov reaction of 3,5-dimethoxybenzylbromide **2** with excess of triethyl phosphite at 160 °C in 84 % yield [1]. Coupling of the phosphonic acid diester **3** with 4-fluorobenzaldehyde **5** under Wittig-Horner-Emmons conditions leads to the formation of pure 3,5-dimethoxy-4'-fluoro-*trans*-stilbene **6** in 62 % yield [2]. Upon reaction with BBr₃ in CH₂Cl₂ at -78 °C, compound **6** was demethylated and gave the resveratrol derivative 3,5-dihydroxy-4'-fluoro-*trans*-stilbene **1** in 57 % yield (see Fig. 1).

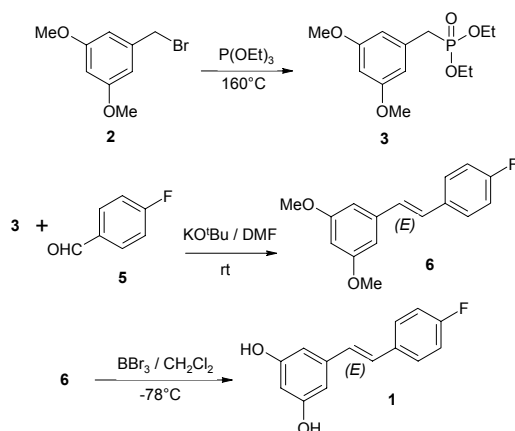


Fig. 1. Synthesis of the labelling precursor **3** and reference compounds **6** and **1**

Compounds **6** and **1** serve as reference substances.

Radiolabelling was performed using the readily available 4-[¹⁸F]fluorobenzaldehyde [¹⁸F]-**5** as coupling partner for the phosphonic acid diester **3**. 4-[¹⁸F]fluorobenzaldehyde was synthesized according to Mäding *et al.* [3] starting from 4-trimethylammonium benzaldehyde triflate **4** as precursor and [¹⁸F]fluoride / Kryptofix-222 in DMF. After cooling, a solution of the phosphonic acid diester **3** and potassium tert-butoxide in DMF was added to the crude reaction mixture containing 4-[¹⁸F]fluorobenzaldehyde. The [¹⁸F]fluorine labelled coupling product 3,5-dimethoxy-4'-[¹⁸F]fluoro-*trans*-stilbene [¹⁸F]-**6** (Fig. 2) was identified by comparison of the retention time with that of the reference compound **6**. The HPLC-determined yield was 76 % related to 4-[¹⁸F]fluorobenzaldehyde.

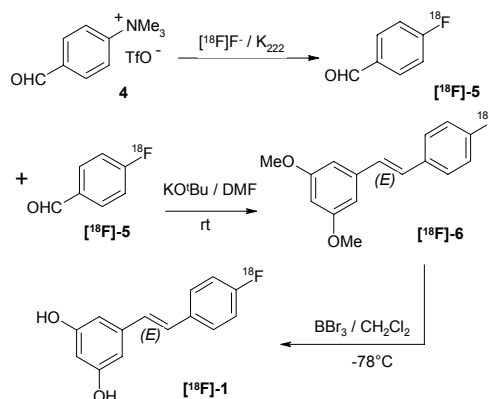


Fig. 2. Synthesis of the radiolabelled resveratrol derivatives [¹⁸F]-**6** and [¹⁸F]-**1**

The demethylation of compound [¹⁸F]-**6** to give the ¹⁸F-radiolabelled resveratrol derivative 3,5-dihydroxy-4'-[¹⁸F]fluoro-*trans*-stilbene [¹⁸F]-**1** is currently under investigation.

References

- [1] Meier, H. *et al.*, J. Org. Chem. 62 (1997) 4821-4826.
- [2] Gerold, J. *et al.*, Eur. J. Org. Chem. (2001) 2757-2763.
- [3] Mäding, P. *et al.*, Annual Report 2001, FZR-340, p. 58.

Synthesis of a ^{18}F -Labelled COX-2 Inhibitor

A. Höhne, F. Wüst

A ^{18}F -labelled derivative of Rofecoxib[®] was synthesized via a Stille cross-coupling reaction of 4-(4-methylsulfonylphenyl)-3-(tributylstannyl)-2(5H)-furanone with $[4\text{-}^{18}\text{F}]$ fluoroiodobenzene. Conversion of $[4\text{-}^{18}\text{F}]$ fluoroiodobenzene into the desired product proceeded in radiochemical yields of up to 76 % related to $[4\text{-}^{18}\text{F}]$ fluoroiodobenzene.

Introduction

Cyclooxygenases control the complex conversion of arachidonic acid to prostaglandins and thromboxanes, which trigger as autocrine and paracrine chemical messengers many physiological and pathophysiological responses. Besides their association with inflammation and pain, the up-regulation of COX-2 expression has also been observed in Alzheimer's disease and in a variety of tumours [1, 2]. The overexpression of COX-2 in several tumours opens an interesting approach for tumour targeting with appropriately radiolabelled ligands for COX-2. Herein we describe the radiosynthesis of a ^{18}F -labelled derivative of Rofecoxib via a Stille reaction with $[4\text{-}^{18}\text{F}]$ fluoroiodobenzene.

Results and Discussion

The synthesis of labelling precursor **5** and reference compound **6** is shown in Fig. 1.

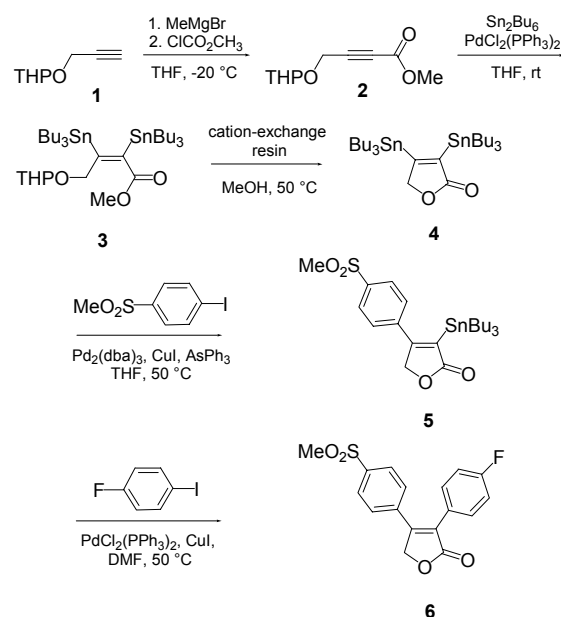


Fig. 1. Synthesis of labelling precursor **5** and reference compound **6**

Briefly, tetrahydro-2-(2-propynyloxy)-2H-pyran **1** was converted into tetrahydro-2-[methyl-2-butynyl-(oxy)-oat]-2H-pyran **2** in 56 % yield using methylmagnesium bromide and methylchloroformate. The introduction of the tributylstannyl groups was achieved by the reaction of

2 with hexabutyldistannane in the presence of PdCl₂(PPh₃)₂ to give the 2,3-bis(tributylstannyl)-propynoate **3** in 76 % yield. Formation of the γ -lactone **4** was accomplished in 72 % yield by the treatment of **3** with cation-exchange resin in MeOH. Regioselective introduction of the 4-methylsulfonylphenyl substituent was achieved by a Stille reaction to give 4-(4'-methylsulfonylphenyl)-3-(tributylstannyl)-2(5H)-furanone **5** in 27 % yield.

Compound **5** was further converted into reference compound 3-(4-fluorophenyl)-4-(4-methylsulfonylphenyl)-2(5H)-furanone **6** in 88 % yield by an additional Stille reaction of **5** with 4-fluoroiodobenzene.

Radiolabelling was performed using $[4\text{-}^{18}\text{F}]$ fluoroiodobenzene as the coupling partner in the Stille reaction (Fig. 2).

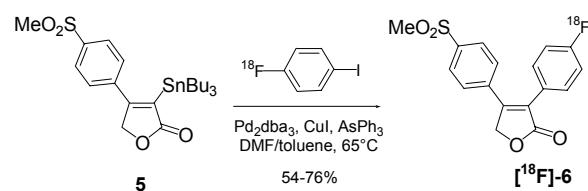


Fig. 2. Stille reaction with $[4\text{-}^{18}\text{F}]$ fluoroiodobenzene

$[4\text{-}^{18}\text{F}]$ fluoroiodobenzene was synthesized according to Wüst *et al.* using 4,4'-diiododiphenyliodonium triflate as precursor [3]. $[4\text{-}^{18}\text{F}]$ fluoroiodobenzene (50-150 MBq) in DMF was added to a reaction vial containing labelling precursor **5** in toluene, Pd₂(dba)₃, AsPh₃ and CuI. After heating the vial at 65 °C for 20 minutes the reaction mixture was filtered and analysed by radio-HPLC. ^{18}F -labelled COX-2 inhibitor $[^{18}\text{F}]$ -**6** was identified by comparison the retention time with that of the corresponding reference compound **6**. The radiochemical yields were determined by radio-HPLC, being 54-76 % related to $[^{18}\text{F}]$ fluoroiodobenzene.

References

- [1] Marnett, L. *et al.*, Trends Pharmacol. Sci. 20 (1999) 465-469.
- [2] Dannhardt, G. *et al.*, Eur. J. Med. Chem. 36 (2001) 109-126.
- [3] Wüst, F. *et al.*, J. Labelled Compd. Radiopharm. 46 (2003) 699-713.

¹⁸F-Labeling of a Potent Nonpeptide CCR1 Antagonist: Synthesis of [¹⁸F]ZK811460 in an Automated Module

P. Mäding, F. Füchtner, B. Johannsen, J. Steinbach¹, C. S. Hilger², R. Mohan³,
M. Halks-Miller³, R. Horuk³

¹Institut für Interdisziplinäre Isotopenforschung, Leipzig; ²Schering AG, Berlin, ³Berlex Biosciences, Departments of Chemistry, Pharmacology, and Immunology, Richmond, California, USA

The two-step one-pot synthesis of the potent nonpeptide CCR1 antagonist [¹⁸F]ZK811460 was adapted to an automated module. The radiochemical yields of the purified and formulated [¹⁸F]ZK811460 ranged between 5 and 15 % (not decay-corrected), the time of the entire manufacturing process was about 90 min.

Introduction

The synthesis of the potent nonpeptide CCR1 antagonist [¹⁸F]ZK811460 is described in [1]. To produce this radiotracer for human studies and on high radioactivity levels, the two-steps one-pot procedure had to be adapted to an automated, remotely-controlled module which is installed in a hot cell.

Results and Discussion

The scheme of the automated module for the synthesis of [¹⁸F]ZK811460 is demonstrated in Fig. 1. It is a commercially available module for nucleophilic fluorination (Nuclear Interface, Münster, Germany) which was modified in terms of program and hardware. The capability of the module includes the radiosynthesis of 4-[¹⁸F]fluorbenzaldehyde and its reductive amination with the appropriate piperazine derivative (ZK258394) to give [¹⁸F]ZK811460 according to ref. [1], the HPLC purification of the final product (see Fig. 2), and its solid phase extraction and formulation.

The isolated (not decay-corrected) radiochemical yields of the purified and formulated [¹⁸F]ZK811460 ranged between 5 and 15 %, the time of the entire manufacturing process

was about 90 min after EOB. The radiochemical purity of [¹⁸F]ZK811460 was greater than 95 %, the chemical purity ≥ 80 % and the enantiomeric purity > 99.5 %. The specific radioactivity was greater than 37 GBq/μmol by using a starting radioactivity level of ≥ 25 GBq.

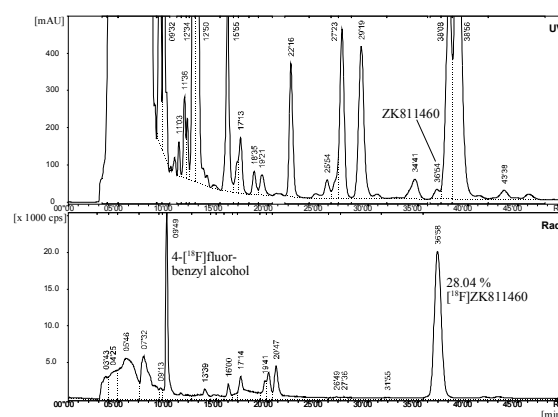


Fig. 2. A semipreparative HPLC chromatogram to purify [¹⁸F]ZK811460 from the reaction mixture

Reference

[1] Mäding, P. *et al.*, *Annual Report 2002*, FZR-363, p. 40.

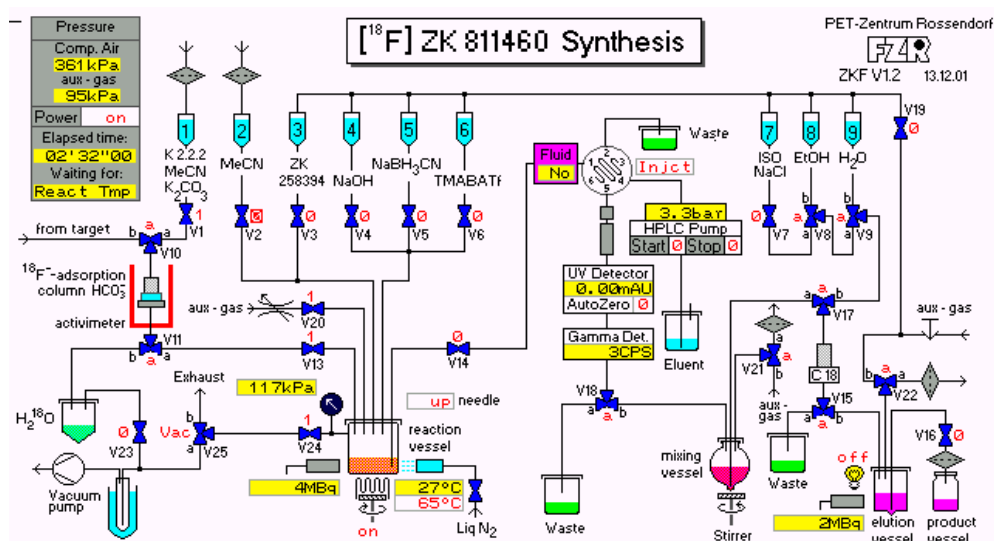


Fig. 1. Scheme of the module for the synthesis of [¹⁸F]ZK811460.

¹¹C-Labeling of a Taxane Derivative Using [1-¹¹C]Acetyl Chloride

P. Mäding, J. Zessin, U. Pleiß¹, F. Wüst
¹Bayer Health Care AG, Wuppertal

The ¹¹C-labelling of the taxane derivative BAY 59-8862 (**1**), a new potent anticancer drug, was developed as a multi-step procedure using an automated module. [¹¹C]**1** was synthesized by reacting [1-¹¹C]acetyl chloride with the secondary hydroxy group of precursor **2** followed by deprotection. The decay-corrected radiochemical yields of the purified and formulated [¹¹C]**1** ranged between 6-19 % (related to [¹¹C]CO₂; n = 11) within 45-50 min after EOB.

Introduction

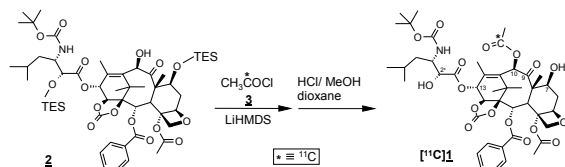
Taxanes are an important class of antitumor agents. These compounds bind to the microtubuli and inhibit their depolymerization into tubulin. Subsequently, the mitosis is disrupted and the cells are not able to divide into daughter cells [1]. Investigations with positron emission tomography (PET) are an important tool to determine the *in vivo* pharmacokinetics of such drugs when they are labelled with positron-emitting radionuclides. An example for such a labelling is given by the synthesis of [¹¹C]paclitaxel by reacting [α-¹¹C]-benzoyl chloride with a corresponding primary amine precursor [2]. Paclitaxel (Taxol) is an effective anticancer drug against solid tumours.

This report describes the ¹¹C-labelling of the taxane derivative BAY 59-8862 (**1**). Compound **1** was shown to be a new potent anticancer drug which is intended for the therapy of breast cancer metastases in the brain. A clinical PET study with female patients is scheduled in collaboration with Bayer Health Care AG using compound [¹¹C]**1**.

Results and Discussion

The acetyl group in compound **1** at position 10 was chosen to introduce carbon-11 by the reaction of 10-deacetyl precursor **2** with [1-¹¹C]acetyl chloride (**3**). With respect to drug metabolism, experiments in human hepatocytes showed that this acetyl position is metabolically stable.

Scheme 1. Synthesis of [¹¹C]**1**

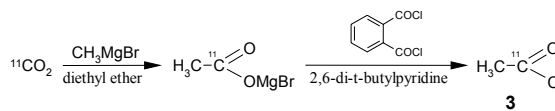


[¹¹C]**1** was synthesized in a multi-step procedure according to Scheme 1 using an automated synthesis module. The remotely controlled synthesis includes: 1. radiosynthesis of **3**; 2. reaction of **3** with the lithium salt of precursor **2**; 3. deprotection and HPLC-purification of [¹¹C]**1**, solid phase extraction, and formulation.

The used module was commercially available as a ¹¹C-methylation module from GE Medical Systems Münster, Germany.

[1-¹¹C]Acetyl chloride (**3**) was synthesized as previously described [3] with some modifications [4] by conversion of [¹¹C]CO₂ with methylmagnesium bromide in diethyl ether followed by quenching the resulting [¹¹C]acetate solution with phthaloyl dichloride in the presence of 2,6-di-*tert.*-butylpyridine (Scheme 2).

Scheme 2. Synthesis of **3**



After evaporation of the solvent, **3** was transferred into a cooled THF solution containing **2** and lithium hexamethyldisilazide. The [¹¹C]acetylation was performed at room temperature. The solvent was evaporated and the residue was treated with a solution of hydrochloric acid in MeOH/dioxane for cleavage of the triethylsilyl protecting groups. The crude product [¹¹C]**1** was purified by semi-preparative RP HPLC and subsequent solid phase extraction using a RP-18-cartridge. The resulting ethanolic solution of [¹¹C]**1** and a saline solution was transferred successively through a sterile filter to obtain the final formulation of [¹¹C]**1**. The decay-corrected radiochemical yields were in the range of 6 to 19 % (related to [¹¹C]CO₂, n = 11). The total synthesis time was 45-50 min. The radiochemical purity exceeded 96 %, and the chemical purity was in the range of 80-99 %. The specific radioactivity of the final product was up to 18 GBq/μmol at EOS starting from 26 GBq of [¹¹C]CO₂.

References

- [1] Georg, G. I. *et al.*, *Taxane Anticancer Agents: Basic Science and Current Status*, American Chemical Society, Washington, DC, 1995.
- [2] Ravert, H. T. *et al.*, *J. Labelled Compd. Radiopharm* 45 (2002) 471-477.
- [3] Le Bars, D. *et al.*, *Appl. Radiat. Isot.* 38 (1987) 1073-1077.
- [4] Holschbach, M., *private communication*.

Synthesis of Sodium [1-¹¹C]Acetate for Clinical Applications

P. Mäding, J. Zessin, F. Füchtner, F. Wüst

The synthesis of sodium [1-¹¹C]acetate, a useful radiopharmaceutical in nuclear cardiology, was developed in an automated module by the reaction of [¹¹C]carbon dioxide with methylmagnesium bromide in diethyl ether followed by quenching the reaction mixture with aqueous hydrochloric acid. The purification was carried out using a silver oxide cartridge and a cation exchange cartridge. After formulation and sterile filtration the decay-corrected radiochemical yields of sodium [1-¹¹C]acetate were in the range of 45-54 % (related to [¹¹C]CO₂) within a synthesis time of 20 min.

Introduction

Sodium [1-¹¹C]acetate has ideal characteristics as a PET tracer of myocardial viability by measurement of the oxidative myocardial metabolism [1]. It is also a suitable marker for estimation of myocardial perfusion. Moreover, oncological studies suggest that the *in vivo* behaviour of [1-¹¹C]acetate is also favourable for clinical detection and evaluation of prostate cancer by PET [1]. Therefore we have developed a simple procedure for the production of sodium [1-¹¹C]acetate for clinical applications based on a ¹¹C synthesis module manufactured by GE Medical Systems.

Results and Discussion

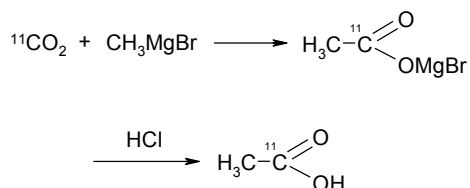
Numerous automated and improved production systems of [1-¹¹C]acetate are reported [1, 2, 3, 4 among others].

We have synthesized sodium [1-¹¹C]acetate according to Scheme 1 using the commercially available ¹¹C-methylation module from GE Medical Systems (former Nuclear Interface, Münster, Germany) which was modified in terms of program and hardware (see Fig. 1).

The preparation of sodium [1-¹¹C]acetate was carried out as follows: carboxylation of methylmagnesium bromide in diethyl ether with [¹¹C]carbon dioxide, quenching the excess of Grignard reagent by ethanol addition, evaporation of the solvents and hydrolysis with diluted aqueous hydrochloric acid. The acidic solution containing [1-¹¹C]acetic acid was purified using two cartridges: a silver oxide cartridge (IC-Ag, Alltech) to remove bromide ions from the reaction mixture and a cation exchange cartridge (SCX, Alltech) to remove magnesium ions. The purified solution was added to an isotonic sodium chloride solution and the mixture was subjected to sterile filtration.

The decay-corrected radiochemical yields of sodium [1-¹¹C]acetate were in the range of 45-54 % (related to [¹¹C]CO₂; n = 10) within a synthesis time of 20 min. Thus in a typical experiment, starting from 40 GBq [¹¹C]carbon dioxide, about 10 GBq of sodium [1-¹¹C]acetate can be synthesized.

Scheme 1. Synthesis of sodium [1-¹¹C]acetate



In this way a chemical and radiochemical pure product was obtained. The radiochemical and chemical purity was determined by HPLC using a CarboPac PA1 column (250 x 4 mm) and 0.1 M sodium hydroxide solution as the eluent. The radiochemical purity exceeds 99.5 %, and the sodium acetate content is lower than 180 ppm. The purification by solid phase extraction works highly efficient. The final sodium [1-¹¹C]acetate solution contains only 0.8-2.5 ppm bromide and 0.2-1.1 ppm magnesium as determined by ion chromatography. The amounts of the solvents diethyl ether, ethanol, and acetone correspond to the limits outlined in the European Pharmacopeia. The pH of the solution varies from 4.6 to 8.5. The product was isotonic, sterile and pyrogen free.

Conclusions

An efficient procedure for the synthesis of sodium [1-¹¹C]acetate was developed based on the ¹¹C-methylation module from GE Medical Systems. The described procedure is very simple and robust by the use of commercially available cartridges for purification. The final product is in compliance with the specifications for radiopharmaceuticals outlined in the European Pharmacopeia.

References

- [1] Moerlein, S. M. *et al.*, Nucl. Med. Biol. 29 (2002) 613-621.
- [2] Pike, V. W. *et al.*, Int. J. Appl. Radiat. Isot. 35 (1984) 623-627.
- [3] Iwata, R. *et al.*, Appl. Radiat. Isot. 46 (1995) 117-121.
- [4] Roeda, D. *et al.*, Appl. Radiat. Isot. 57 (2002) 857-860.

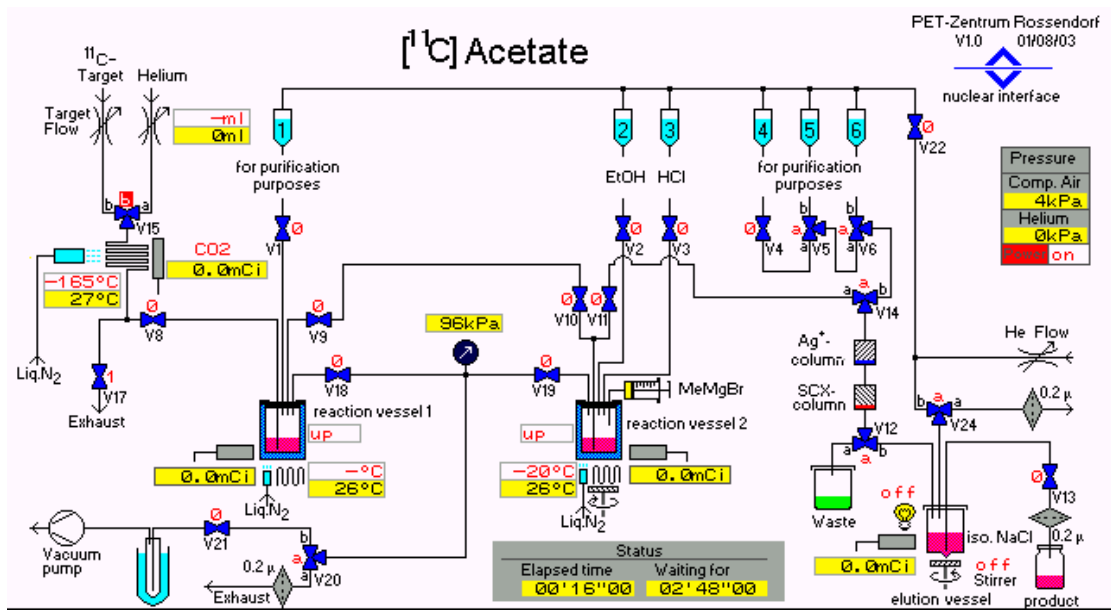


Fig. 1. Scheme of the module for the synthesis of sodium [¹¹C]acetate

Tissue Transglutaminase: a Minireview

J. Pietzsch, R. Bergmann

Transglutaminases (TGs) are a family of Ca^{2+} -dependent enzymes that mediate the post-translational modification of proteins by catalyzing acyl-transfer reactions yielding to the formation of new amide bonds between γ -carboxamide groups of protein glutamine side chain residues and various primary amines. Glutamine residues serve as acyl-donors and the most common acyl-acceptors are ϵ -amino groups of protein lysine side chain residues or primary amino groups of some naturally occurring polyamines, like putrescine, spermidine, and spermine (Fig. 1) [1, 2].

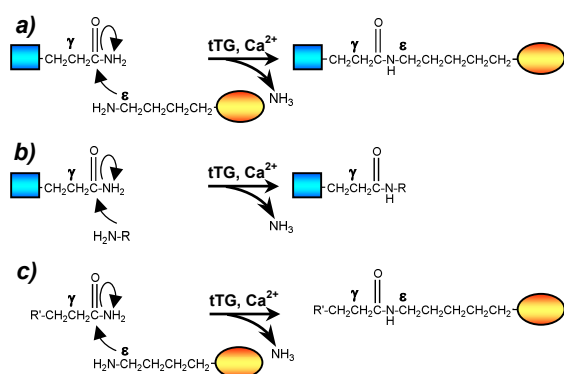


Fig. 1. tTG-catalyzed transamidation reactions. Transamidation can cause **a)** protein crosslinking by forming a N^ϵ -(γ -glutamyl)lysine isopeptide bridge between the deprotonated lysine donor residue of one protein (orange ellipse) and the acceptor glutamine residue of another protein (blue rectangle), **b)** the incorporation of an amine into the glutamine side chain residue of the acceptor protein (diamines and polyamines can act as a tether in a bis-glutamyl adduct between two acceptor molecules), and **c)** the acylation of a lysine side chain residue of the donor protein (according to Lorand and Graham [1]). Reactions **b)** and **c)** compete against crosslinking that is shown in **a)**. R represents the side chain in a primary amine, R' represents a glutamine containing peptide.

The active site cysteine reacts first with the γ -carboxamide group of a glutamine residue forming a γ -glutamyl thioester and releasing ammonia. The transient acyl-enzyme intermediate then reacts with any nucleophilic primary amine, yielding either an isopeptide bond or a (γ -glutamyl) polyamine bond. TGs are ubiquitous, with each enzyme having a distinct set of substrates, giving them distinct physiological roles. Among the most recognized members of the TG family is tissue TG (tTG, also abbreviated TG2; EC 2.3.2.13.). tTG is a monomeric globular protein with a molecular mass of about 77 kDa and shows a high degree of sequence similarity to the α -subunit of factor XIII. tTG is expressed in the majority of cells and tissues. Its subcellular localization is the

cytosolic fraction and no interactions with other specific subcellular compartments are described [2, 3].

tTG activity has been demonstrated to play a crucial role in stabilization of the basement membrane and adhesion of cells and tissue mineralization, respectively, which are important processes in angiogenesis, wound healing, and bone remodelling. tTG has been shown to crosslink all major extracellular matrix (ECM) proteins, including fibronectin, laminin, vitronectin, and collagen, thus forming a stable ECM, because these crosslinks are resistant to proteolytic and mechanical damage. tTG also participates in normal protective cellular response contributing to tissues homeostasis. In this line, several *in vitro* and *in vivo* models demonstrate direct relationship between the expression and activity of tTG and apoptosis. Coupled with the potential importance of tTG in the organization of ECM and programmed cell death, respectively, the finding that tTG activity is increased, often markedly, in various inflammatory and fibrotic conditions (such as rheumatoid arthritis, atherosclerosis, liver, renal and pulmonary fibrosis, Huntington's and Alzheimer's disease, and coeliac disease), led to its implication in the pathogenesis of these disorders. It is also hypothesized that transglutaminase ECM-promoting abilities form an important part of the host response mechanism against tumour growth and tumour invasion [3-5].

Given the potential importance of tTG in such varied cellular and extracellular processes, it is of interest to understand perturbations in tTG activity through abnormal expression, genetic deficiencies, or autoimmune disorders *in vivo*. One promising approach is the use of fluorine-18 labelled polyamines as potential substrates of tTG for positron emission tomography (PET) imaging and quantitative characterization, respectively, of tTG activity and expression in animal models *in vivo*.

References

- [1] Lorand, L. *et al.*, Nat. Rev. 4 (2003) 140-156.
- [2] Folk, J. E. *et al.*, J. Biol. Chem. 255 (1980) 3695-3700.
- [3] Aeschlimann, D. *et al.*, Connect Tissue Res. 41 (2000) 1-27.
- [4] Folk, J. E. *et al.*, Adv. Protein Chem. 31 (1997) 1-133.
- [5] Auld, G. C. *et al.*, Arterioscler. Thromb. Vasc. Biol. 21 (2001) 1689-1694.

Synthesis of Fluorinated *N*-Benzoylpolyamines as Substrates of Tissue Transglutaminase

K. Knop, C. Hultsch, K. Rode, T. Kniess, F. Wüst, R. Bergmann, J. Pietzsch

Introduction

Tissue transglutaminase (tTG) catalyzes acyl-transfer reactions between protein glutamine side chain residues and primary amines, including naturally occurring polyamines, like putrescine, spermidine, and spermine. In this report we describe a method for labelling of polyamines putrescine and spermine, respectively, with ^{18}F by means of [^{18}F]SFB.

Methods

Preparation of *n.c.a.* *N*-succinimidyl 4- ^{18}F -fluorobenzoate ([^{18}F]SFB) was achieved within 40 min in decay-corrected radiochemical yields of $50\pm 5\%$ and a radiochemical purity of $>95\%$ [1]. For coupling, polyamines (100 μM to 100 mM in 800 μl borate buffer, pH 8.3) were incubated with 5-10 MBq [^{18}F]SFB (200 μl , in acetonitrile). The reaction mixture (various polyamine concentrations) was kept at different pH and temperatures, and aliquots were taken at different time points for analysis. The analysis was performed by radio-TLC. The synthesis of reference compounds was accomplished by using an excess of polyamine in the coupling reaction with [^{19}F]SFB. Reference compounds (*N*- ^{19}F fluorobenzoylated polyamines) were analysed by HPLC and mass spectrometry.

Results and Discussion

The incorporation of ^{18}F into polyamines requires the use of a prosthetic group. The acylation of primary amino groups with [^{18}F]SFB has been shown to be a suitable and versatile ^{18}F -labelling method in terms of radiochemical yield and *in vivo* stability [1, 2]. In a series of labelling experiments at analytical scale the effects of time, temperature, polyamine concentration, and pH on the coupling reaction of polyamines with [^{18}F]SFB were studied. Our findings revealed the use of 20 mM polyamine at room temperature for 20 min at pH 8.5 to be the optimum condition for efficient coupling of both putrescine and spermine with [^{18}F]SFB. Figures 1 and 2 show the reaction schemes for the formation of [^{18}F]FB putrescine and [^{18}F]FB spermine, respectively. As expected, the coupling reaction of the symmetric molecules putrescine and spermine, respectively, with *n.c.a.* [^{18}F]SFB resulted in only one *N*- ^{18}F fluorobenzoylated product. This result correlates well with the sub-stoichiometric amounts of [^{18}F]SFB in the course of the reactions with polyamines.

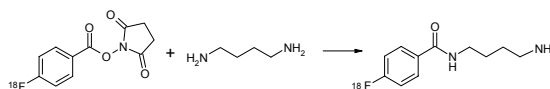


Fig. 1. Reaction scheme of [^{18}F]fluorobenzoylation of putrescine

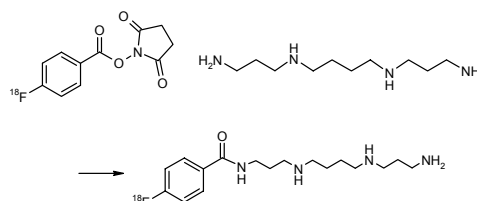


Fig. 2. Reaction scheme of [^{18}F]fluorobenzoylation of spermine

The formation of both [^{18}F]FB putrescine and [^{18}F]FB spermine was confirmed by comparison of the retention times with the corresponding reference compounds. Employing optimum reaction conditions, the radiochemical synthesis of *N*- ^{18}F fluorobenzoylated polyamines can be accomplished within 85 min after EOB. The radiochemical yield amounted to $35\pm 5\%$ and the radiochemical purity to $95\pm 4\%$ (Fig. 3).

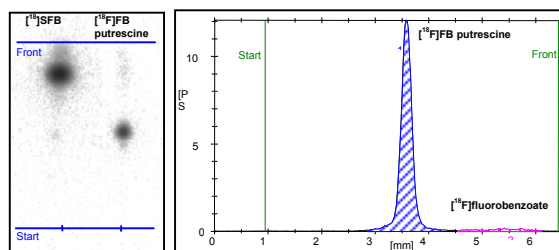


Fig. 3. Radio-TLC of purified [^{18}F]fluorobenzoylated putrescine

In conclusion, the use of the found optimum reaction conditions provided radiolabelled polyamines in radiochemical yields suitable for further biological evaluation as potential substrates of tTG *in vitro* and *in vivo*.

Acknowledgements

The authors wish to thank S. Preusche, M. Grote, and T. Krauss for expert technical assistance.

References

- [1] Wuest, F. *et al.*, Appl. Radiat. Isot. 59 (2003) 43-48.
- [2] Wester, H. J. *et al.*, Nucl. Med. Biol. 23 (1996) 365-372.

Biological Evaluation of Fluorinated N-Benzoylpolyamines as Substrates of Tissue Transglutaminase Activity: Polyamination of N,N'-Dimethylcasein

J. Pietzsch, K. Knop, K. Rode, R. Bergmann

Introduction

Tissue transglutaminase (tTG) catalyzes acyl-transfer reactions between protein glutamine residues and primary amines. We report the identification of [^{18}F]fluorobenzoylated polyamines putrescine and spermine as substrates of tTG *in vitro*.

Preparation of *n.c.a.* N-succinimidyl 4- ^{18}F -fluorobenzoate (^{18}F SFB) was achieved within 40 min with radiochemical yields of $50\pm 5\%$ and purity of $>95\%$ [1]. Polyamine labelling with ^{18}F SFB and purification of [^{18}F]fluorobenzoylated (^{18}F FB) polyamines resulted in radiochemical yields of $35\pm 5\%$ and purity of $>95\%$ [2]. tTG transamidation activity was evaluated by measuring the incorporation of [^{18}F]FB polyamines into N,N'-dimethylcasein and the recovery of [^{18}F]FB polyamine-protein conjugates, respectively, according to Rossi *et al.* with some modifications [3]. In brief, the reaction mixture contained 150 mM Tris-HCl buffer (pH 8.3), 90 mM NaCl, 10 mM DTT, 15 mM CaCl_2 , 12.5 mg N,N'-dimethylcasein per mL, and 0.1, 0.2, 0.5, and 1.0 MBq purified [^{18}F]FB polyamines. 50 ng (0.25 U) of guinea pig liver tTG were incubated with the reaction mixture in a final volume of 200 μl for 20 min at 37°C. The reaction was stopped by spotting 60 μl aliquots onto 3MM filter paper. Unbound [^{18}F]FB polyamine was removed by washing with large volumes of ice-cold 30%, 15%, and 10% trichloroacetic acid and absolute ethanol. Filters were dried and the amount of polyamine incorporation was measured by scintillation counting. In addition, 20 μl aliquots were subjected to SDS-polyacrylamide gelelectrophoresis (SDS-PAGE) as described previously [4]. Gels were analysed by radioluminography.

Results and Discussion

Evaluation of tTG activity is based on the incorporation of labelled polyamines into N,N'-dimethylcasein. The use of N,N'-dimethylcasein, where the lysine residues are blocked by methylation, instead of casein as the substrate protein prevents the intra-chain reaction between glutamine and lysine residues and favors the binding with amino groups of polyamines. As shown in Figs. 1 and 2, incorporation of the [^{18}F]FB spermine into N,N'-dimethylcasein was observed. Similar results could be observed for [^{18}F]FB putrescine (data not shown in detail).

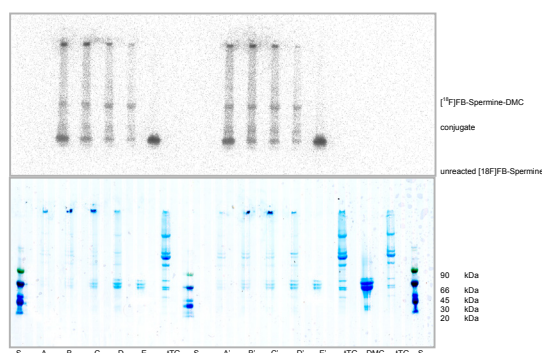


Fig. 1. Evaluation of [^{18}F]FB spermine incorporation into N,N'-dimethylcasein by SDS-PAGE (representative gel). The unreacted [^{18}F]FB spermine was observed at the bottom of the gel as also seen in the control (without enzyme). Samples were subjected to electrophoresis on a 8-18% acrylamide gradient gel. Samples and protein standards (S; Amersham Rainbow™ low molecular weight mixture) were reduced prior to electrophoresis. Radioluminography (top) and Coomassie blue protein staining (bottom) served for identification of [^{18}F]FB spermine incorporation into N,N'-dimethylcasein. Samples (complete reaction mixture) containing 0.1, 0.2, 0.5, and 1.0 MBq purified [^{18}F]FB spermine were incubated at 4 °C (A, B, C, D) and at 37 °C (A', B', C', D'). Controls (without enzyme; E, E') contained 0.1 MBq purified [^{18}F]FB spermine. tTG, guinea pig liver tTG; DMC, N,N'-dimethylcasein

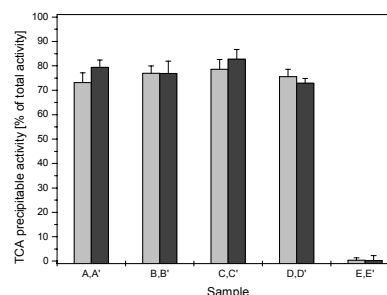


Fig. 2. Evaluation of tTG transamidation activity as determined by *n.c.a.* [^{18}F]FB spermine incorporation into N,N'-dimethylcasein assay. Samples (complete reaction mixture) containing 0.1, 0.2, 0.5, and 1 MBq purified [^{18}F]FB spermine were incubated at 4 °C (A, B, C, D) and at 37 °C (A', B', C', D'). Controls (without enzyme; E, E') contained 0.1 MBq purified [^{18}F]FB spermine.

In conclusion, we have shown that both [^{18}F]FB spermine and [^{18}F]FB putrescine are substrates for tTG catalyzed transamidation reaction *in vitro*.

References

- [1] Wuest, F. *et al.*, Appl. Radiat. Isot. 59 (2003) 43-48.
- [2] Knop, K. *et al.*, *this report*, p. 36.
- [3] Rossi, A. *et al.*, J. Invest. Dermatol. 115 (2000) 731-739.
- [4] Pietzsch, J. *et al.* Biochim. Biophys. Acta 1254 (1995) 77-88.

Biological Evaluation of Fluorinated *N*-Benzoylpolyamines as Substrates of Tissue Transglutaminase Activity: Insights from Animal PET Studies

J. Pietzsch, R. Bergmann, K. Knop, K. Rode, F. Wüst, J. van den Hoff

Introduction

Given the potential importance of tissue transglutaminase (tTG) in various cellular and extracellular processes, it is of interest to understand perturbations in tTG activity under pathological conditions *in vivo*. We report a first approach using [¹⁸F]fluoro-benzoylated ([¹⁸F]FB) polyamines as potential tTG substrates for PET imaging and quantitative characterization of tTG activity and expression, respectively, in animal models *in vivo*.

Methods

Preparation of [¹⁸F]FB polyamines was accomplished within 85 min with radiochemical yields of 35±5 % and radiochemical purity of >95 % [1]. The metabolic fate of [¹⁸F]FB polyamines in male Wistar rats was delineated by both biodistribution studies *ex vivo* and dynamic PET studies using a dedicated small animal tomograph (microPET; spatial resolution of <2 mm) *in vivo*.

Results and Discussion

Fig. 1 shows the biodistribution of the [¹⁸F]FB polyamines putrescine and spermine in male Wistar rats 5 and 60 min *p.i.* Data revealed high *in vivo* stability of [¹⁸F]FB polyamines. High concentration of radioactivity was detected in kidneys, liver, adrenals, and lungs. The main excretory organs are the kidneys.

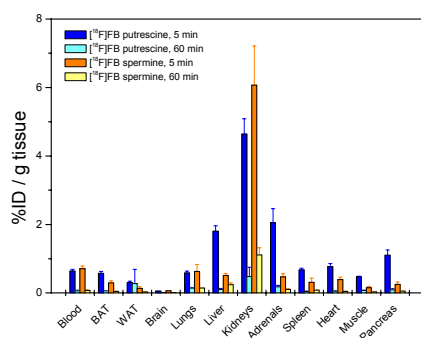


Fig. 1. Representative biodistribution (% ID/g) of both [¹⁸F]FB putrescine and [¹⁸F]FB spermine in male Wistar rats (100-120 g) after i.v. injection (2.0 MBq; radiochemical purity 95 %) at 5 and 60 min *p.i.* (mean±SD; n = 4).

In Wistar rats, first data of biodistribution as well as dynamic PET studies (Figs 2 and 3) are likely to reflect the high expression of tTG in epithelial tissue, particularly in lungs, liver and kidney [2].

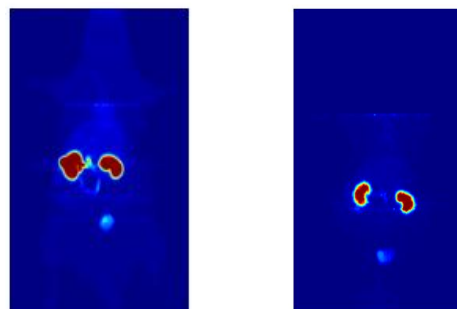


Fig. 2. *In vivo* distribution of [¹⁸F]FB putrescine (left) and [¹⁸F]FB spermine (right) in the rat at 45 min *p.i.*

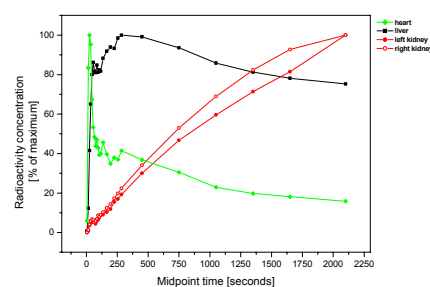
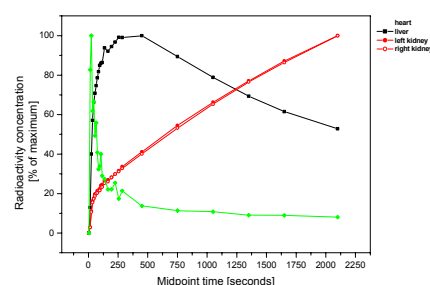


Fig. 3. Kinetics ([¹⁸F]FB putrescine, top; [¹⁸F]FB spermine, bottom) of the radioactivity derived from PET measurements for selected regions of interest. In a typical imaging experiment, 10 MBq of [¹⁸F]FB polyamine was administered as a 0.5 ml bolus injection to male Wistar rats. Data were acquired by the animal tomograph for 45 min post-injection in 21 frames divided as follows: 10 × 10 s, 6 × 30 s, 5 × 300 s, and 2 × 600 s. The volume of interest (heart, liver, kidneys) was centered in the 8 cm field of view. Data were reconstructed using the OSEM algorithm into images with 128 voxels × 128 voxels × 63 voxels, using a voxel size of 0.5 mm × 0.5 mm × 1.2 mm.

In conclusion, [¹⁸F]fluorobenzoylation of polyamines putrescine and spermine, respectively, and the use of high resolution animal PET are supposed to be a valuable approach to mapping sites of tTG activity and expression in animal models *in vivo*.

References

- [1] Knop, K. *et al.*, *this report*, p. 36.
- [2] Pietzsch, J. *et al.*, *in preparation*.

Measurement of 5-Hydroxy-2-Aminovaleric Acid as a Specific Marker of Iron-Mediated Oxidation of Proline and Arginine Residues of Low Density Lipoprotein Apolipoprotein B-100 in Human Atherosclerotic Lesions

J. Pietzsch, R. Bergmann

γ -Glutamyl-semialdehyde (γ GSA) is a major product of iron-mediated oxidation of apolipoprotein (apo) B-100 proline and arginine residues. By reduction γ GSA forms 5-hydroxy-2-aminovaleric acid (HAVA). HAVA levels were markedly increased in LDL from early (10.25 ± 3.49 mol/mol apoB-100; $P < 0.01$), intermediate (11.18 ± 2.37 mol/mol apoB-100; $P < 0.01$), and advanced (9.91 ± 2.15 mol/mol apoB-100; $P < 0.01$) lesions, when compared with LDL from normal aortic tissue (0.05 ± 0.01 mol/mol apoB-100). These findings support the hypothesis that pathways involving iron-mediated oxidation of LDL apoB-100 are of pathological significance for atherogenesis.

Introduction

Oxidative modification of LDL apoB-100 is regarded as a crucial event in atherogenesis. Direct oxidation of apoB-100 amino acid residues finally results in the formation of new epitopes that are specifically recognized by scavenger receptors [1]. There is effectual evidence supporting the hypothesis that among important mechanisms of apoB-100 oxidation are metal-catalyzed processes [3]. These processes involve binding of either free or, physiologically more relevant, complexed (porphyrin-bound) redox-active iron ($\text{Fe}^{2+}/\text{Fe}^{3+}$) to discrete binding sites of LDL and apoB-100, respectively, thus forming centers for redox cycling and repeated radical production. A major product of iron-mediated protein oxidation is γ GSA, which by reduction forms HAVA [1]. In the present study we used specific GC-MS methodology to demonstrate that levels of HAVA are markedly elevated in LDL apoB-100 recovered from human aortic vascular lesions. Lesion LDL were isolated from the intima of normal and atherosclerotic specimen of human thoracic aortas obtained at necropsy within 10 h of sudden death (20 male accident victims, aged 26 to 45 years; no signs of severe acute diseases). Aortic intima was dissected from the medium and homogenized for 2 h at 4°C (30 mg wet tissue/mL phosphate buffered saline, pH 7.2). All buffers and solutions were degassed and stored under argon. Lesion LDL were then isolated by very fast ultracentrifugation [1]. Delipidation of LDL, formation of HAVA by reduction of γ GSA with sodium borohydride, enzymatic hydrolysis of apoB-100, isolation and derivatisation of free amino acids, and GC-MS analysis were performed as described elsewhere [1]. HAVA content in all samples is expressed as mol/mol apoB-100.

Results and Discussion

Fig. 1 shows the HAVA content in aortic intima from various stages of lesion evolution. The HAVA content was significantly higher in LDL recovered from all types of lesion when com-

pared with normal aortic tissue (paired Student's *t* test). The overall yield of HAVA that has been found in lesion LDL is remarkably high and indicates that proline and arginine residues are good targets for iron-mediated oxidative attack in atherosclerotic tissue. HAVA content in both atherosclerotic and normal aortic tissue exceeded the physiological level of HAVA formerly found in native LDL obtained from healthy normolipidemic subjects (0.012 ± 0.004 mol/mol apoB-100) [1]. The experiments support the hypothesis that a pathway involving iron-mediated oxidation of LDL apoB-100 may be of pathological significance for atherogenesis [2]. However, additional work is needed to understand the specific consequences of γ GSA formation for the metabolic fate of apoB-containing lipoproteins *in vivo*.

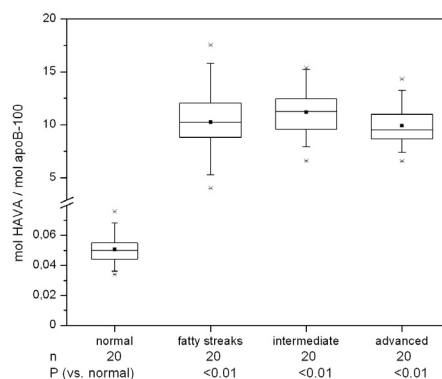


Fig. 1. Boxplots showing LDL apoB-100 HAVA content in intima from various stages of lesion evolution in human thoracic aorta. Normal and atherosclerotic tissue (fatty streaks, intermediate, and advanced plaques) was classified according to the criteria of the *Pathobiological Determinants of Atherosclerosis in Youth Study* [3].

References

- [1] Pietzsch, J., *Biochem. Biophys. Res. Comm.* 270 (2000) 852-857.
- [2] Pietzsch, J. *et al.*, *J. Clin. Pathol.* 56 (2003) 622-623.
- [3] PDAY Research Group., *Arterioscler. Thromb.* 13 (1993) 1291-1298.

Increased Cholesteryl Ester Transfer Protein (CETP) Activity in Impaired Glucose Tolerance: Relationship to High Density Lipoprotein Metabolism

J. Pietzsch, S. Nitzsche¹, K. Fuecker¹

¹Lipoprotein Laboratory, Department of Internal Medicine, Medical Faculty, University of Technology Dresden

Introduction

Impaired glucose tolerance (IGT) is characterized by insulin resistance and hyperinsulinemia and is associated with dyslipidemia (elevated plasma triglycerides, decreased high density lipoprotein (HDL) levels, and a preponderance of smaller, more dense low density lipoprotein (LDL) particles). Our previous studies focused on the regulation of HDL metabolism in subjects with IGT. By investigating the *in vivo* kinetics of HDL apolipoproteins (apo) A-I and A-II using a stable isotope approach, we demonstrated that increased catabolism of HDL apoA-I in IGT was related to the increased triglyceride content of HDL particles and accounted for lower HDL levels. In this context, increased fasting cholesteryl ester transfer protein (CETP) activity appeared to be directly associated with HDL apoA-I catabolism and with plasma and HDL triglycerides. CETP facilitates the exchange of neutral lipids among plasma lipoproteins. This results in net transfer of cholesteryl esters from HDL to triglyceride-rich lipoproteins in exchange for triglycerides. This redistribution process should have consequences for HDL composition and consequently for the HDL metabolism. Indeed, increased CETP activity in humans has been reported in several metabolic disorders with low HDL cholesterol, including type 1 diabetes, overt type 2 diabetes, obesity, nephrotic syndrome, and hypercholesterolemia. The present study was designed to further explore the mechanisms and dynamics of cholesteryl ester transfer and their specific link with low plasma HDL concentrations and an altered HDL composition under insulin resistant / hyperinsulinemic conditions [1].

The CETP activity in 44 non-obese, normo- or mildly hypertriglyceridemic IGT subjects (plasma triglycerides 1.56 ± 0.64 mmol/l; HDL cholesterol 0.96 ± 0.25 mmol/l; plasma insulin 78 ± 8 pmol/l) and in 42 normoglycemic controls (0.88 ± 0.41 mmol/l, $p < 0.05$; 1.48 ± 0.29 mmol/l, $p < 0.05$; 38 ± 14 pmol/l, $p < 0.01$) was measured using a new fluorometric assay [1].

Results and Discussion

CETP activity was elevated in IGT subjects by 47 % (39.5 ± 7.8 vs. 26.8 ± 6.8 nmol/ml \times h⁻¹, $p < 0.05$). Linear regression analysis showed that CETP activity in IGT subjects is significantly correlated with the following parameters:

plasma triglycerides ($\rho = 0.614$, $p < 0.05$), HDL-triglycerides ($\rho = 0.595$, $p < 0.05$), HDL-triglyceride % ($\rho = 0.667$, $p < 0.05$), HDL cholesterol ester % ($\rho = -0.751$, $p < 0.01$), HDL phospholipid % ($\rho = 0.648$, $p < 0.05$), 2-h-insulin ($\rho = 0.668$, $p < 0.05$), and 2-h-proinsulin ($\rho = 0.658$, $p < 0.01$). In a subgroup of 13 IGT subjects, CETP activity correlated with HDL apoA-I fractional catabolic rate ($\rho = 0.701$, $p < 0.01$). In normoglycemic controls significant correlations were only seen between CETP activity and HDL-triglyceride % ($\rho = 0.541$, $p < 0.05$), HDL cholesteryl ester % ($\rho = -0.639$, $p < 0.01$), 2-h-proinsulin ($\rho = 0.642$, $p < 0.05$), and HDL apoA-I fractional catabolic rate ($n = 10$, $\rho = 0.587$, $p < 0.05$) [1]. This study showed that fasting CETP activity, measured by a new fluorescent spectrophotometric method, was significantly increased in normo- or mildly hypertriglyceridemic subjects with IGT. The assay used measured CETP activity as the specific cholesteryl linoleate transfer from HDL (donor) particles to VLDL (acceptor) particles. By using this method and VLDL- and LDL-depleted plasma as the CETP source, the influence of endogenous lipoproteins was avoided. The CETP activity therefore reflected more likely the CETP mass. CETP activity was directly associated with parameters highly indicative for an insulin resistant / hyperinsulinemic situation. Furthermore, we found CETP activity to be directly associated with parameters of HDL particle composition, particularly with the HDL triglyceride and cholesteryl ester content. In conclusion, our observations suggest that neutral lipid transfer mediated by CETP is crucial for the modification of HDL composition in subjects with IGT. Under insulin resistant/hyperinsulinemic conditions, increased CETP activity modulates HDL metabolism more drastically than in normoglycemic conditions. This modulation may be explained by the increased availability of triglyceride-rich lipoproteins for neutral lipid exchange in IGT. As a consequence, HDL cholesterol is decreased in IGT. Low HDL is an integral part of the atherogenic lipoprotein phenotype in diabetic and prediabetic states [1].

Reference

- [1] Pietzsch, J. *et al.*, Croat. Med. J. 44 (2003) 171-177.

RADIOMETAL THERAPEUTICS

Novel Procedures for Preparing '4+1' ^{188}Re Complexes

S. Seifert, E. Schiller, H.-J. Pietzsch

Improved methods for the preparation of '4+1' ^{188}Re mixed ligand complexes are presented. The use of copper isocyanide complexes facilitates storage stability and allows kit formulations. Moreover, the formation of ^{188}Re complexes in acidic solution becomes possible using that stabilised form of isocyanides.

Introduction

'4+1' $^{99\text{m}}\text{Tc}$ complexes are prepared following a two-step procedure to prevent the formation of reduced hydrolysed species [1]. At first, the precursor complex $^{99\text{m}}\text{Tc-EDTA}$ is formed in neutral solution. In a second step it reacts with optimised ligand amounts to the desired '4+1' complex. Attempts to prepare the corresponding ^{188}Re complexes were only successful using phosphines as monodentate ligands. '4+1' isocyanide complexes were not formed following this reaction route. They could be prepared in low yields only in neutral solutions from the phosphine complexes by ligand exchange reaction. The aim of this work was to establish suitable preparation conditions for both phosphine and isonitrile '4+1' ^{188}Re complexes.

Results and Discussion

The comparable tendency of ^{188}Re to form reduced hydrolysed species requires the two-step procedure too. However the preparation of $^{188}\text{Re-EDTA}$ failed in neutral solution, but it succeeds in acidic solution at room temperature using the following kit formulation:

A mixture of 3–5 ml perrhenate eluate and 0.5 ml of 0.1 N HCl is added to a vial containing 5 mg EDTA, 5 mg mannitol, and 1.0 mg SnCl_2 in freeze-dried form under nitrogen. After standing for 10 min yields of >95 % are obtained.

Lower Sn^{2+} concentrations or pH-values >3 lead to incomplete reduction of perrhenate. The addition of both ligands for the second step of reaction has to occur in the acidic solution. That was unproblematically in case of phosphines. However, isocyanides are not stable under acidic conditions, but react with water to give the corresponding formamide and finally the amine. The use of copper isocyanide complexes widely prevents the degradation of isocyanides and allows so the preparation of the corresponding '4+1' ^{188}Re complexes in a two-step procedure. Moreover it allows to prepare freeze-dried kit formulations as following:

The complex $[\text{Cu}(\text{TBI})_4]\text{Cl}$ (TBI = *tert.* butyl isonitrile) was prepared and for optimum reaction conditions per vial 0.05 mg of the copper complex was lyophilized together with 0.1 mg of NS_3 -oxalate. For reconstitution the $^{188}\text{Re-EDTA}$ solution was added with a syringe to the kit vial and the '4+1' ^{188}Re complex was formed

with yields of 85-90 % by incubation the reaction solution for 30 min at 90 °C or 60 min at 50 °C.

The preparation of the corresponding $^{99\text{m}}\text{Tc}$ complexes at room temperature for 30–45 minutes or by heating at 50 °C for 15 minutes leads to yields of 90-97 % determined by HPLC.

The novel two-step procedure allows "kit-like" preparations of '4+1' $^{99\text{m}}\text{Tc}$ and ^{188}Re complexes. Using oxalate salts of NS_3 -ligands and copper isocyanide complexes or phosphonium salts as monodentate ligands, kit formulations can be prepared and reconstituted with per-technetate or perrhenate in high yields. Only micromolar amounts of the monodentate ligand are needed and that results in high specific activity labelling of interesting molecules. The reduction of perrhenate has to be performed in acidic solutions and needs more quantities of EDTA and of the reducing agent stannous chloride, but not of the NS_3 ligand and the isocyanide or phosphine. Thus, high labelling yields are possible at low ligand concentration also with ^{188}Re . Reactions were performed with both NS_3 and its carboxylic derivative, the latter allows to control lipophilicity [2]. Examples are shown in Table 1.

Table 1. Partition coefficients log P (octanol/0.1 M phosphate buffer pH 7.4) of '4+1' $^{99\text{m}}\text{Tc}$ and ^{188}Re complexes (n = 3)

Ligands		Log P	
tetradentate	monodentate	$^{99\text{m}}\text{Tc}$	^{188}Re
NS_3	PPh_3	1.83	1.78
NS_3COOH	PPh_3	1.54	1.01
NS_3	PMe_2Ph	1.27	1.25
NS_3COOH	PMe_2Ph	1.10	0.96
NS_3	TBI	1.28	1.14
NS_3COOH	TBI	0.31	0.46
NS_3	MIBI	1.35	1.34
NS_3COOH	MIBI	-0.42	-0.27

References

- [1] Seifert, S. *et al.*, *Annual Report 2001*, FZR-340, p. 49.
- [2] Schiller, E. *et al.*, *this report*, p. 44.

Hydrophilic Rhenium-188 Complexes for Attaching the Metal to Biomolecules

1. General Considerations

E. Schiller, H.-J. Pietzsch, H. Spies

In efforts to find appropriate ligands forming rhenium-188 complexes with high in vitro and in vivo stability, the '4+1' mixed ligand approach is a suitable tool to achieve this goal.

Introduction

Rhenium-188 is an attractive candidate for therapeutic applications in oncology due to its nuclide properties ($E_{\beta\text{max}} = 2,1 \text{ MeV}$, $t_{1/2} = 16,9 \text{ h}$) and its daily availability from a $^{188}\text{W}/^{188}\text{Re}$ generator [1, 2]. Target-specific radiotherapeutics must be developed to spare healthy tissue from irradiation. This can be achieved by linking the radionuclide to biomolecules.

One approach for attaching rhenium-188 to biomolecules is the '4+1' mixed ligand concept [3]. Here the metal is coordinated at oxidation state +III by the tetradentate chelator tris-(2-mercaptoethyl)amine (NS_3) and a phosphine or isonitrile as monodentate ligand. This ligand also serves as a linker for coupling target-searching biomolecules such as peptides, antibodies and oligonucleotides (Fig. 1).

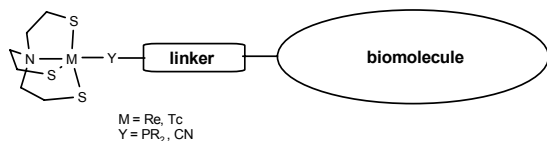


Fig. 1. The '4+1' mixed ligand approach.

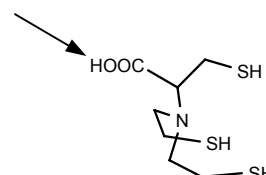
To achieve a fast renal clearance of radioactive metabolites and to minimize exposure of radiation-sensitive organs we searched for hydrophilic complexes derived from hydrophilic NS_3 -ligands and linkers for the '4+1' approach. Furthermore, ligands should bind to the rhenium central atom in a radiolytic and metabolic stable way and they must have an anchor group for attaching biomolecules.

Results

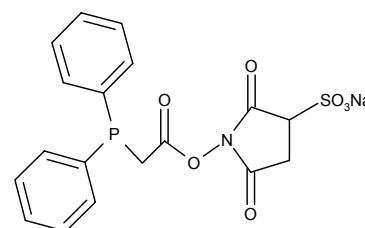
To meet these requirements we synthesized three novel ligands for the '4+1' approach:

- a carboxyl group-containing tripodal tetradentate ligand (1),
- a sulfohydroxysuccinimidyl active ester of carboxymethyl diphenylphosphine (2) and
- a hydroxymethylene-functionalized phosphine (3).

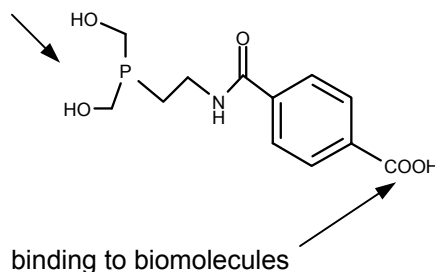
- (1) increase of hydrophilicity/binding to biomolecules



- (2)



- (3) increase of hydrophilicity



For description of the syntheses and further investigations see [4].

References

- [1] Knapp, F. F. *Cancer Biotherapy & Radiopharmaceuticals* 13 (1998) 337.
- [2] Blower, P. J. *et al.*, *Perspectives on Bioinorganic Chemistry* 4 (1999) 91.
- [3] Pietzsch, H.-J. *et al.*, *Bioconjugate Chem.* 12 (2001) 538.
- [4] Schiller, E. *et al.*, *this report*, p. 45.

Hydrophilic Rhenium-188 Complexes for Attaching the Metal to Biomolecules

2. Synthesis and Characterisation of a Novel Hydrophilic Ligand

E. Schiller, W. Kraus¹, H.-J. Pietzsch, H. Spies
¹Bundesanstalt für Materialforschung und -prüfung, Berlin

A synthetic route for a novel carboxyl group-containing ligand derived from tris-(2-mercaptoethyl)amine was developed. A '4+1' model complex with the new ligand was synthesized and characterized by X-ray diffraction.

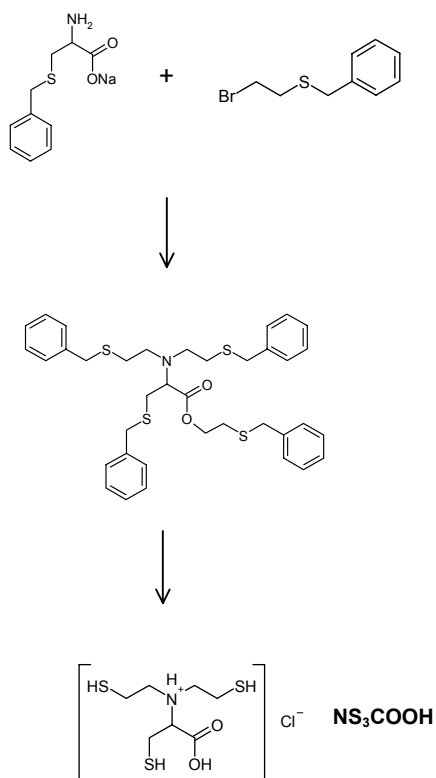
Introduction

Until now '4+1' complexes of technetium and rhenium with the tris-(2-mercaptoethyl)amine chelator (NS₃) and several isocyano or phosphine ligands are predominantly of lipophilic nature. Development of more hydrophilic ligands aims at fast renal excretion of radioactive metabolites as well as at radiolabelling of biomolecules like antibodies and peptides in aqueous solution [1].

Introduction of a carboxyl group into the NS₃ framework may lead firstly to an increase of hydrophilicity and gives secondly the opportunity to attach biomolecules via an amide bond.

Results and Discussion

The carboxyl group-containing ligand NS₃COOH was prepared by double alkylation of a cysteine derivative followed by hydrolysis of the ester bond and deprotection of the mercapto groups.



The ligand was characterised as hydrochloride by ¹H NMR, ¹³C NMR and mass spectrometry.

A rhenium model complex was synthesized by a similar method to that previously reported by Spies *et al.* [2]. Ammonium perrhenate, NS₃COOH and an excess of triphenylphosphine PPh₃ was refluxed in acetonitrile under argon for two hours. The complex was obtained as dark-green needles.

The X-ray crystal structure analysis shows a trigonal-bipyramidal geometry around the metal centre. S- and R-isomers were found. Obviously, racemization occurs despite starting from S-cysteine.

Fig. 2 shows the molecular structure of the S-isomer of [Re(NS₃COOH)PPh₃].

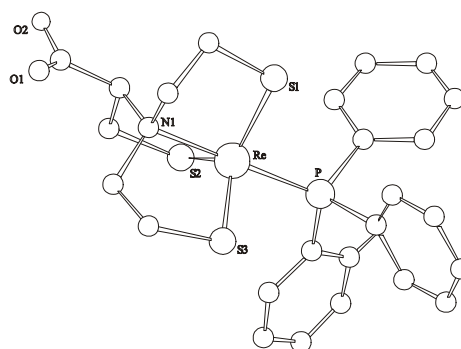


Fig. 2. Molecular structure of the S-isomer of [Re(NS₃COOH)PPh₃]

References

- [1] Schiller, E. *et al.*, *this report*, p. 44.
- [2] Spies, H. *et al.*, *Inorg. Chim. Acta* 240 (1995) 465.

Hydrophilic Rhenium-188 Complexes for Attaching the Metal to Biomolecules

3. Physicochemical and Biological Evaluation of Model Complexes

E. Schiller, S. Seifert, R. Bergmann, H.-J. Pietzsch, H. Spies

Technetium-99m '4+1' complexes derived from the novel carboxyl group-containing ligand NS₃COOH and tris-(2-mercaptoethyl)amine NS₃, respectively, serving as surrogates for ¹⁸⁸Re complexes, were compared concerning their lipophilicity and behaviour in vivo.

Introduction

The introduction of a carboxyl group into tris-(2-mercaptoethyl)amine (NS₃) aims at hydrophilic water-soluble rhenium-188 complexes with enhanced renal excretion.

Both technetium and rhenium complexes exhibit similar physicochemical and biological properties. The evaluation of '4+1' complexes derived from the novel ligand NS₃COOH in comparison with complexes derived from the NS₃ ligand was carried out with technetium-99m complexes because they are easier to prepare and to handle than their rhenium-188 analogues.

Results and Discussion

The preparation of the technetium complexes was described elsewhere [1]. At first the octanol/water partition coefficient at physiological pH was determined to study the influence of the carboxyl group on lipophilicity. Fig. 1 shows the log D values at pH 7.4 of the NS₃COOH complexes in comparison with their NS₃ analogues. As expected the carboxyl group highly controls the lipophilicity. Especially complexes with ether-derivatised monodentate ligands (TMPP, MIBI) or a small isonitrile (TBI) show increased hydrophilicity. The effect is less intensive using small phosphines as monodentate ligands (PMe₂Ph, PPh₃).

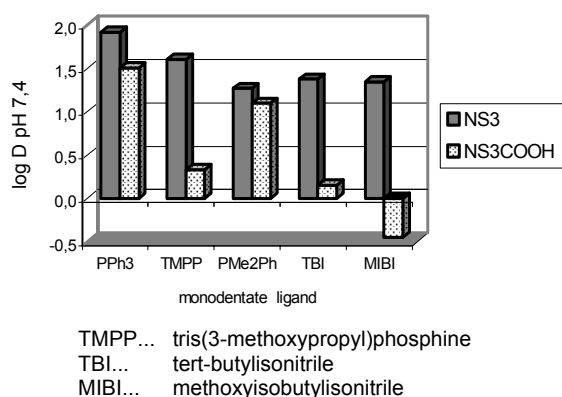


Fig. 1. Octanol/water partition coefficients of '4+1' model complexes.

Biodistribution studies were done to evaluate the influence of introducing the COOH group into the tripodal ligand on excretion. Three technetium-99m complexes with NS₃COOH and different monodentate ligands (MIBI, TBI, PMe₂Ph) were compared with their NS₃ analogues. As an example the biodistribution of complexes with MIBI as monodentate ligand is shown in Fig. 2.

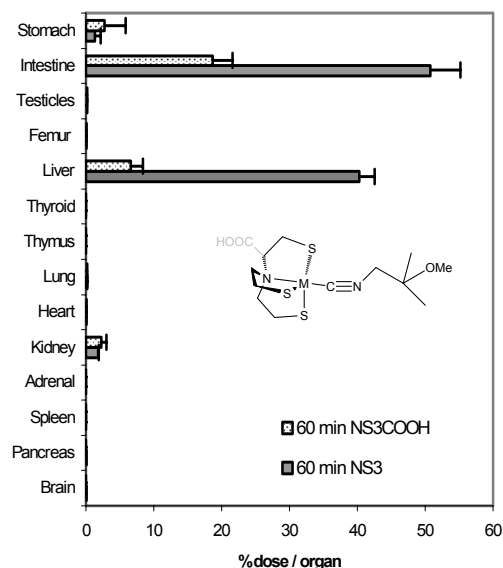


Fig. 2. Biodistribution of '4+1' model complexes with and without carboxyl group one hour post injection in male Wistar rats.

The biodistribution experiments in male Wistar rats showed the expected differences. The radioactivity level of carboxyl group-containing '4+1' complexes in the liver is decreased and a faster renal clearance is observed. The influence is weaker when PMe₂Ph and TBI are used as monodentate ligands. Considering these results our current work is focussed on the development of more hydrophilic monodentate ligands.

Reference

[1] Seifert, S. *et al.*, Annual Report 2001, FZR-340, p. 49.

Routes to Modification of Rhenium Cluster Core Ligand Environment with Organic Ligands

K. Brylev¹, H.-J. Pietzsch, H. Stephan, V. E. Fedorov, H. Spies
¹Institute of Inorganic Chemistry, Russian Academy of Science, Novosibirsk, Russia

Main goal of this investigation is the synthesis of octahedral Re cluster core containing complexes with organic ligands which will be soluble in water and stable in vivo.

Introduction

The investigations for modification of octahedral cluster core ligand environment are intended to make available metal clusters that allow to deposit metals such as molybdenum or rhenium in high density in animal cells. Sufficient metal concentration is a prerequisite for a high efficacy of subsequent irradiation by monochromatic photons that will activate the metal to emit Auger electrons. These electrons lead to the damage of the targeted cells. This procedure is known as Photon Activation Therapy (PAT) [1].

In this context, polynuclear metal compounds may have considerable potential as metallic drugs. So, some types of polyoxometallates (derived from Mo, W, Re and others) are able to be transported into cells and mitochondria, in particular. Some of these representatives show antiviral and antitumor properties. Multi-nuclear metal compounds such as clusters may have also good properties to deposit the respective metal in high density in the target cells.

Discussion

Octahedral clusters of rhenium were intensively studied in last years [2]. The main goal of our further investigations is the modification of ligand environment of cluster core with organic ligand in chalcogenide anionic cluster complexes $[\text{Re}_6(\mu_3\text{-Q})_8\text{Br}_6]^{n-}$ (Q = S, Se; n = 3 or 4). In such complexes Re_6 octahedron (Fig. 1a) is inscribed into a cube of eight $\mu_3\text{-Q}$ atoms (inner ligands). Such "octahedron into cube" forms cluster core $[\text{Re}_6(\mu_3\text{-Q})_8]$ (Fig. 1b). The six apical positions are fully occupied by Br atoms (Fig. 1c). The anticipated substitutional lability of these outer bromide ligands makes $[\text{Re}_6(\mu_3\text{-Q})_8\text{Br}_6]^{n-}$ clusters a reasonable point of departure for synthesis cluster complexes with organic apical ligands in which $[\text{Re}_6\text{Q}_8]$ core is viewed as the fundamental building block.

From recent investigations it is known that nitrogen and phosphorous can prove themselves as donor atom of organic apical ligands [3]. For obtaining cluster complexes with organic ligands different approaches were used: a) substitution apical halogen ligands by strong nucleophilic organic ligands in solution;

b) removal apical halogen ligands using Ag^+ in presence of organic ligand which can coordinate to Re;

c) substitution loosely ligated apical ligands in cluster complexes.

It is important to note that up to now all reactions of substitution apical halogen ligands in cluster core described in literature, were carried out in solution and as starting compounds the salts with oxidated cluster anions $[\text{Re}_6\text{Q}_8\text{L}_6]^{3-}$ (Q = S, Se; L = Cl, Br, I) were used (most part of investigations was applied to selenium halogenide cluster complexes of rhenium).

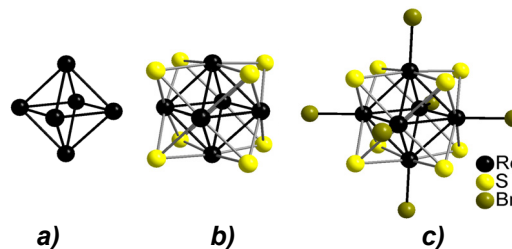


Fig. 1. Structure of cluster anion $[\text{Re}_6\text{Q}_8\text{Br}_6]^{n-}$

It is possible to suppose that in reactions of ligand substitution not oxidated cluster anions $[\text{Re}_6\text{Q}_8\text{L}_6]^{4-}$ can be involved. Very likely that special approach can be used for such reactions. One of the possible approaches is reaction with melted ligands. In this case it is necessary to use ligands which are stable in melt such as of 3,5-dimethylpyrazole (Fig. 2a) or 1H-benzotriazol (Fig. 2b).

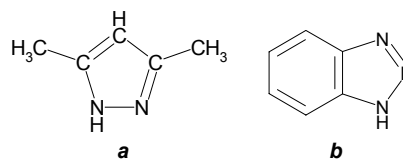


Fig. 2. Structure of 3,5-dimethylpyrazole (a) and 1H-benzotriazol (b).

References

- [1] Larsson, B. *Hadrontherapy in Oncology*. In: U. Amaldi and B. Larsson (Eds.), Elsevier (1994) p. 33.
- [2] Mironov, Y. V. *et al.*, J. Am. Chem. Soc. 119 (1997) 493.
- [3] Zheng, Z. P. *et al.*, J. Am. Chem. Soc. 119 (1997) 2163.

Characterization of Cu(II)-Cyclam Complexes by Laser-Induced Fluorescence Spectroscopy

D. Appelhans¹, D. Tabuani¹, B. Voit¹, G. Geipel², G. Bernhard², H. Spies, H. Stephan
¹Institut für Makromolekulare Chemie, IPF Dresden; ²Institut für Radiochemie

Time-resolved laser-induced fluorescence spectroscopy (TRFLS) has been used to study the interaction of copper(II) with different cyclam derivatives. The fluorescence emission and lifetime are strongly dependent on the structure of the complexes formed.

Introduction

Copper complexes with cyclam **1** have applications in radiopharmaceutical chemistry [1-3]. We have chosen cyclam as core unit for the synthesis of novel dendritic molecules. Here, we want to report on the spectroscopic (TRFLS) properties of star-like cyclams **2** and **3**.

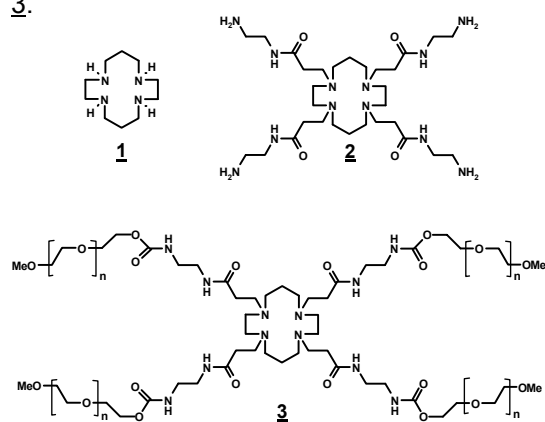


Fig. 1. Cyclam derivatives investigated

Results and Discussion

Cyclam **1** was purchased from Aldrich. **2** was prepared according to the known procedure [4]. The PEG (polyethylene glycol having an average molecular weight of 550) appended cyclam derivative **3** was obtained via hydroxy group activation of polyethylene glycol using 4-nitrophenylchloroformate. This intermediate was finally treated with the cyclam tetraamine **2**. To form the copper complexes, $\text{Cu}(\text{CF}_3\text{SO}_3)_2$ dissolved in acetonitrile was added to a acetonitrile solution of cyclam derivative (0.023 M) until Cu was equimolar. The complexation process was maintained overnight at room temperature. TRFLS experiments were performed as described recently [5]. The excitation wavelength was set to be 266 nm. As can be seen from Fig. 2 the intensity of the emitted fluorescence signal increases with changes of the ligand. Also a change of fluorescence decay times and a small change of the maximum of the fluorescence emission was found. This can be interpreted by a decrease of the quench effect of the metal ion on the fluorescence of the ligand due to increasing shielding of the metal ion.

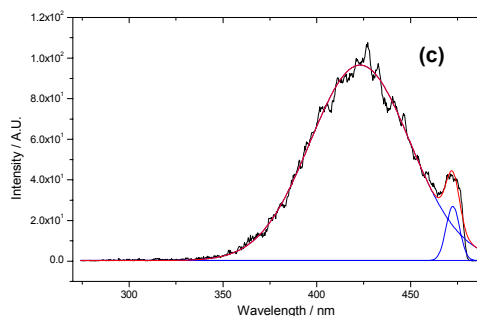
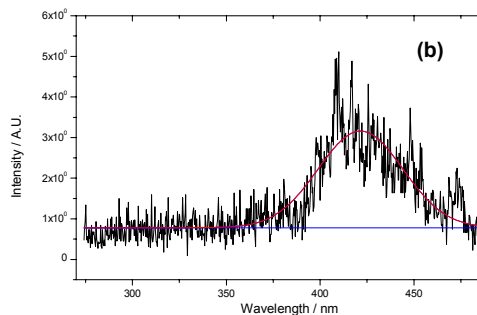
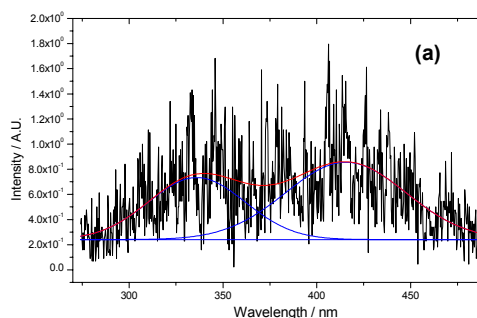


Fig. 2. Time resolved fluorescence spectra of **1** (a), **2** (b) and **3** (c) with $\text{Cu}(\text{CF}_3\text{SO}_3)_2$ in acetonitrile.

References

- [1] Parker, D., Chem. Soc. Rev. 19 (1990) 271-291.
- [2] Blower, P. J. et al., Nucl. Med. Biol. 23 (1996) 957-980.
- [3] Sun, X. et al., J. Med. Chem. 45 (2002) 469-477.
- [4] Zhuo, R. X. et al., J. Contr. Release 57 (1999) 249-257.
- [5] Geipel, G. Annual Report 2001, FZR-343, p. 7.

Calorimetric and Potentiometric Study of PAMAM Dendrimers: Protonation and Interactions with Human Serum Albumin

R. Kirchner¹, J. Seidel¹, H. Stephan, B. Johannsen

¹Institut für Physikalische Chemie, TU Freiberg

The protonation of dendrimers and their interactions with HSA were studied by combined potentiometric and calorimetric titration experiments. The thermodynamic data of protonation were calculated and assigned to the different protonable sites. No significant interactions of the PAMAM dendrimers with HSA could be detected.

Introduction

The particular structural features of dendrimers cause a rapidly expanding scientific as well as practical interest for dendritic molecules [1, 2], e.g. drug and gene delivery systems, contrast agent carrier, tumour targeting etc., and motivate to comprehensive investigations of the underlying physico-chemical processes. It is known that the structure and consequently, the complexation behaviour and interactions of dendrimers in solution strongly depend on the pH (degree of protonation of functional groups) and ionic strength [3]. This work presents results of potentiometric and calorimetric pH-titration experiments with aqueous solutions of polyamidoamino-based dendrimers (PAMAM) carrying different terminal functional groups (-NH₂, -OH, -COONa) and calorimetric results of their interactions with HSA.

Results and Discussion

The potentiometric titration curves (Fig. 1) can be adequately described using minimal three simultaneous protonation equilibria (three characteristic pK_a values). The results are consistent with the polyelectrolyte effect.

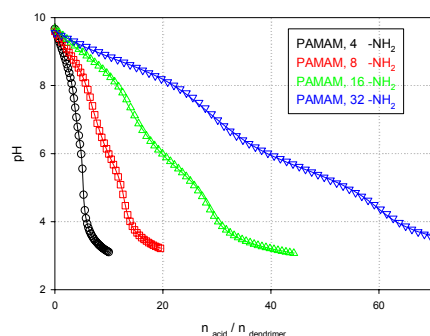


Fig. 1. Experimental (symbols) and calculated (lines) potentiometric titration curves.

The calorimetric titration results (Fig. 2) reflect the complex nature of the underlying processes more clearly. Despite of distinct steps in the calorimetric titration curves that can be assigned to different protonation equilibria, endothermic effects could be observed which are not yet fully understood. Therefore, a complete quantitative thermodynamic description of the calorimetric results based on protonation

equilibria (pK_a values from potentiometric experiments and protonation enthalpies as additional parameters) failed.

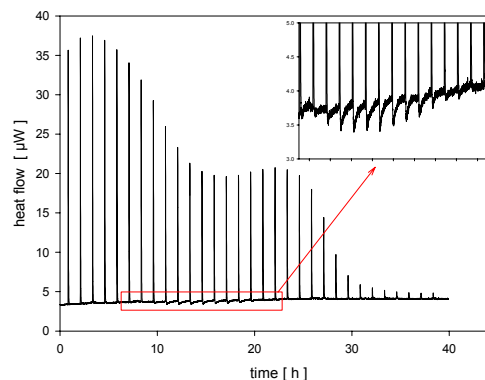


Fig. 2. Typical calorimetric titration results, (PAMAM-16-NH₂).

ITC studies of dendrimer-HSA-interactions at different pH levels (Fig. 3) show very small caloric effects for all types of dendrimers investigated (PAMAM-16-NH₂, PAMAM-16-COONa, PAMAM-16-OH) indicating very weak interactions. This finding is confirmed for the interactions of dendrimers with BSA [4].

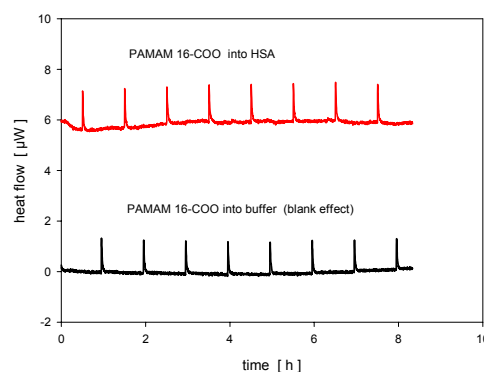


Fig. 3. Typical ITC results for the interaction of PAMAM's with HSA.

References

- [1] Fischer, M. *et al.*, *Angew. Chem.* 111 (1999) 76-94.
- [2] Stiriba, S.-E. *et al.*, *Angew. Chem.* 114 (2002) 1385-1390.
- [3] Koper, G. J. M. *et al.*, *J. Am. Chem. Soc.* 119 (1997) 6512-21.
- [4] Klajnert, B. *et al.*, *Bioelectrochem.* 55 (2002) 33-35.

Hydrolytic Stability of Polyoxotungstates

H. Stephan, D. John, A. S. Raji, A.-K. Sawatzki, L. Jelínek¹, P. Houserová¹, Z. Matějka¹
¹Institute of Chemical Technology Prague

The hydrolytic stability of four different polyoxotungstates has been investigated by UV/vis spectroscopy. It was found that $\text{Na}_6[\text{W}_{12}\text{O}_{39}]$ and $\text{K}_7[\text{Ti}_2\text{W}_{10}\text{PO}_{40}]$ are stable at $\text{pH} = 7.6$. In contrast to this, $\text{H}_3[\text{PW}_{12}\text{O}_{40}]$ and $(\text{NH}_4)_{18}[\text{NaSb}_9\text{W}_{21}\text{O}_{86}]$ are remarkably decomposed at physiologically relevant pH values.

Introduction

Polyoxometalates (POMs) show unique transport behaviour into living cells, and may act as antiviral and antitumoral agents [1]. Among a great variability of different metal clusters formed, *Keggin type* $[\text{XW}_{12}\text{O}_{40}]^x$, *double-Keggin type* $[\{\text{A}-\alpha\text{-SiO}_4\text{W}_9\text{O}_{30}(\text{OH})_3\text{M}_3\}_2(\text{OH})_3]^{11-}$ and *HPA-23* [2] seem to be the most important compounds for medical applications (Fig. 1). But there are only few information about the hydrolytic stability at physiologically relevant pH values.

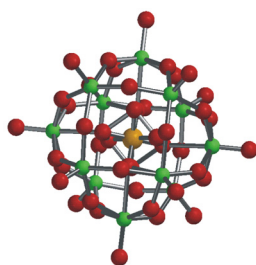


Fig. 1. X-ray structure of $[\text{PW}_{12}\text{O}_{40}]^{3-}$ [3]

Thus, we want to report on the stability of different POMs in aqueous solution using UV/vis measurements.

Results and Discussion

We have chosen four different POMs: $\text{Na}_6\text{W}_{12}\text{O}_{39}$ (Sigma-Aldrich), $\text{H}_3[\text{PW}_{12}\text{O}_{40}]$ (Fluka), HPA-23 (prepared according to [4]), and $\text{K}_7[\text{Ti}_2\text{W}_{10}\text{PO}_{40}]$ (prepared according to [5]). Owing to a characteristic $\text{O}_b \rightarrow \text{W}$ (O_b is bridging oxygen in W-O-W bond) charge transfer band (240...260 nm), UV/vis spectroscopy can be preferably applied to study the hydrolytic stability. This band disappears after degradation of the cluster structure to the WO_4^{2-} . First experiments were performed with aqueous solutions of POMs (10^{-5} M) at $\text{pH} = 7.4$ adjusted with 0.001 M NaOH. A remarkable pH drift into the acidic media was observed for $\text{H}_3[\text{PW}_{12}\text{O}_{40}]$ and HPA-23 indicating the decomposition of the polyanionic structure. On the other hand the initial pH of $\text{Na}_6[\text{W}_{12}\text{O}_{39}]$ and $\text{K}_7[\text{Ti}_2\text{W}_{10}\text{PO}_{40}]$ solutions remain almost constant. In order to compare the POMs investigated, buffered solutions were used. At first HEPES-NaOH buffer was applied. But the absorbance of this buffer lies very near to the

charge transfer band of the polyanion. The most reliable results were obtained with a HCl-borate buffer ($\text{pH} = 7.6$). Under these experimentally chosen conditions $\text{H}_3[\text{PW}_{12}\text{O}_{40}]$ and HPA-23 are rather unstable (Fig. 2). So, $\text{H}_3[\text{PW}_{12}\text{O}_{40}]$ is almost completely decomposed after 90 min. HPA-23 is stable for appr. 90 min. But a remarkable degradation was observed after 1 day.

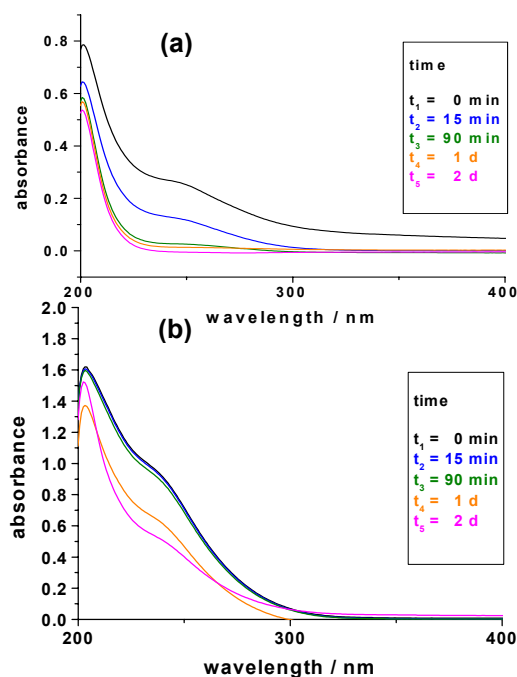


Fig. 2. UV/vis spectra of $\text{H}_3[\text{PW}_{12}\text{O}_{40}]$ (a) and HPA-23 (b) at $\text{pH} = 7.6$ (0.05 M HCl-borate buffer) for different times.

On the other hand, $\text{Na}_6[\text{W}_{12}\text{O}_{39}]$ and $\text{K}_7[\text{Ti}_2\text{W}_{10}\text{PO}_{40}]$ are very stable under these conditions. Thus, the absorbance of $\text{Na}_6[\text{W}_{12}\text{O}_{39}]$ and $\text{K}_7[\text{Ti}_2\text{W}_{10}\text{PO}_{40}]$ remains almost unchanged for three days pointing to a high hydrolytic stability.

References

- [1] Rhule, J. T. *et al.*, Chem. Rev. 98 (1998) 327-357.
- [2] $(\text{NH}_4)_{18}[\text{NaSb}_9\text{W}_{21}\text{O}_{86}]$: HPA-23 = heteropolyacid (23 represents sodium).
- [3] Gabriel, J.-C. P. *et al.*, J. Solid. State Chem. 129 (1997) 257.
- [4] Bountiff, L., *PhD Thesis* (1982), University of Reading.
- [5] Domaille, P. J. *et al.*, Inorg. Chem. 22 (1983) 818-822.

PET IN DRUG AND FOOD RESEARCH

Biodistribution and Catabolism of ^{18}F -Labelled Isopeptide N^ϵ -(γ -Glutamyl)-L-Lysine

C. Hultsch, R. Bergmann, B. Pawelke, F. Wüst, J. Pietzsch, T. Knieß, B. Johannsen, T. Henle¹

¹Institute of Food Chemistry, TU Dresden

After synthesis of fluorine-18 labelled analogues of N^ϵ -(γ -glutamyl)-L-lysine by conjugation with *N*-succinimidyl-4- ^{18}F fluorobenzoate, biodistribution and catabolism of these labelled compounds were studied.

Introduction

A peptide bond between the ϵ -amino group of lysine and the γ -carboxamide group of glutamine is called an isopeptide bond. Such isopeptide bonds are formed during strong heating of pure proteins or, more important, by enzymatic reaction mediated by transglutaminases [1]. Therefore transglutaminases are used in food biotechnology to modify certain properties of food, such as milk, meat or fish products [2]. Up to now little is known about the metabolic fate of this bond. For this reason biodistribution, catabolism and elimination of radioactive labelled N^ϵ -(γ -glutamyl)-L-lysine was investigated.

Results and Discussion

N-succinimidyl-4- ^{18}F fluorobenzoate was used to modify N^ϵ -(γ -glutamyl)-L-lysine at each of its two free α -amino groups. The coupling reaction resulted in the respective 4- ^{18}F fluorobenzoylated derivatives (Fig. 1), which were separated by semipreparative HPLC [3].

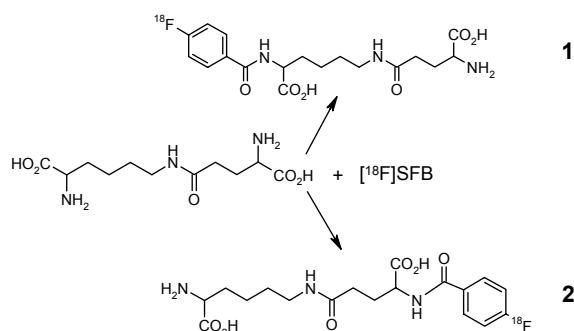


Fig. 1. Conjugation of isopeptide with ^{18}F SFB.

A quite different biochemical behaviour of the two labelled isopeptides was observed in Wistar rats. For compound **2** a strong accumulation in the kidneys was found while compound **1** was rapidly excreted through the kidneys into the urine (Figs. 2 and 3).

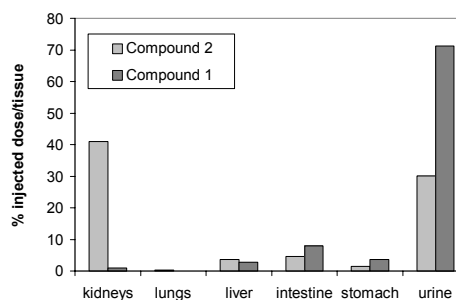


Fig. 2. Biodistributions (60 min p.i.).

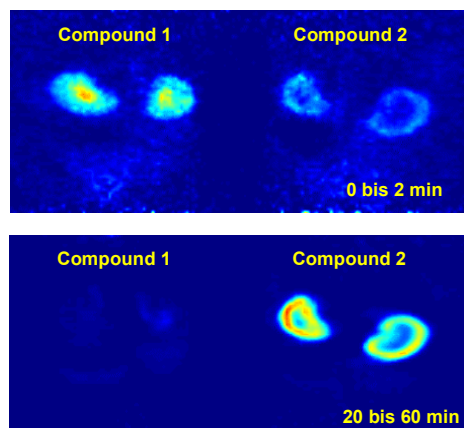


Fig. 3. Transversal plane of summed PET images.

Furthermore catabolism of the isopeptide derivatives was investigated. After application of compound **1** formation of 4- ^{18}F fluorobenzoylated lysine could be observed. Application of compound **2** also led to formation of metabolites but none of them was identified as the 4- ^{18}F fluorobenzoylated glutamate. These results suggest that cleavage of the isopeptide bond is possible if the γ -glutamyl moiety is not substituted. The metabolic fate of isopeptide should therefore be dependent on how it is reabsorbed – free or peptide bound.

References

- [1] Folk, J. E. *et al.*, *Adv. Protein Chem.* 31 (1977) 1-133.
- [2] Nielsen, P. M., *Food Biotechnology* 9 (1995) 119-156.
- [3] Wüst, F. *et al.*, *Appl. Radiat. Isot.* 59 (2003) 43-48.

CYCLOTRON OPERATION

Operation of the Rossendorf PET Cyclotron "CYCLONE 18/9" in 2003

St. Preusche, F. Wüst

Routine operation

The routine operation of the CYCLONE 18/9 for the production of radiopharmaceuticals started at the beginning of June 2003 after finishing the rebuilding of the radiopharmaceutical production laboratories due to stronger GMP rules. The radionuclides produced in routine operation in 2003 were F-18, C-11, O-15 available as $[^{18}\text{F}]\text{F}^-$, $[^{18}\text{F}]\text{F}_2$, $[^{11}\text{C}]\text{CO}_2$, and $[^{15}\text{O}]\text{H}_2\text{O}$. Table 1 gives an overview of the 2003 radionuclide production. There were no demands for production of ^{13}N .

The daily operating time of the CYCLONE 18/9 varied between two and four hours as ever.

In March 2003 we received a new operating licence from our authority. Now we are able to

- increase the maximum target activity produced by the ($\text{N}_2 + 1\% \text{O}_2$) target for the production of $[^{15}\text{O}]\text{H}_2\text{O}$
- use the solid target system [1] for the production of non-standard radionuclides
- produce ^{86}Y , ^{60}Cu , ^{61}Cu and ^{64}Cu with the solid target system.

First tests for the production of the radionuclide ^{86}Y have started in summer 2003.

Table 1. Radionuclide production in 2003

RN	Radionuclide production	
	Number of irradiations	SumA _{EOB} [GBq]
$[^{18}\text{F}]\text{F}^-$	253	7975
$[^{18}\text{F}]\text{F}_2$	133 ^{*)}	748
^{11}C	120	2336
^{15}O	53	1045
^{86}Y	4	1.7

^{*)}including pre-irradiations

Fig. 1 shows the number of irradiations of our radionuclides and Fig. 2 the total amount of activity produced from 1997 to 2003. The decrease in the produced activities (see Fig. 2) is due to five months without routine operation to produce radiopharmaceuticals at least.

Investigations at the cyclotron

- Beam tests on the solid target system

Comprehensive beam tests were carried out on the solid target system to find the optimum irradiation conditions for the production of ^{86}Y [2].

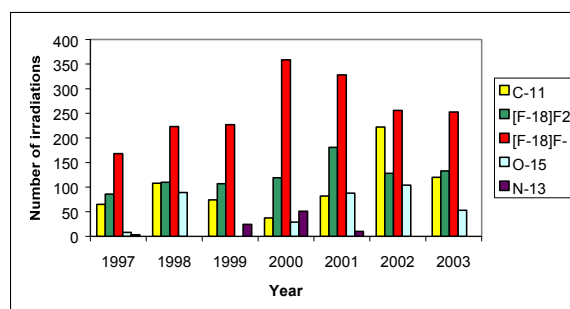


Fig. 1. Number of irradiations of radionuclides produced

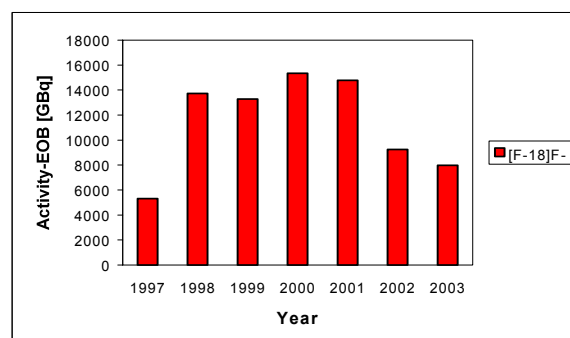
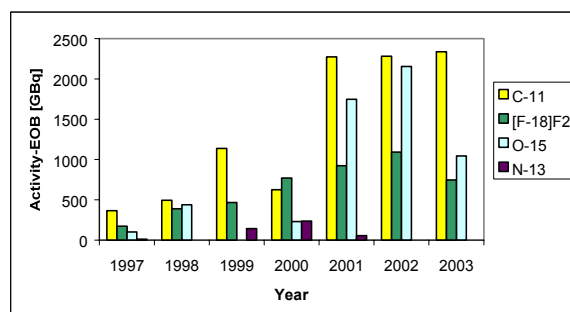


Fig. 2a, b. Total amount of activity produced

Maintenance and service

The main reasons for opening the cyclotron were maintenance and service work at both ion sources and destroyed stripper foils.

The annual check of the CYCLONE 18/9 facility by the TÜV Sachsen organization (TÜV = Association for Technical Inspection) under § 66 (2) of the Radiation Protection Regulation was carried out in the second half of September. There were no objections to the further operation of the cyclotron.

Radiation protection

- *Emission of radionuclides with the exhaust air*
The emission of radionuclides with the exhaust air is routinely monitored. As shown in Table 2, it is well below the limit of 2.0E11 Bq.

Table 2. Emission of radionuclides with the exhaust air in 2003 as a result of cyclotron operation

Radionuclide	Emission [Bq/a]
⁴¹ Ar	1.6E10
¹⁸ F	3.1E09
Sum	1.9E10
Percentage of the annual limit	9.7

- *Exposure to radiation of the cyclotron staff*

The cyclotron staff belong to category A of occupational exposed persons. The average exposure to radiation of the cyclotron staff over the years is shown in Table 3.

Table 3. Average exposure to radiation of the cyclotron staff

Year	Exposure [mSv]
1997	1.8
1998	2.9
1999	3.5
2000	6.2
2001	4.6
2002	1.7
2003	1.1*

*) 2003: (Jan. – Oct.)

References

- [1] Preusche, St. *et al.*, *Annual Report 2002*, FZR-363, p. 69.
- [2] Preusche, St. *et al.*, *this report*, p. 58.

Ion Beam Tests on the Solid Target System of the Rossendorf CYCLONE 18/9 Cyclotron

St. Preusche, H. Roß

Ion beam tests were carried out on the solid target system to find the optimum irradiation conditions for the production of the radionuclide ^{86}Y .

Introduction

The Rossendorf solid target system (see Fig. 1) [1] consists of an irradiation chamber to irradiate targets with rectangular shape (*rectangle targets*) and a module connected to the chamber to irradiate targets with circular shape (*disk targets*).

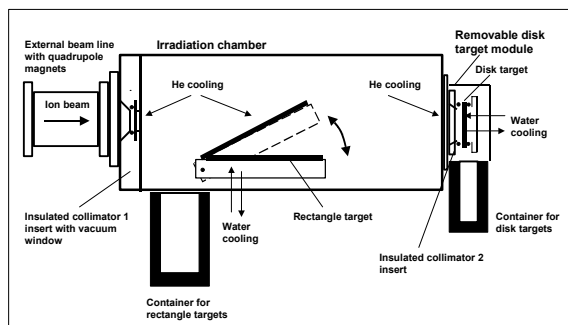


Fig. 1. Principle of the solid target system

After receiving the new licence for routine operation of the CYCLONE 18/9 in March 2003 ion beam tests on both target systems were carried out to find the optimum irradiation conditions for the production of non-standard PET radionuclides. The main topic was turned towards the disk target for the production of ^{86}Y . All tests were done with proton beam.

Ion beam on the disk target

To irradiate the disk target the target holder of the rectangle target must be in the horizontal position. A disk target area of only 12 mm in diameter was chosen due to the expensive target material though the diameter of the proton beam is larger than 15 mm. Unavoidable beam losses were accepted.

Ion beam currents were measured on the stripper foil (I_S), the collimator 1 (I_{C1}) and on the target (I_T).

Operating conditions

Accelerating parameters

$I_{MAG} = 195.5 \text{ A}$, $U_{DEE} = 30.8 \text{ kV}$,

$I_S = 200 \text{ mA}$

Focusing conditions (quadrupole magnets of the external beam transport line)

$I_{QM1} = 98.8 \text{ A}$, $I_{QM2} = 86.0 \text{ A}$

Ion beam currents

$I_S \sim 43 \mu\text{A}$, $I_{C1} = 23 \mu\text{A}$, $I_T = 8 \mu\text{A}$.

Results

Extraction ratio: $I_T / I_S \sim 20 \%$

$I_T = (10 - 13) \mu\text{A}$ are possible on the disk target. Fig. 2 shows the result of a test irradiation on the disk target with typical parameters monitored in the 'real current display window' of the control computer.

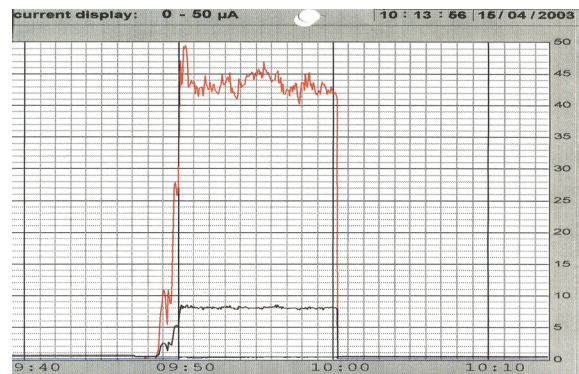


Fig. 2. Plot of the 'real current display window'
 $I_S \sim 43 \mu\text{A}$, $I_T = 8 \mu\text{A}$

Ion beam on the rectangle target

The rectangle target was planned to irradiate sensitive target materials. The angle between the target and the ion beam is variable to enlarge the beam area on the target and thus reduce the beam density. The target holder plate has an area of $(85 \times 35) \text{ mm}^2$ with an usable target area of maximum $(65 \times 15) \text{ mm}^2$.

The accelerating and focusing conditions of the proton beam were similar to those during the irradiation of the disk target.

Results

Extraction ratio: $I_T / I_S \sim 40 \%$. There are less beam losses than for the disk target.

$I_T \sim 15 \mu\text{A}$ are possible on the rectangle target.

Reference

[1] Preusche, St. *et al.*, *Annual Report 2002*, FZR-363, p. 69.

Factors Affecting the Specific Activity of [¹⁸F]Fluoride from a Water Target

F. Füchtner, S. Preusche, J. Steinbach

Introduction

The reaction $^{18}\text{O}(p,n)^{18}\text{F}$ is the method of choice for routine production of n.c.a. [¹⁸F]fluoride to synthesize labelled compounds as well as on high activity level and with high specific activity (SA). For quite a few PET radiopharmaceuticals the SA has to be high in order to prevent physiological response at the studied system (e.g. agonistic and toxic effects). We found that the SA shows considerable variation, as also reported in the literature [1-3]. The SA of the radiopharmaceutical mainly depends on the SA of the [¹⁸F]fluoride used for the syntheses. Initial investigations indicated that the main origin of ¹⁹F is the [¹⁸O]water dispensing and delivery system of the target (see Fig. 1) and is not originated from the starting [¹⁸O]water.

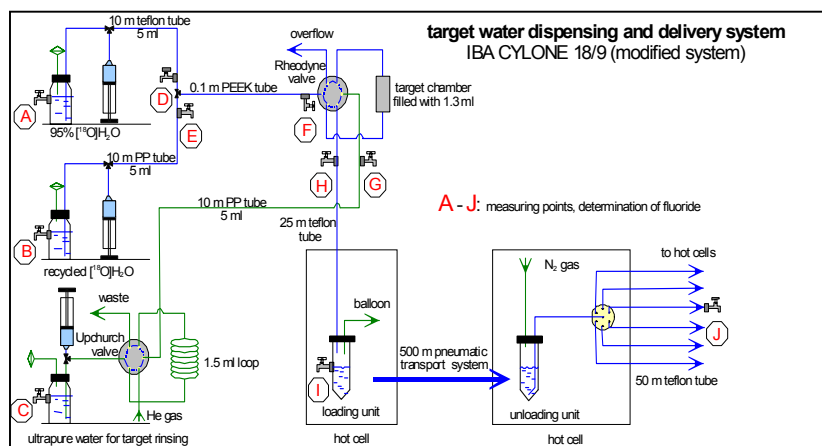
Results and Discussion

• The starting [¹⁸O]water is of good quality and contains not significant amounts of [¹⁹F]fluoride. Also a considerable contribution of the target irradiation process to the [¹⁹F]fluoride amount was not found.

- The Table 1 shows the partial contribution of the different parts of the target system to the [¹⁹F]fluoride amount. The [¹⁹F]fluoride amount depends mainly on the radiation dose, which the tube gets near the target/cyclotron, as well as on the water/tube contact time and the tube and valve material.
- The PTFE tube of the dispensing system (between A and D) is the main origin of [¹⁹F]fluoride. Avoiding PTFE tubes and changing to PP tubes in the target dispensing system the limit for SA can be reliably ensured.
- If very high SA is required repeated rinsing of the whole system with ultra pure water becomes necessary.

References

- [1] Dence, C. *et al.*, *Proceedings Vancouver* (1995) 199-205.
- [2] Kilbourn, M. R. *et al.*, *Int. J. Appl. Radiat. Isot.* 35 (1984) 599-602.
- [3] Nishijima, K. *et al.*, *Appl. Radiat. Isot.* 57 (2002) 443-449.



Scheme of the [¹⁵O]H₂O production module

Table 1. Partial contribution of the different constructive parts of the target dispensing and delivery system to the [¹⁹F]fluoride amount in the target water

sample	[¹⁹ F]fluoride content [nmol]						sum total
	reservoir	in front of target		target	after transport		
		dispensing tubs	target filling system		to pneumatic system	to the hot cell	
95% [¹⁸ O]H ₂ O	A	D	F	H	I	J	A - J
	0.53 ± 0.13	0.5 - 380	0.3 - 17.2	0.8 - 29.8	-	-	3 - 410
recycled [¹⁸ O]H ₂ O	B	E	F	H	I	J	A - J
	0,58 ± 0.34	0.2 - 10.0	0.5 - 6.5	0.9 - 28.5	-	-	3 - 34
ultra pure water	C	G	-	H	I	J	A - J
	0.1 ± 0.1	0.1 - 0.8	-	0.1 - 6.4	2.2 - 20.5	5.3 - 10.6	2 - 27

II. PUBLICATIONS, LECTURES, PATENTS AND AWARDS OF THE INSTITUTE AND THE PET- CENTRE ROSSENDORF

PUBLICATIONS

- Bauer, R.; Walter, B.; Brust, P.; Füchtner, F.; Zwiener, U.
Impact of asymmetric intrauterine growth restriction on organ function in newborn piglets.
Eur. J. Obstet. Gynecol. Reprod. Biol. 110 (2003) 40-49.
- Bernard, J.; Ortner, K.; Spingler, B.; Pietzsch, H.-J.; Alberto, R.
Aqueous synthesis of derivatized cyclopentadienyl complexes of technetium and rhenium directed towards radiopharmaceutical application.
Inorg. Chem. 42 (2003) 1014-1022.
- Beuthien-Baumann, B.; Bredow, J.; Burchert, W.; Füchtner, F.; Bergmann, R.; Alheit, H.-D.; Reiss, G.; Hliscs, R.; Steinmeier, R.; Franke, W.-G.; Johannsen, B.; Kotzerke, J.
3-O-Methyl-6-[¹⁸F]fluoro-L-DOPA and its evaluation in brain tumour imaging.
Eur. J. Nucl. Med. Mol. Imaging 30 (2003) 1004-1008.
- Beuthien-Baumann, B.; Hahn, G.; Winkler, C.; Heubner, G.
Differentiation between recurrent tumor or radiation necrosis in a child with anaplastic ependymoma after chemotherapy and radiation therapy.
Strahlentherapie Onkologie 179 (2003) 819-822.
- Beuthien-Baumann, B.; Handrick, W.; Schmidt, T.; Burchert, W.; Oehme, L.; Schackert, G.; Schuewer, U.; Kropp, J.; Franke, W.-G.
Brain perfusion and cerebral glucose metabolism in patients in persistent vegetative state.
Nucl. Med. Commun. 24 (2003) 643-650.
- Brust, P.; Hinz, R.; Kuwabara, H.; Hesse, S.; Zessin, J.; Pawelke, B.; Stephan, H.; Bergmann, R.; Steinbach, J.; Sabri, O.
In vivo measurement of the serotonin transporter with (S)-([¹⁸F]fluoromethyl)-(+)-McN5652.
Neuropsychopharmacology 28 (2003) 2010-2019.
- Brust, P.; Zessin, J.; Kuwabara, H.; Pawelke, B.; Kretzschmar, M.; Hinz, R.; Bergman, J.; Eskola, O.; Solin, O.; Steinbach, J.; Johannsen, B.
Positron emission tomography imaging of the serotonin transporter in the pig brain using [¹¹C](+)-McN5652 and S-([¹⁸F]fluoromethyl)-(+)-McN5652.
Synapse 47 (2003) 143-151.
- Buchert, R.; van den Hoff, J.; Mester, J.
Accurate determination of metabolic rates from dynamic positron emission tomography data with very-low temporal resolution.
J. Comp. Ass. Tomography 27 (2003) 597-605.
- Buchert, R.; Wilke, F.; van den Hoff, J.; Mester, J.
Improved statistical power of the multilinear reference tissue approach to the quantification of neuroreceptor ligand binding by regularization.
J. Cereb. Blood Flow Metab. 23 (2003) 612-620.
- Farrell, D.; Gloe, K.; Gloe, K.; Gerotzki, G.; McKee, V.; Nelson, J.; Nieuwenhuyzen, M.; Pál, I.; Stephan, H.; Town, R. M.; Wichmann, K.
Towards promising oxoanion extractants: azacages and open-chain counterparts.
J. Chem. Soc., Dalton Trans. (2003) 1961-1968.
- Füchtner, F.; Steinbach, J.
Efficient synthesis of the ¹⁸F-labelled amino acid 3-O-methyl-6-[¹⁸F]fluoro-L-DOPA.
Appl. Radiat. Isot. 58 (2003) 575-578.
- Gloe, K.; Stephan, H.; Grotjahn, M.
Where the anion extraction is going?
Chem. Eng. Technol. 26 (2003) 1107-1117.

- Johannsen, B.
Möglichkeiten und Trends in Diagnostik und Therapie.
Pharm. Zeitg. 148 (2003) 2884-2893.
- Knieß, T.; Fernandes, C.; Santos, I.; Kraus, W.; Spies, H.
Silylated mixed-ligand rhenium complexes with the [PNS/S] donor atom set.
Inorg. Chim. Acta 348 (2003) 237-241.
- Knieß, T.; Grote, M.; Noll, B.; Johannsen, B.
Synthesis and enzymatic evaluation of nucleosides derived from 5-iodo-2'-halo-2'-deoxyuridines.
Z. Naturforsch. 58b (2003) 226-230.
- Kopprasch, S.; Pietzsch, J.; Kuhlisch, E.; Gräßler, J.
Lack of association between serum paraoxonase (PON1) activities and increased oxidized LDL levels in impaired glucose tolerance and newly diagnosed diabetes mellitus.
J. Clin. Endocrinol. Metab. 88 (2003) 1711-1716.
- Kopprasch, S.; Pietzsch, J.; Grässler, J.
Validation of different chemiluminescent substrates for detecting extracellular generation of reactive oxygen species by phagocytes and endothelial cells.
Luminescence 18 (2003) 268-273.
- Kotzerke, J.; Volkmer, B. G.; Glattig, G.; van den Hoff, J.; Gschwend, J. E.; Messer, P.; Reske, S. N.; Neumaier, B.
Intraindividual comparison of [¹¹C]acetate and [¹¹C]choline PET for detection of metastases of prostate cancer.
Nuklearmedizin 42 (2003) 25-30.
- Kretschmar, M.; Brust, P.; Zessin, J.; Cumming, P.; Bergmann, R.; Johannsen, B.
Autoradiographic imaging of the serotonin transporter in the brain of rats and pigs using S-([¹⁸F]Fluoromethyl)-(+)-McN5652.
Eur. Neuropsychopharmacology 13 (2003) 387-397.
- Marjamäki, P.; Zessin, J.; Eskola, O.; Grönroos, T.; Haaparanta, M.; Bergman, J.; Lehtikoinen, P.; Forsback, S.; Brust, P.; Steinbach, J.; Solin, O.
S-[¹⁸F]fluoromethyl-(+)-McN5652, a PET tracer for the serotonin transporter: evaluation in rats.
Synapse 47 (2003) 45-53.
- Naumann, R.; Beuthien-Baumann, B.
What is evidence for positron emission tomography in the management of patients with indolent non-Hodgkin's lymphoma? [Commentary]
Clinical Lymphoma 4 (2003) 50-51.
- Pietzsch, H.-J.; Seifert, S.; Syhre, R.; Tisato, F.; Refosco, F.; Leibnitz, P.; Spies, H.
Synthesis, characterization and biological evaluation of technetium(III) complexes with tridentate/bidentate S,E,S/P,S coordination (E = O, N(CH₃), S): a novel approach to robust technetium chelates suitable for linking the metal to biomolecules.
Bioconjugate Chem. 14 (2003) 136-143.
- Pietzsch, J.; Kopprasch, S.; Bergmann, R.
Analysis of 3-chlorotyrosine as a specific marker of protein oxidation: the use of N(O,S)-ethoxycarbonyl trifluoroethyl ester derivatives and gas chromatography/mass spectrometry.
Rapid Commun. Mass Spectrom. 17: 767-770.
- Pietzsch, J.; Fuecker, K.
Increased cholesteryl ester transfer protein (CETP) activity in impaired glucose tolerance: relationship to high density lipoprotein metabolism.
Croat. Med. J. 44 (2003) 171-177.

- Pietzsch, J.; Bergmann, R.; Wüst, F.
Flavonoide: Wirkmechanismen und neue Anwendungsmöglichkeiten (Teil 1).
Bioforum 5 (2003) 289-291.
- Pietzsch, J. Bergmann, R.; Wüst, F.
Flavonoide: Wirkmechanismen und neue Anwendungsmöglichkeiten (Teil 2)
Bioforum 6 (2003) 284-285.
- Pietzsch, J.; Bergmann, R.
Measurement of 5-hydroxy-2-aminovaleric acid as a specific marker of iron-mediated oxidation of proline and arginine residues of low density lipoprotein apolipoprotein B-100 in human atherosclerotic lesions
J. Clin. Pathol. 56 (2003) 622-623.
- Pietzsch, J.
Fortschritte in der Aminosäureanalytik: N(O,S)-Ethoxycarbonyl-(trifluoro)ethylester-Derivate.
Bioforum 9 (2003) 643-645.
- Roesky, C. E. O.; Weber, E.; Rambusch, T.; Stephan, H.; Gloe, K.; Czugler, M.
A new cryptophane receptor featuring three endo-carboxylic acid groups: synthesis, host behavior and structural study.
Chemistry, A European Journal 9/5 (2003) 1104-1112.
- Schiller, L.; Jähkel, M.; Kretzschmar, M.; Brust, P.; Oehler, J.
Autoradiographic analyses of 5-HT_{1A} and 5-HT_{2A} receptors after social isolation in mice.
Brain Research 980 (2003) 169-178.
- Seifert, S.; Syhre, R.; Spies, H.; Johannsen, B.
Novel tumour tropic ester derivatives of ^{99m}Tc(V)-mesoDMSA with low affinity for bone tissue.
Nucl. Med. Commun. 24 (2003) 1175-1183.
- Weigl, M.; Müllich, U.; Geist, A.; Gompper, K.; Zevaco, T.; Stephan H.
Alkyl-substituted 2,6-dioxadiazolopyridines as selective extractants for trivalent actinides.
J. Radioanal. Nucl. Chem. 256/3 (2003) 403-412.
- Wiegrebe, W.; Johannsen, B.
Herausforderung und Chance für Apotheker.
Pharm. Ztg., 17 (2003) 26-30.
- Wiegrebe, W.; Johannsen, B.;
Therapie mit Radionukliden.
Pharm. Ztg., 18 (2003) 24-25.
- Wüst, F.; Zessin, J.; Johannsen, B.
A new approach for ¹¹C-C bond formation: synthesis of 17 α -(3'-[¹¹C]prop-1-yn-1-yl)-3-methoxy-3,17 β -estradiol.
J. Labelled Compd. Radiopharm. 46 (2003) 333-342.
- Wüst, F.; Carlson, K. E.; Katzenellenbogen, J. A.
Synthesis of novel arylpyrazolo corticosteroids as potential ligands for imaging brain glucocorticoid receptors.
Steroids 68 (2003) 177-191.
- Wüst, F.; Hultsch, C.; Bergmann, R.; Johannsen, B.; Henle T.
Radiolabelling of isopeptide N ϵ -(γ -glutamyl)-L-lysine by conjugation with N-succinimidyl-4-[¹⁸F]fluorobenzoate.
Appl. Radiat. Isot. 59 (2003) 43-48.

Wüst, F.; Knieß, T.
Synthesis of 4-¹⁸Ffluoriodobenzene and its application in Sonogashira cross-coupling reactions.
J. Labelled Compd. Radiopharm. 46 (2003) 699-713.

Zippe, C.; Hoppe, D.; Fietz, J.; Hampel, U.; Hensel, F.; Mäding, P.; Prasser, M.; Zippe, W.
Berührungslose Messung von Phasen- und Konzentrationsverteilungen in Blasensäulen mit positronenemittierenden Radionukliden.
Wissenschaftlich-Technische Berichte FZR-289, September 2003.

PROCEEDINGS

Bergmann, R.; Pawelke, B.; Hultsch, C.; Pietzsch, J.; Wüst, F.; Henle, T.; Johannsen, B.
Biodistribution and catabolism of [¹⁸F]fluorobenzoylated amino acids, peptides and proteins.
In: Cancer Biotherapy & Radiopharmaceuticals 18 (2003) 280-281.

Jelínek, L.; Matejka, Z.; Novotná, M.; Burda, R.; Sawatzki, A.-K.; Stephan, H.
Interaction of polyoxotungstates with aminosaccharides.
XVIIIth International Symposium "Ars Separatoria 2003", Z. Potok, Poland (2003) 74-76.

Julius, U.; Pietzsch, J.
Spezifische Glukoseverstärkung der Hämin-(Fe³⁺)-katalysierten LDL-Oxidation in vitro und in vivo.
In: Heinle, H.; Schulte, H.; Hahmann, H. Geschlechtsspezifische Mechanismen der Arteriosklerose; 16. Jahrestagung der Deutschen Gesellschaft für Arterioskleroseforschung, Köhler Druck, Tübingen (2003) 70-74.

Julius, U.; Kirschner, E.; Pietzsch, J.
Intravasal lipid transfer in impaired glucose tolerance (IGT): role of the cholesterol ester transfer protein (CETP).
In: Proceedings of the 21th International Symposium on Diabetes and Nutrition – Diabetes and Nutrition Study Group (DNSG) of the European Association for the Study of Diabetes (EASD), Bruges, Belgium, 19-22 June, 2003

Kopprasch, S.; Pietzsch, J.; Kuhlisch, E.; Graessler, J.
Chemiluminescence as a tool to assess hyperglycemia-induced systemic oxidative stress in different insulin-resistant states.
In: Stanley P. E.; Kricka L. J. Bioluminescence and Chemiluminescence: Progress and Current Applications. World Scientific Publishing Company, New Jersey (2003) 261-264.

Kopprasch, S.; Roch, B.; Pietzsch, J.; Kuhlisch, E.; Graessler, J.
Luminescence studies of blood phagocyte oxygenation activities in patients with antiphospholipid syndrome.
In: Stanley P. E.; Kricka L. J. Bioluminescence and Chemiluminescence: Progress and Current Applications. World Scientific Publishing Company, New Jersey (2003) 265-268.

Pietzsch, J.
Analysis of non-protein amino acids as specific markers of protein oxidation: the use of N(O,S)-ethoxycarbonyltrifluoroethyl ester derivatives and GC-MS.
In: Proceedings of the 2nd International Conference on Biomedical Spectroscopy, London, UK, July 5-8, 2003.

van den Hoff, J.
Principles of quantitative positron emission tomography in the lung.
In: IV. Postgraduate Course on Respiratory Intensive Care Medicine (2003) 10-12.

ABSTRACTS

Beuthien-Baumann, B.; Eckhardt, M.; Herrmann, Th.; Hliscs, R.; Oehme, L.; van den Hoff, J.; Kumpf, R.; Geyer, P.; Blank, H.; Baumann, M.

Monitoring postradiotherapeutic changes of lung tissue with PET and SPECT.
Int. J. Radiat. Oncol. Biol. Physics (2003) 499.

Beuthien-Baumann, B.; Zündorf, G.; Lüdecke, S.; Triemer, A.; Schierz, K.; Herholz, K.; Holthoff, V.
Regional cerebral metabolism in unipolar depression: the relationship with clinical characteristics.
J. Cereb. Blood Flow Metab. 23 (2003) 642.

Beuthien-Baumann, B.; Eckhardt, M.; Herrmann, Th.; Hliscs, R.; van den Hoff, J.; Kumpf, R.; Blank, H.; Baumann, M.

Monitoring postradiotherapeutic changes of lung tissue with CT, PET and SPECT.
12th International Congress of Radiation Research, Brisbane, Australia, Abstract Book (2003) 270.

Bühler, P.; Just, U.; Will, E.; Kotzerke, J.; van den Hoff, J.
An accurate method for correction of head movement in PET.
Eur. J. Nucl. Med. 30 (2003) S174/116.

Bühler, P.; Just, U.; Will, E.; Zühl, K.; Kotzerke, J.; van den Hoff, J.
Korrektur bewegungsbedingter Fehlortung individueller Koinzidenzereignisse in der PET.
Nuklearmedizin 42 (2003) A26.

Füchtner, F.; Preusche, S.; Steinbach, J.
Factors affecting the specific activity of [¹⁸F]fluoride from a water target.
J. Labelled Compd. Radiopharm. 46 (2003) S218.

Holthoff, V.A.; Lüdecke, S.; Beuthien-Baumann, B.; Zündorf, G.; Triemer, A.; Schellong, J.
Major-Depression im höheren Lebensalter: Regionale Hirnfunktion und kognitive Leistungsfähigkeit in Abhängigkeit vom Erkrankungsalter
J. Cereb. Blood Flow Metab. 23 (2003) 631.

Julius, U.; Kirschner, E.; Pietzsch J.
Intravascular lipid transfer in impaired glucose tolerance (IGT): role of the cholesterol ester transfer protein (CETP).
Diabetes 52 (2003) (suppl. 1) A211-A212.

Just, U.; Will, E.; Beuthien-Baumann, B.; Bredow, J.; Bühler, P.; van den Hoff, J.
Nutzbarmachung der List-Mode Akquisition an der PET-Kamera ECAT EXACT HR⁺.
Nuklearmedizin 42 (2003) A93.

Pawelke, B.; Bergmann, R.; Künstler, J.-U.; Kretzschmar, M.; Wittrisch, H.; Johannsen, B.
Untersuchung der Metabolisierung von Neurotensin (8-13) mit ^{99m}Tc- und ¹⁸F-Markierung.
Nuklearmedizin 42 (2003) A94.

Pietzsch, J.
Specific hemin catalyzed low density lipoprotein oxidation reactions: implications for metabolic and inflammatory diseases.
Amino Acids 25 (2003) 120.

Pietzsch, J.; Bergmann, R.; Wüst, F.; Grote, M.; Hultsch, C.; Pawelke, B.; van den Hoff, J.
Assessment of metabolism of native and oxidized low density lipoprotein in vivo: insights from animal positron emission tomography (PET) studies.
Amino Acids 25 (2003) 120.

Pietzsch, C.; Beuthien-Baumann, B.; van den Hoff, J.
Teilautomatisierte Segmentierung zur Quantifizierung von Metastasen bei der FDG-PET.
Nuklearmedizin 42 (2003) A26.

van den Hoff, J.; Fricke, H.; Wielepp, P.; Burchert, W.
Dynamische ^{15}O - H_2O -PET zur Erzeugung quantitativer 3D-Polar-Maps der Myocardperfusion.
Nuklearmedizin 42 (2003) A27.

van den Hoff, J.; Börner, A.; Behrens, G.; Meyer, G. J.; Knapp, W. H.
Untersuchung des Glukosestoffwechsels bei Patienten mit HIV-Infektion unter hochaktiver antiretrovi-
raler Therapie (HAART) mittels quantitativer dynamischer FDG-PET.
In: Nuklearmedizin als Paradigma molekularer Bildgebung, Eds.: I. Brink, S. Högerle, E. Moser,
Blackwell Verlag, Berlin (2002) p. 16.

LECTURES AND POSTERS

Lectures

Antonoli, B.; Gloe, K.; Goretzki, G.; Glenn, M. W.; Schröder, M.; Herrmann, E.; Stephan, H.
Oxathiaza-Makrocyclen: Potentielle Extraktionsmittel für Metallionen und Metallsalze.
DECHEMA-Sitzung „Das Neue geschieht an den Grenzflächen“, Würzburg, 05.-07.03.2003.

Bergmann, R.
Status and perspectives in neurotensin receptor PET imaging.
International workshop “Radiolabelled peptides in tumour research”, Leipzig, 26.05.2003.

Bergmann, R.
Experience with neurotensin and bombesin labelled with fluorine-18.
European Association of Nuclear Medicine Annual Congress 2003, Amsterdam, The Netherlands, 23.-
27.08.2003.

Beuthien-Baumann, B.; Eckhardt, M.; Herrmann, Th.; Hliscs, R.; Oehme, L.; van den Hoff, J.; Kumpf,
R.; Geyer, P.; Blank, H.; Baumann, M.
Monitoring postradiotherapeutic changes of lung tissue with PET and SPECT.
ICTR 2003 Lugano, 16.-19.03.2003.

Brust, P.; Zessin, J.; Solin, O.; Steinbach, J.
Comparison of [^{11}C](+)-McN5652 and S-([^{18}F]fluoromethyl)-(+)-McN5652 for PET imaging of the sero-
tonin transporter.
15th International Symposium on Radiopharmaceutical Chemistry, Sydney, Australia, 07.-18.08.2003.

Bühler, P.; Just, U.; Will, E.; Kotzerke, J.; van den Hoff, J.
An accurate method for correction of head movement in PET.
European Association of Nuclear Medicine Annual Congress 2003, Amsterdam, The Netherlands, 23.-
27.08.2003.

Bühler, P.; Just, U.; Will, E.; Zühl, K.; Kotzerke, J.; van den Hoff, J.
Korrektur bewegungsbedingter Fehlortung individueller Koinzidenzereignisse in der PET.
41. Jahrestagung der DGN, Essen, 02.-05.04.2003.

Farrell, D.; Gloe, K.; Goretzki, G.; McKee, V.; Nelson, J.; Nieuwenhuyzen, M.; Pal, I.; Stephan, H.;
Town, R. M.; Wichmann, K.
Towards promising oxoanion extractants: azacages and open-chain counterparts.
Dalton Discussion 5 “Ligand Design for Functional Complexes”, Noordwijkerhout, The Netherlands,
10.-12.04.2003.

Füchtner, F.
Erfahrungen bei der Verwendung von kommerziellen Ausrüstungen für die PET-Radiopharmaka-
herstellung.
11. Jahrestagung der AG Radiochemie/Radiopharmazie, Leipzig-Brehna, 18.09.2003.

Heinrich, T.

Synthetische Arbeiten in der medizinischen Chemie und der Re/Tc-Chemie.
Dies Academicus 2003, Zittau, 04.06.2003.

Holthoff, V.A.; Lüdecke, S.; Beuthien-Baumann, B.; Zündorf, G.; Triemer, A.; Schellong, J.
Major-Depression im höheren Lebensalter: Regionale Hirnfunktion und kognitive Leistungsfähigkeit in Abhängigkeit vom Erkrankungsalter.
6. Jahrestagung der Deutschen Gesellschaft für Gerontopsychiatrie und –psychotherapie, München, 02.-05.04.2003.

Holthoff, V.; Herholz, K.; Lüdecke, S.; Spirling, S.; Kalbe, E.; Lenz, O.; Zündorf, G.; Beuthien-Baumann, B.
Behavioral disturbances and regional cerebral metabolism in probable Alzheimer's disease.
Brain and BrainPET 2003, 29.06.-03.07.2003, Calgary, Canada.

Hultsch, C.

Untersuchungen zur Bioverteilung und Elimination des Isopeptides N-ε-(γ-Glutamyl)-lysin mittels Positronen-Emissions-Tomographie.
11. Jahrestagung der AG Radiochemie/Radiopharmazie, Leipzig-Brehna, 18.09.2003.

Jelínek, L.; Matejka, Z.; Novotná, M.; Burda, R.; Sawatzki, A.-K.; Stephan, H.
Interaction of polyoxotungstates with aminosaccharides.
XVIIIth International Symposium "Ars Separatoria 2003", Z. Potok, Poland, 02.-05.06.2003.

Johannsen, B.

Zur Zulassungsproblematik und spezifischen Anwendung von GMP bei PET-Radiopharmaka.
Arbeitstagung der pharmazeutischen und veterinärmedizinischen Überwachungsbeamtinnen und –beamten der Länder, Workshop Radiopharmazeutika, Erfurt, 24.09.2003.

Johannsen, B.

Radiopharmazeutika – gestern, heute und morgen.
Bad Berkaer Gespräche Nuklearmedizin, Bad Berka, 12.11.2003.

Johannsen, B.

Biologische Funktionen – ihre Aufklärung mit Hilfe von Metallkomplexverbindungen.
Adlershofer Analytisches Kolloquium der BAM, Adlershof, 25.11.2003.

Julius, U.; Kirschner, E.; Pietzsch, J.

Intravasal lipid transfer in impaired glucose tolerance (IGT): role of the cholesterol ester transfer protein (CETP).
21th International Symposium on Diabetes and Nutrition – Diabetes and Nutrition Study Group (DNSG) of the European Association for the Study of Diabetes (EASD), Bruges, Belgium, 19.-22.06.2003.

Marjamäki, P.; Eskola, O.; Haaparanta, M.; Grönroos, T.; Fagerholm, V.; Bergman, J.; Lehtikoinen, P.; Savisto, N.; Zessin, J.; Solin, O.
Sex differences in the uptake of [¹⁸F]FMe-McN in rat brain.
15th International Symposium on Radiopharmaceutical Chemistry, Sydney, Australia, 07.-18.08.2003.

Mäding, P.

¹⁸F-Labeling of the CCR1 antagonist ZK811460 for the diagnosis of the Alzheimer's disease.
Technical Exchange Meeting on Alzheimer Imaging, Berlin, 30.10.2003.

Mäding, P.; Zessin, J.; Pleiß, U.; Wüst, F.

Synthesis of a ¹¹C-labelled taxan derivative by [1-¹¹C]acetylation.
11th Conference of the Central European Division e. V. of the International Isotope Society, Bad Soden, 25.-26.09.2003.

Pietzsch, H.-J.; Spies, H.
Radiometals for nuclear medicine.
18th KAIF/KNS Annual Conference, Korea Atomic Industrial Forum, Inc. (KAIF), Korean Nuclear Society (KNS), Seoul, 09.-13.04.2003 (invited lecture).

Pietzsch, H.-J.; Spies, H.
Radiometals for nuclear medicine.
Korea Cancer Center Hospital Seoul, Dept. of Nuclear Medicine, 09.04.2003 (invited lecture).

Pietzsch, H.-J.
Mixed-ligand complexes of Tc(III) serving as flexible tools for binding the metal to small biomolecules.
IAEA-Tagung, Ferrara, Italy, 04.-09.05.2003 (invited lecture).

Pietzsch, H.-J.
Radiometalle in der nuklearmedizinischen Diagnostik und Therapie.
Kolloquium des GDCh-Ortsverbandes Lausitz, FH Zittau, 22.10.2003 (invited lecture).

Pietzsch, J.
Untersuchungen zur *in vivo*-Kinetik humaner Lipoproteine mittels stabiler Isotope: Störungen des Lipoproteinstoffwechsels bei Diabetesvorstadien.
Lebensmittelchemisches Kolloquium, Universität Hohenheim, 30.01.2003 (invited lecture).

Pietzsch, J.
Analysis of non-protein amino acids as specific markers of protein oxidation: the use of N(O,S)-ethoxy-carbonyltrifluoroethyl ester derivatives and GC-MS.
2nd Int. Conference on Biomedical Spectroscopy, London, UK, 05.-08.06.2003 (invited lecture).

Pietzsch, J.
Analysis of non-protein amino acids as specific markers of protein oxidation: the use of N(O,S)-ethoxy-carbonyltrifluoroethyl ester derivatives and GC-MS.
London, UK, 05.-08.07.2003 (invited lecture).

Pietzsch, J.
Specific hemin catalyzed low density lipoprotein oxidation reactions: implications for metabolic and inflammatory diseases.
8th Int. Congress on Proteins and Amino Acids, Rome, Italy, 05.-09.09.2003.

Pietzsch, J.; Bergmann, R.; Wüst, F.; Grote, M.; Hultsch, C.; Pawelke, B.; van den Hoff, J.
Assessment of metabolism of native and oxidized low density lipoprotein *in vivo*: insights from animal positron emission tomography (PET) studies.
8th Int. Congress on Proteins and Amino Acids, Rome, Italy, 05.-09.09.2003.

Pietzsch, J.
Untersuchungen zum *in vivo*-Metabolismus nativer und oxidierter Lipoproteine am Tiermodell mittels PET.
11. Jahrestagung der AG Radiochemie/Radiopharmazie, Leipzig-Brehna, 18.09.2003.

Schiller, E.
Hydrophile ^{99m}Tc/¹⁸⁸Re-Komplexe zur Kopplung an Biomoleküle.
11. Jahrestagung der AG Radiochemie/Radiopharmazie, Leipzig-Brehna, 18.09.2003.

Stephan, H.
Neue Rhenium- und Kupfer-Koordinationsverbindungen für die Radiotherapie.
Institutskolloquium, Universität Heidelberg, Institut für Anorganische Chemie, Heidelberg, 30.06.2003 (invited lecture).

Stephan, H.; Sawatzki, A.-K.
Preparation and characterization of polyoxotungstates.
Institutskolloquium, Institute of Chemical Technology Prague, Prague, Czech Republic, 20.08.2003.

- Stephan, H.
Dendritic receptors for binding therapeutically relevant copper and rhenium radionuclides.
10th International Conference "Separation of Ionic Solutes", Podbanske, Slovakia, 06.-11.09.2003.
- Stephan, H.
Development of rhenium complexes and metal clusters for therapy.
Kolloquium, Department of Chemical Processes and Environments, University Kitakyushu, Kitakyushu, Japan, 11.11.2003 (invited lecture).
- Stephan, H.
Development of rhenium complexes and metal clusters for therapy.
Kolloquium, Department of Applied Chemistry, Saga University, Saga, Japan, 14.11.2003 (invited lecture).
- Stephan, H.
Novel approaches for binding therapeutically relevant copper and rhenium radionuclides.
Kolloquium, Department of Chemistry, Tohoku University, Sendai, Japan, 19.11.2003 (invited lecture).
- Stephan, H.
Solvent extraction as a helpful tool for the characterisation of supramolecular receptors.
Kolloquium, Department of Environmental Chemistry and Engineering, Tokyo Institute of Technology, Tokyo, Japan, 25.11.2003 (invited lecture).
- Stephan, H.
Dendritic carriers and cage compounds for radionuclides.
Kolloquium, Department of Materials Science, JAERI, Tokaimura, Japan, 26.11.2003 (invited lecture).
- van den Hoff, J.
Linearisations in compartment modelling.
XV. Annual PET Pharmacokinetic Course, Montreal, Canada, 25.-30.06.2003 (invited lecture).
- van den Hoff, J.
Principles of quantitative positron emission tomography in the lung.
IV. Postgraduate Course on Respiratory Intensive Care Medicine, 12.09.2003 (invited lecture).
- Wüst, F.
Positron Emission Tomography (PET): Fundamentals and the potential role in drug research and development.
PET-Tagung der BAYER AG, Wuppertal, 16.06.2003 (invited lecture).
- Wüst, F.; Füchtner, F.
Synthesis of 4-[¹⁸F]fluoriodobenzene and its application in Sonogashira cross-coupling reactions.
15th International Symposium on Radiopharmaceutical Chemistry, Sydney, Australia, 07.-18.08.2003.
- Wüst, F.
Carbon-11 labelled compounds in the development of pharmaceuticals.
11th Conference of the International Isotope Society, Bad Soden, 25.-26.09.2003.
- Wüst, F.
¹⁸F-markierte Corticosteroide als Liganden für die Darstellung von Glucocorticoidrezeptoren (GR) im Gehirn mittels PET.
Gemeinsames Institutskolloquium der Klinik und Poliklinik für Nuklearmedizin und des Instituts für Interdisziplinäre Isotopenforschung, Leipzig, 23.10.2003.
- Zessin, J.
Radionuklide in der medizinischen Diagnostik.
Ehrenkolloquium zum 60. Geburtstag von Frau Prof. G. Schmidt, TU Clausthal-Zellerfeld, 11.04.2003 (invited lecture).

Posters

Appelhans, D.; Clausnitzer, C.; Gloe, K.; Gloe, K.; Johannsen, B.; Spies, H.; Stephan, H.; Stute, S.; Voit, B.

Development of dendrons for binding rhenium radionuclides.

3rd International Dendrimer Symposium, Berlin, 17.-20.09.2003.

Bergmann, R.; Pawelke, B.; Hultsch, C.; Pietzsch, J.; Wüst, F.; Henle, T.; Johannsen, B.

Biodistribution and catabolism of [¹⁸F]fluorobenzoylated amino acids, peptides and proteins.

16th International Meeting of the International Research Group in Immunoscintigraphy and Immunotherapy (IRIST), Capri, Italy, 08.-10.05.2003.

Beuthien-Baumann, B.; Eckhardt, M.; Herrmann, T.; Hliscs, R.; Oehme, L.; van den Hoff, J.; Kumpf, R.; Geyer, P.; Blank, H.; Baumann, M.

Monitoring postradiotherapeutic changes of lung tissue with PET and SPECT.

International Congress of Translation Research, Lugano, Switzerland, 16.-18.03.2003.

Beuthien-Baumann, B.; Eckhardt, M.; Herrmann, T.; Hliscs, R.; van den Hoff, J.; Kumpf, R.; Blank, H.; Baumann, M.

Monitoring postradiotherapeutic changes of lung tissue with CT, PET and SPECT.

12th International Congress of Radiation Research, Brisbane, Australia, 17.-22.08.2003.

Beuthien-Baumann, B.; Zündorf, G.; Lüdecke, S.; Triemer, A.; Schierz, K.; Herholz, K.; Holthoff, V.

Regional cerebral metabolism in unipolar depression: the relationship with clinical characteristics.

Brain and BrainPET 2003, Calgary, Canada, 29.06.-03.07.2003.

Fernandes, C.; Kniess, T.; Seifert, S.; Spies, H.; Gano, L.; Santos, I.

Síntese, Caracterização e Avaliação Biológica de Complexos Lipofílicos de ^{99m}Tc.

Contendo Grupos Siloxo Hidrolisáveis, 1^o Congresso da Sociedade Portuguesa de Ciências Farmacêuticas, Lisbon, Portugal, 04.-16.04.2003.

Fernandes, C.; Bergmann, R.; Correia, J. D. G.; Gano, L.; Santos, I.; Spies, H.; Seifert, S.

Novel Re and ^{99m}Tc '3+1' oxocomplexes with high affinity for the 5-HT_{1A} receptor.

7th FIGIPS Meeting in Inorganic Chemistry, Lisbon, Portugal, 11.-15.06.2003.

Holthoff, V.; Herholz, K.; Lüdecke, S.; Spirling, S.; Kalbe, E.; Lenz, O.; Zündorf, G.; Beuthien-Baumann, B.

Behavioral disturbances and regional cerebral metabolism in probable Alzheimer's Disease.

Brain and BrainPET 2003, Calgary, Canada, 29.06.-03.07.2003.

Julius, U.; Kirschner, E.; Pietzsch J.

Intravascular lipid transfer in impaired glucose tolerance (IGT): role of the cholesterol ester transfer protein (CETP).

63rd Scientific Sessions of the American Diabetes Association (ADA), New Orleans, USA, 13.-17.06.2003.

Kirchner, R.; Seidel, J.; Gloe, K.; Stephan, H.

Kalorimetrische und potentiometrische Untersuchungen an Dendrimeren auf PAMAM Basis: Protonierung und Wechselwirkung mit HSA.

15. Ulm-Freiberger Kalorimetrietage, Freiberg, 19.-21.03.2003.

Kirchner, R.; Seidel, J.; Gloe, K.; Stephan, H.

Calorimetric and potentiometric study of PAMAM dendrimers: protonation and interactions with human serum albumin.

3rd International Dendrimer Symposium, Berlin, 17.-20.09.2003.

Naumann, R.; Beuthien-Baumann, B.; Reiss, A.; Kühnel, G.; Schulze, J.; Haenel, A.; Bredow, J.; Kropp, J.; Haenel, M.; Laniado, M.; Ehninger, G.

Impact of FDG positron emission tomography in addition to conventional staging procedures in patients with Hodgkin's lymphoma.

45th Meeting of the American Society of Haematology, San Diego, USA, 06.-09.12.2003.

Pawelke, B.; Bergmann, R.; Helling, R.; Wittrisch, H.; Wüst, F.; Johannsen, B.
Biodistribution and catabolism studies of ^{18}F -labeled amino acid and peptid derivatives.
6. Deutsches Peptidsymposium, Berlin, 23.-26.03.2003.

Pawelke, B.; Bergmann, R.; Künstler, J.-U.; Kretzschmar, M.; Wittrisch, H.; Johannsen, B.
Untersuchung der Metabolisierung von Neurotensin (8-13) mit $^{99\text{m}}\text{Tc}$ - und ^{18}F -Markierung.
41. Jahrestagung Deutsche Gesellschaft für Nuklearmedizin, Essen, 02.-05.04.2003.

Pietzsch, J.

Analysis of non-protein amino acids as specific markers of protein oxidation: the use of N(O,S)-ethoxy-carbonyltrifluoroethyl ester derivatives and GC-MS.

2nd International Conference on Biomedical Spectroscopy, London, UK, 05.-08.06.2003.

PATENTS

Dinkelborg, L.; Blume, F.; Hilger, C.-S.; Heldmann, D.; Platzek, J.; Niedballa, U.; Miklautz, H.; Speck, U.; Duda, S.; Tepe, G.; Noll, B.; Görner, H.

Stents with a radioactive surface coating, processes for producing the same and their use for restenosis prevention.

EP0979108 A2

AWARDS

Dr. Christian Jung

FZR-Doktorandenpreis 2003

Synthese und Charakterisierung von fettsäuretragenden Technetiumkomplexen und deren Vorstufen.



DIPLOMA

Christian Pötzsch

Teilautomatisierte Abgrenzung dreidimensionaler Strukturen zur erweiterten quantitativen Analyse von dynamischen und statischen Datensätzen in der Positronen-Emissions-Tomographie.
Hochschule für Technik und Wirtschaft Dresden, 13.02.2003.

Christina Hultsch

Untersuchungen zur Bioverteilung und Elimination des Isopeptides N-e-(g-Glutamyl)-lysin mittels Positronen-Emissions-Tomographie.
Technische Universität Dresden, 11.07.2003.

Jörg Stolzenburg

Aufbau und Validierung einer automatischen Injektionsapparatur für Patientenuntersuchungen in der Positronen-Emissions-Tomographie.
Berufsakademie Bautzen, 25.09.2003.

Denise Tiebel

Entwicklung und Anwendung eines Atemtriggersystems für Patientenuntersuchungen in der Positronen-Emissions-Tomographie.
Berufsakademie Bautzen, 25.09.2003.

PhD THESES

Christian Jung

Synthese und Charakterisierung von fettsäuretragenden Technetiumkomplexen und deren Vorstufen.
Technische Universität Dresden, 20.10.2003.

Aneta Jordanova

Investigations to electrophilic fluorination with n.c.a. ^{18}F .
Technische Universität Dresden, 28.11.2003.

III. SCIENTIFIC COOPERATION

COOPERATIVE RELATIONS AND JOINT PROJECTS

In multidisciplinary research such as carried out by this Institute, collaboration, the sharing of advanced equipment and, above all, exchanges of ideas and information play an important role. Effective collaboration has been established with colleagues at universities, in research centres and hospitals.

The Technische Universität Dresden has been a major partner in our cooperative relations. Cooperation with various groups in the Department of Chemistry and the Faculty of Medicine was again significantly extended last year. Common objects of radiopharmacological and medical research link the Institute with the Dresden University Hospital, above all with its Department of Nuclear Medicine (Prof. Kotzerke). A joint team of staff members from both the Institute and the Clinic of Nuclear Medicine is currently working at the Rossendorf PET Centre. Cooperation with The Institute of Analytical Chemistry (Prof. Salzer) in tumour research has been continued. Application of the positron emission tomography modality has been successfully proceeded in collaboration with the Institute of Food Chemistry (Prof. Henle). Bioinorganic research activities are closely linked with the Department of Coordination Chemistry (Prof. Gloe).

Special thanks go to Schering AG Berlin (Dr. Dinckelborg) for the long-standing valuable collaboration in radiotracer development. Recently, cooperation with the pharmaceutical industry and regional enterprises has been intensified and extended. Joint projects exist with Bayer AG, ABX advances biochemical compounds, ROTOP Pharmaka GmbH, Wälischmiller GmbH, AEA Technology QSA GmbH, Nihon-Medi-Physics, Apogepha Arzneimittel GmbH and A.R.T. Hersching.

The identification of common objects in PET radiopharmacy has led to collaborative research with the Institut für Interdisziplinäre Isotopenforschung Leipzig (Prof. Steinbach). Both institutes constitute an alliance of research in radiopharmaceutical sciences.

Cooperation in PET tracer chemistry and radiopharmacology has been established with the Turku Medical PET Centre (Dr. Solin), Washington University (Prof. Welch), Harvard School of Medicine (Dr. Neumeyer), North-Eastern University Boston (Dr. Hanson), University of Illinois (Prof. Katzenellenbogen).

Cooperation in technetium and rhenium chemistry exists with the University of Ferrara (Prof. Duatti), CNR Padova (Dr. Tisato, Dr. Refosco), University of Tunis (Prof. Saidi) and, more recently, with the Korean Research Centre KAERI (Dr. Park), as well as with the University of Kitakyushu, Japan (Prof. Yoshizuka). The Institute works with the Humboldt University Berlin, Charité Hospital (Dr. Fischer) and with University Hospital Leipzig (Prof. Emmrich), on radioimmunochemistry.

Very effective cooperation exists with the Federal Material Research Institute in Berlin (Dr. Reck, Mr. Kraus), whose staff members carried out X-ray crystal structure analysis of new technetium and rhenium complexes.

In the field of supramolecular chemistry, successful cooperation exists with the Kekulé Institute of Organic Chemistry and Biochemistry (Prof. Vögtle) of the University of Bonn.

LABORATORY VISITS

Dr. H.-J. Pietzsch
Korea Atomic Energy Research Institute (KAERI), HANARO, Div. of Radioisotope Production, Korea
07.-13.04.2003

Dr. M. Grote
Paul Scherrer Institut, Zürich, Switzerland
11.-18.05.2003

Dr. H.-J. Pietzsch,
Universität Ferrara, FZ Padua, Italy
09.-14.11.2003

Dr. H. Spies
Universität Ferrara, FZ Padua, Italy
09.-14.11.2003

Dr. H. Stephan	
University of Kitakyushu, Japan	02.-18.11.2003
Tohoku University, Japan	19.-21.11.2003
Tokyo Institute of Technology, Japan	24.-25.11.2003
Japan Atomic Energy Research Institute, Japan	26.-27.11.2003

E. Schiller
Universität Ferrara, FZ Padua, Italy
23.11.-12.12.2003

GUESTS

Dr. Wu
Nihon Medi-Physics Co., Ltd., Japan
19.03.2003

Dr. L. Jelinek
Institute of Chemical Technology, Prague, Czech Republic
01.-31.07.2003
01.-05.12.2003

P. Houserova
Institute of Chemical Technology, Prague, Czech Republic
21.-25.07.2003
01.-05.12.2003

Dr. K. A. Brylev
Russian Academy of Science, Novosibirsk, Russia
01.09.-01.12.2003

S. Raji
Kwame Nkrumah University of Science and Technology, Kumasi, Ghana
01.09.2003 – 28.02.2004

F. Aggrey
University of Cape Coast (U.C.C.), Ghana
01.09.2003 – 28.02.2004

Dr. S. H. Park
Korea Atomic Energy Research Institute, Korea
15.09.–31.10.2003

Dr. R. Lambrich
AEA Technology QSA, Braunschweig
29.09.2003

Dr. U. Schwarz
AEA Technology QSA, Braunschweig
29.09.2003

Dr. K. B. Park
Korea Atomic Energy Research Institute, Vice President HANARO, Korea
24.10.2003

Dr. M. Saidi
Centre National des Sciences et Technologie Nucléaires Tunis, Tunisia
08.09.-08.11.2003

E. Hesemann
AEA Technology, Braunschweig
27.11.2003

Dr. H. Parschova
Institute of Chemical Technology Prague, Czech Republic
01.-05.12.2003

P. Krotka
Institute of Chemical Technology Prague, Czech Republic
01.-05.12.2003

E. Mistova
Institute of Chemical Technology Prague, Czech Republic
01.-05.12.2003

Dr. L. Tellmann
Forschungszentrum Jülich
10.12.2003

Dr. R. Folton
University of Sydney and Royal Prince Alfred Hospital, Australia
10.12.2003

Prof. V. E. Fedorov
Institute of Inorganic Chemistry, Siberian Branch of the Russian Academy of Sciences, Novosibirsk,
Russia
11.-17.12.2003

TEACHING ACTIVITIES

Summer term 2003

B. Johannsen, H.-J. Pietzsch

One term course on Metals in Biosystems (Introduction into Bioinorganic Chemistry)

J. Pietzsch

Chemistry for medical students

Winter term 2003/2004

F. Wüst

One term course on Radiopharmaceutical Chemistry

J. Pietzsch

Chemistry for medical students

OTHER ACTIVITIES

B. Johannsen

Chairman of the DGN Working Group on Radiochemistry and Radiopharmacy

B. Johannsen

Co-editor of the Journal "Nuclear Medicine and Biology"

IV. SEMINARS

TALKS OF VISITORS

Prof. Dr. B. Voit, Institut für Polymerforschung Dresden
Design von biokompatiblen und bioaktiven Grenzflächen für die Anwendung in der Medizin
31.01.2003

Prof. Dr. J. L. Neumeyer, Harvard Medical School, Belmont, USA
Some recent developments in PET and SPECT ligands: phenyltropanes and morphinans
28.02.2003

Jeffrey Iqbal
Jugend forscht: Endos, Exos und mehr – Die Welt der Fullerene II
07.04.2003

Prof. Dr. P. Comba, Ruprecht-Karls-Universität Heidelberg
Vier-, fünf- und sechszählige Bispidine: Mögliche neue Ligandensysteme für die Radiopharmazeuti-
sche Chemie
24.04.2003

Dr. W. von der Saal, Roche Diagnostics GmbH, Penzberg
Medizinische Chemie in der Krebsforschung
10.07.2003

Dr. M. Horn, Universität Göteborg,
Magnetresonanzverfahren als Fenster zur Physiologie in vivo
23.07.2003

Dr. Stanislaw Schastak, Klinik für Augenheilkunde, Universitätsklinikum Leipzig
Photodynamische Therapie von Tumoren mit neuartigem Photosensitizer
29.08.2003

Dr. A. Daubinet, Ruprecht-Karls-Universität Heidelberg
Molecular modelling of rhenium (V) complexes with DMSA
23.10.2003

Dr. St. Heymann, Institut für Informatik, Humboldt-Universität Berlin
Spleißformen eines Neurotensin-Rezeptors auf dem Prüfstand – Data Warehouse Strategien in der
Bioinformatik
14.11.2003

Dr. R. Buchert, Abteilung für Nuklearmedizin, Universitätskrankenhaus Hamburg
McN5652-PET zum Nachweis von Veränderungen der Serotonintransporter-Verfügbarkeit
17.11.2003

INTERNAL SEMINARS

K. Rode

In vitro- und in vivo-Untersuchungen zur Stabilität eines Tc-„4+1“-Komplexes
29.01.2003

C. Heichert

Stand der Arbeit zu Substraten der HSV-1-Thymidinkinase und der entsprechenden Präkursoren für die ¹⁸F-Markierung
26.02.2003

F. Wüst

PET-Corticosteroide
09.04.2003

P. Bühler

Bewegungskorrektur bei PET-Untersuchungen
30.04.2003

E. Will

Performance-Messungen am neuen MicroPET-Scanner
21.05.2003

Ch. Pönisch

Rechnergestützte Verfahren zur Verbesserung der tomographischen Bildrekonstruktion am MicroPET-Scanner
11.06.2003

E. Schiller

Kopplungsfähige hydrophile „4+1“-Chelatsysteme zur Bindung von Metallen an Biomoleküle
25.06.2003

F. Füchtner

Spezifische Aktivität bei nukleophilen [¹⁸F]Fluorierungen
27.08.2003

T. Knieß

4-[¹⁸F]Fluoriodbenzen als Markerungsbaustein in der ¹⁸F-Chemie
17.09.2003

J. Pietzsch

Untersuchungen zum Metabolismus nativer und oxidierter Lipoproteine
08.10.2003

B. Beuthien-Baumann

PET in der Demenz-Diagnostik
05.11.2003

R. Bergmann

Bioverteilung und Metabolismus von Proteinen und Peptiden
18.12.2003

V. ACKNOWLEDGEMENTS

ACKNOWLEDGEMENTS FOR FINANCIAL SUPPORT

The Institute is part of the Research Center Rossendorf Inc., which is financed by the Federal Republic of Germany and the Free State of Saxony on a fifty-fifty basis.

The Institute participated in the following two projects supported by Commission of the European Communities:

Network for Efficiency and Standardization of Dementia Diagnosis
NEST-DD
in collaboration with Belgium, France, Italy
01/2002 – 12/2003.

Radiotracers for *in vivo* assessment of biological function
COST B12
in collaboration with Sweden, Italy and Switzerland
02/1999 – 02/2004.

Three research projects concerning tracer design, biochemistry and PET radiochemistry were supported by the Deutsche Forschungsgemeinschaft (DFG):

^{18}F labelled substrates of bacterial cytosindeaminase for monitoring gene expression of cancer cells
NO 418/1-1 (B. Noll), 06/2001 - 05/2003.

Molecular encapsulated ^{188}Re complexes: Development of robust and tunable radioactive rhenium complexes on the basis of novel chelators derived from dimercaptosuccinic acid (DMSA)
PI 255/5-1 (H.-J. Pietzsch) 12/2002 – 11/2004.

F-18 labelled corticosteroides as ligands for imaging brain glucocorticoid-receptors by means of PET
WU 340/1-1 (F. Wüst) 01/2002 – 12/2003.

The Sächsisches Staatsministerium für Wissenschaft und Kunst provided support for the following project:

Development and characterization of nanoscale metal-based drugs targeting tumors
SMWK-No. 4-7531.50-03-0370-01/4, 06/2001 – 12/2003.

and for the stay of scientists from Czech Republic and Russia.

The Bundesministerium für Bildung und Forschung supported cooperation with

Czech Republic: polyoxometallo compounds
WTZ, 08/2002 – 07/2005

Russia: Polynuclear metallo drugs
WTZ, 07/2003 – 09/2004

The Bundesministerium für Wirtschaft und Arbeit supported cooperation with AEA Technology QSA GmbH:

Y-86 for nuclear medical application
08/2003 – 01/2005

The following projects were supported by cooperations with the industry:

Cooperation in nuclear diagnostics

Schering AG Berlin
07/1996 – 12/2004

Cooperation in functional diagnostics

ABX advanced biomedical compounds GmbH Dresden
04/2001 - 11/2004

Synthesis of precursors for PET-radiopharmaceuticals

ABX advanced biomedical compounds GmbH Dresden
01/2003 – 12/2004

Cooperation in drug development

Bayer AG Leverkusen
05/2002 – 02/2004

Cooperation in movement tracking for PET

A.R.T. Hersching
09/2002 – 12/2004

Cooperation in pharmacokinetics and metabolism of propiverin

Apogepha Arzneimittel GmbH
07/2003 – 02/2004

Development and evaluation of technetium-99m-labelled fatty acids

Nihon-Medi-Physics (Japan/USA)
01/2003 – 12/2004

Several laboratory visits were supported by the “Deutscher Akademischer Austauschdienst” (DAAD).

VIGONI-Project with Padova (Italy):

Labelling Dithiol Ligands with a TcN-Synthon
01/2002 – 12/2003

VI. PERSONNEL

Director

Dr. Spies, H.

Administrative Staff

Forker, S.

Neubert, G.

Scientific Staff

Dr. Bergmann, R.
Dr. Füchtner, F.
Dr. Grote, M.*
Dr. Knieß, T.
Kretzschmar, M.
Künstler, J.-U.*
Lange, S.
Mäding, P.

Dr. Noll, B.
Dr. Noll, S.
Dr. Pietzsch, H.-J.
Dr. Pietzsch, J.
Dr. Pönisch, F.*
Preusche, S.
Dr. Rother, A.*

Dr. Seifert, S.
Dr. Stephan, H.*
Prof. van den Hoff, J.
Dr. Walther, M.*
Dr. Will, E.
Dr. Wüst, F.
Dr. Zessin, J.

Technical Staff

Barth, M.*
Dohn, N.
Gläser, H.
Görner, H.
Große, B.
Hentges, A.*
Herrlich, R.
Herzog, W.

Jährig, P.*
Kasper, H.
Kolbe, U.
Krauß, E.
Krauß, T.*
Kreisl, B.
Kunadt, E.
Landrock, K.

Lehnert, S.
Lenkeit, U.**
Lipps, B.
Lücke, R.
Rode, K.
Roß, H.
Sterzing, R.**
Suhr, A.**

Post Docs

Dr. Müller, M.*

Dr. Pawelke, B.*

PhD Students

Gester, S.
Hecht, M.
Heinrich, T.

Hultsch, C.
Just, U.

Pöttsch, C.
Schiller, E.

Former Personnel

(who left during the period covered by the report)

Director: Prof. Dr. Johannsen, B.

Administrative Staff: Kersten, M.

Scientific Staff: Dr. Heichert, C.* Dr. Syhre, R.

Technical Staff: Kunadt, E.

PhD Students: Habala, L. Rother, A.
Jordanova, A. Schneider, A.
Jung, Ch. Wardwilai, C.

* term contract

** on maternity leave